The role of deubiquitinase USP7 in the regulation of pancreatic pro-endocrine factor NGN3

Manea, Thea

Awarding institution:
King's College London

The role of deubiquitinase USP7 in the regulation of pancreatic pro-endocrine factor NGN3

Teodora Manea

ID: 1733197

Thesis submitted for the degree of Doctor of Philosophy (PhD)

First Supervisor: Dr Rocio Sancho

Second Supervisor: Prof Francesca Spagnoli

Centre for Gene Therapy and Regenerative Medicine

King's College London

30th of March 2022

Abstract

Transient expression of the transcription factor Neurogenin 3 (NGN3) during pancreatic development is essential for the specification of endocrine progenitors that give rise to all endocrine cell types in the pancreas. These include insulin-secreting β cells, which are vital in maintaining glucose homeostasis, with their loss resulting in type 1 diabetes. NGN3 overexpression in ductal and acinar cells of the exocrine pancreas promotes exocrine-to-endocrine transdifferentiation, generating α, β and δ cells. Accordingly, transient NGN3 expression is a hallmark of *in vitro* β cell differentiation protocols. Absence of pancreatic islets and the development of a diabetic phenotype have been described for Ngn3 knockout mice and pigs, while null NGN3 mutations in human patients result in neonatal diabetes. Due to its importance in endocrine development and to its ability to induce pancreatic plasticity, a better understanding of NGN3 regulation could help improve the yield and maturity of β cells generated *in vitro*, as well as provide strategies for promoting exocrine-to-β-cell transdifferentiation *in situ*.

In this thesis, I identified two new NGN3 interactors, USP7 and HUWE1, with known roles in the ubiquitin-proteasome pathway, and investigated their role in NGN3 post-translational regulation. I used HEK293A cells and iPSC-derived pancreatic progenitors to assess whether modulating HUWE1 and USP7 activity affected NGN3 ubiquitination and stability, while also analysing the role of NGN3 phosphorylation in these interactions. Inhibiting HUWE1 activity had no effect on NGN3 stability. However, USP7 overexpression led to the deubiquitination and stabilisation of NGN3 in HEK293A cells, while USP7 inhibition impaired the generation of NGN3+ endocrine progenitors and β-like cells during iPSC-to-β-cell differentiation. Furthermore, these findings were recapitulated in a Usp7 conditional knockout mouse model, with adult mice exhibiting smaller islets and increased blood glucose levels.

This study uncovers a new USP7-dependent mechanism for NGN3 post-translational regulation. During pancreatic development, USP7-mediated deubiquitination of NGN3 reduces its ubiquitination by ligases such as FBW7, preventing its proteasomal degradation. In turn, this results in NGN3 accumulation in the cell, promoting endocrine specification and allowing for the generation of pancreatic islets.

Acknowledgements

First and foremost, I would like to thank my main supervisor, Dr Rocio Sancho, for the insight and support she has provided throughout my PhD and during the writing of this thesis. Her guidance has been fundamental not only in the completion of this project, but also in my growth as a research scientist.

I would also like to thank my 2nd supervisor, Prof Francesca Spagnoli, as well as Dr Davide Danovi, Dr Aileen King and Prof Agi Grigoriadis, who formed my PhD committee, for their valuable help and advice. Many thanks to our collaborator Dr Jessica Nelson, for her help with the *in vivo* experiments described in this thesis.

Further thanks to the Wellcome Trust for funding this project, and Dr Fay Minty, who in her role as the administrator of this programme has provided me with much-appreciated assistance, making the entire process a lot easier to navigate.

I wish to thank the members of the Sancho lab, Cristina Garrone, Dr Sergio Pedraza-Arevalo, Dr Mario Alvarez-Fallas and Theoni Demcollari for their support, friendship, and for the collegial environment they helped create. Alongside our colleagues at the CSCRM, you are an essential part of what made working here such an amazing experience.

Apart from my friends in the lab, I would like to offer even more thanks to those outside of it, whose outspoken hatred of their consultancy jobs has achieved the considerable feat of reinforcing my decision to pursue a career in academia.

Finally, I would like to thank my family for their unwavering support throughout my life, including during my PhD. I am privileged to have them and the safety net that they have always provided, even from 1,000 miles away.

Table of contents

Table of figures

Table of tables

List of abbreviations

AMY2B	Amylase 2B
HEPES	4-(2-hydroxyethyl)-1-piperazineethanesulfonic acid
DAPI	4',6-Diamidino-2-Phenylindole
ASCL1	Achaete-Scute Family BHLH Transcription Factor 1
ATP	Adenosine triphosphate
ATCC	American Type Culture Collection
ANOVA	ANalysis Of VAriance
ARX	Aristaless Related Homeobox
ARM	Armadillo (repeat-like domains)
ATOH1	Atonal BHLH Transcription Factor 1
bHLH	basic Helix-Loop-Helix
BH3	Bcl-2 homology region 3
BSA	Bovine serum albumin
C57BL/6	C57 black 6
CPA1	Carboxypeptidase A1
CK2	Casein kinase II
CRISPR	Clustered Regularly Interspaced Short Palindromic Repeat
cDNA	Complementary DNA
CRL4B	Cullin4B-Ring E3 ligase complex
Ct	cycle threshold
CDK1	Cyclin Dependent Kinase 1
CHX	Cycloheximide
CK19	Cytokeratin 19
DE	Definitive Endoderm
DUB	Deubiquitinase
D	Differentiation day
DMSO	dimethyl sulfoxide

DNTM1	DNA methyltransferase 1
DMEM	Dulbecco's Modified Eagle's Medium
E1B-55K	E1B 55-kilodalton protein
E	Embryonic day
ESC	Embryonic Stem Cells
W	Embryonic week
EP	Endocrine Progenitors
EGFP	Enhanced Green Fluorescent Protein
EGF	Epidermal Growth Factor
EBNA1	Epstein-Barr nuclear antigen 1
EDTA	Ethylenediaminetetraacetic acid
FBW7	F-box and WD repeat domain-containing 7
FGF	Fibroblast Growth Factor
FGF10	Fibroblast Growth Factor 10
FR3T3	Fisher rat 3T3
FBS	Foetal Bovine Serum
FOXA2	Forkhead boX A2
GATA4	GATA-binding protein 4
GO	Gene Ontology
GLIS3	Glis family zinc finger 3
GCG	Glucagon
GAPDH	Glyceraldehyde-3-Phosphate Dehydrogenase
GSK3	Glycogen Synthase Kinase 3β
GFP	Green Fluorescent Protein
GMP	Guanosine monophosphate
H2AX	H2A histone family member X
HSPC	Haematopoietic stem and progenitor cells
HUWE1	HECT, UBA And WWE Domain Containing E3 Ubiquitin Protein Ligase 1

HA	Hemagglutinin
H&E	Haematoxylin-and-Eosin
HNF1A	Hepatocyte nuclear factor-1 alpha
HNF6	Hepatocyte nuclear factor 6
HAUSP	Herpesvirus-associated ubiquitin-specific protease
HES1	Hes Family BHLH Transcription Factor 1
His	Histidine (tag)
HECT	Homologous to E6-AP Carboxy Terminus
HRP	Horseradish peroxidase
HEK293	Human Embryonic Kidney 293
HEK293A	Human Embryonic Kidney 293A
HEK293T	Human Embryonic Kidney 293A
ICP0	Human Herpes Virus (HHV) Infected Cell Polypeptide 0
HIV	Human immunodeficiency virus
HipSci	Human Induced Pluripotent Stem Cell Initiative
hNGN3	human NGN3
IP	Immunoprecipitation
iPSCs	Induced Pluripotent Stem Cells
INS	Insulin
ITS-X	Insulin-Transferrin-Selenium-Ethanolamine
JMS	Juberg-Marsidi syndrome
KGF	Keratinocyte growth factor
LB	Liquid Broth
MAGE-L2	MAGE Family Member L2
MRI	Magnetic resonance imaging
MS	Mass spectrometry
MonoUb	Monoubiquitination
MDM2	Mouse double minute 2 homolog
MIN6	Mouse insulinoma 6

MAFA	Musculoaponeurotic Fibrosarcoma oncogene family, A
MAFB	Musculoaponeurotic Fibrosarcoma oncogene family, B
MCL-1	Myeloid leukemia 1
NGN3	Neurogenin 3
NEUROD1	Neuronal Differentiation 1
NKX2.2	NK2 Homeobox 2
NKX6.1	NK6 Homeobox 1
NEAA	Non-essential amino acids
NT	Not treated
NOTCH1	Notch homolog 1, translocation-associated
OCT	Optimal cutting temperature compound
O/N	Overnight
PAX4	Paired Box 4
PTF1A	Pancreas Associated Transcription Factor 1a
PANC1	Pancreatic Adenocarcinoma-1
PDX1	Pancreatic And Duodenal Homeobox
PDAC	Pancreatic ductal adenocarcinoma
PFA	Paraformaldehyde
PHF8	PHD Finger Protein 8
PMSF	Phenylmethylsulfonyl fluoride
PTEN	Phosphatase and tensin homolog
PBS	Phosphate Buffered Saline
PLK1	Polo Like Kinase 1
PEI	Polyethylenimine
PCR	Polymerase chain reaction
PP	Polypeptide positive
PolyUb	Polyubiquitination
PVDF	Polyvinylidene fluoride
PGT	Primitive gut tube

PCA	Principal Component Analysis
PCNA	Proliferating cell nuclear antigen
PHD3	Prolyl hydroxylase 3
p53	Protein p53
PPM1G	Protein Phosphatase, Mg2+/Mn2+ Dependent 1G
RT-qPCR	Real time quantitative polymerase chain reaction
RING	Really Interesting New Gene
RING2	Really Interesting New Gene 2
RBR	RING-between-RING
RT	Room temperature
Ser-Pro	Serine-Proline
SNP	Single nucleotide polymorphism
scRNA	single-cell RNA
SDS	Sodium dodecyl sulfate
SDS-PAGE	Sodium dodecyl sulfate–polyacrylamide gel electrophoresis
SST	Somatostatin
SHH	Sonic Hedgehog
SOX9	SRY (sex-determining region Y)-box 9
SEM	Standard error of the mean
TUBE2	Tandem Ubiquitin Binding Entities 2
TEMED	Tetramethylethylenediamine
TRAF	TNF receptor associated factor
TRIM27	Tripartite Motif Containing 27
TBS-T	Tris-buffered saline-Tween
T1D	Type 1 Diabetes
T2D	Type 2 Diabetes
Ub	Ubiquitin
USP7	Ubiquitin Specific Peptidase 7
USP	Ubiquitin Specific Proteases

UBA	Ubiquitin-associated
UPS	Ubiquitin-proteasome system
UBL	Ubiquitin-like
UMAP	Uniform Manifold Approximation and Projection
UCN3	Urocortin 3
HUBL	USP7/HAUSP UBL domains
HUBL12	USP7/HAUSP UBL domains 1-2
HUBL123	USP7/HAUSP UBL domains 1-2-3
HUBL45	USP7/HAUSP UBL domains 4-5
vIRF1	Viral Interferon Regulatory Factor 1
W	Embryonic Week
WT	Wildtype
WASH	Wiskott-Aldrich syndrome protein and SCAR homolog
XLID	X-Linked Intellectual Disabilities

Chapter 1: Introduction

1.1 The pancreas

1.1.1 Human pancreas development

In humans, the pancreas is located on the posterior wall of the abdominal cavity, between the stomach and the duodenum. It is a mixed gland, consisting of a large exocrine compartment comprising the pancreatic ducts and acini, and a much smaller endocrine compartment organised in pancreatic islets (Fig. 1). Acinar cells are arranged in grape-like clusters, each connected to the ductal system via centroacinar cells found at the ductal periphery. They secrete digestive enzymes, such as trypsin, lipase, and amylase into the ductal network, which eventually drain into the main duct (the duct of Wirsung). In turn, the main duct then empties into the duodenum, where secreted enzymes participate in the digestion of ingested proteins, lipids, and carbohydrates.

Pancreatic islets, also called the islets of Langerhans, are located between acinar clusters, and contain endocrine α, β, δ, ε and polypeptide-positive (PP) cells, which secrete glucagon, insulin, somatostatin, ghrelin, and pancreatic polypeptide, respectively. Despite its relatively small size, the endocrine compartment of the pancreas plays an essential role in glucose metabolism. Low blood glucose levels induce α-cells to secrete glucagon, a catabolic hormone. Glucagon triggers glycogenolysis in the liver, increasing glucose and fatty acid concentrations in the blood. In contrast, high blood glucose levels trigger secretion of insulin by β cells. Insulin is an anabolic hormone that promotes glucose absorption into liver, fat, and skeletal muscle cells. Glucagon itself has been shown to induce β-cell insulin secretion (Samols, Marri, and Marks 1966). This enacts a negative feedback loop in which β-cell-secreted factors such as

insulin and zinc inhibit glucagon secretion from α-cells (Franklin et al. 2005). The interplay between glucagon and insulin secretion is a crucial part of maintaining glucose homeostasis.

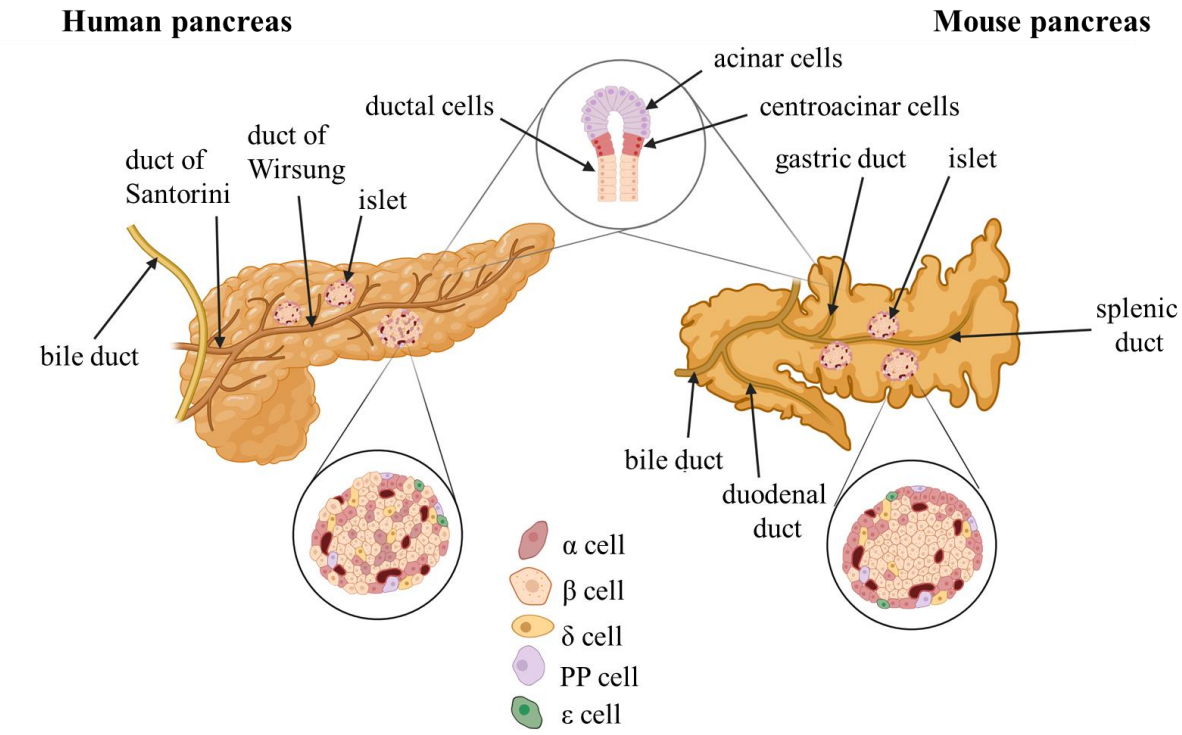

Figure 1. Schematic diagram of the human and mouse pancreas. In both human and mouse, the pancreas is made up of a large exocrine compartment containing the acini and pancreatic ducts, and a smaller endocrine compartment organised in islets and containing α, β, δ, ε and PP cells. In the human pancreas, acinar secretions first drain into intercalated ducts, which then drain into intralobular ducts, followed by interlobular ducts, to finally converge into the duct of Wirsung, which runs alongside the whole pancreatic gland and empties into the duodenum adjacent to the entrance of the common bile duct; in the mouse pancreas, the three lobes (gastric, splenic and duodenal) each drain into their corresponding duct, with the gastric and splenic duct merging, before all three empty into the bile duct. At the islet level, while the standard β-cell core/non-β-cell mantle islet type can be found in both mice and humans, the human pancreas will often exhibit increased islet heterogeneity, with bigger islets showing a more dispersed pattern with non-β cells present in the islet core.

As an additional regulatory layer, β-cell activation results in secretion of Urocortin 3 (UCN3), a hormone found to stimulate somatostatin secretion in pancreatic δ-cells, which, in turn, inhibits β-cell insulin secretion (Van Der Meulen et al. 2015) and may also play a role in the inhibition of glucagon secretion by α-cells (Huising et al. 2018). Somatostatin secretion, as well as secretion of pancreatic polypeptide, has been shown to also be stimulated by ε-cell-

secreted ghrelin (Arosio et al. 2003), known as the “hunger hormone” for its role in regulating food intake. Finally, pancreatic polypeptide secreted by PP cells has been shown to play a role in gall bladder relaxation and inhibition of enzyme secretion by the exocrine pancreas (Greenberg et al. 1978), slowing down digestion.

In chick (Matthias Hebrok, Kim, and Melton 1998) and mouse (F. C. Pan and Wright 2011) embryogenesis, pancreatic development is initiated when, due to signalling from the notochord, the adjacent foregut loses expression of sonic hedgehog (SHH), allowing expression of pancreatic and duodenal homeobox factor 1 (PDX1). In the chick, notochord expression of FGF2 and ActivinβB represses SHH expression in the pre-pancreatic region (Matthias Hebrok, Kim, and Melton 1998; S. K. Kim, Hebrok, and Melton 1997), while in mouse mutation of activin receptors ActRIIA and ActRIIB leads to pancreatic hypoplasia and foregut patterning defects (S. K. Kim et al. 2000), indicating a similar role for activin signalling in murine pancreatic development. Furthermore, loss of SHH signalling inhibitors PTCH1 and HHIP in mice resulted in a similarly impacted pancreas, suggesting that these may also facilitate the initiation of normal pancreatic development (M. Hebrok et al. 2000; Kawahira et al. 2003). Contact with endothelial cells from the dorsal aortae, which, in the mouse, become interposed between the notochord and the dorsal foregut endoderm at E9, further aids the expansion of the dorsal bud (Jacquemin et al. 2006). In contrast to the dorsal region of the foregut, initiation of pancreatic development in the ventral region depends on signalling from tissues other than the notochord, such as the cardiac mesoderm and the vitelline veins (Azizoglu and Cleaver 2016; Deutsch et al. 2001; Lammert, Cleaver, and Melton 2001).

PDX1 is a key transcription factor for pancreatic development, with PDX1+ progenitors giving rise to all main pancreatic lineages (Jonsson et al. 1994; Offield et al. 1996), and impaired PDX1 activity resulting in pancreatic agenesis (Stoffers et al. 1997). During human embryonic

development, SHH expression is excluded from the presumptive pancreatic endoderm by week 4 (W4) and PDX1 expression visible by W5 (Jennings et al. 2013). PDX1+ cells then give rise to a dorsal pancreatic bud and two ventral buds, marked by expression of PDX1, SRY (sex-determining region Y)-box 9 (SOX9) and GATA binding protein 4 (GATA4) (Fig. 2). At this time, microlumens start developing within the dorsal pancreas that will later generate a luminal network for the drainage of acinar secretions into the intestine (Jennings et al. 2013).

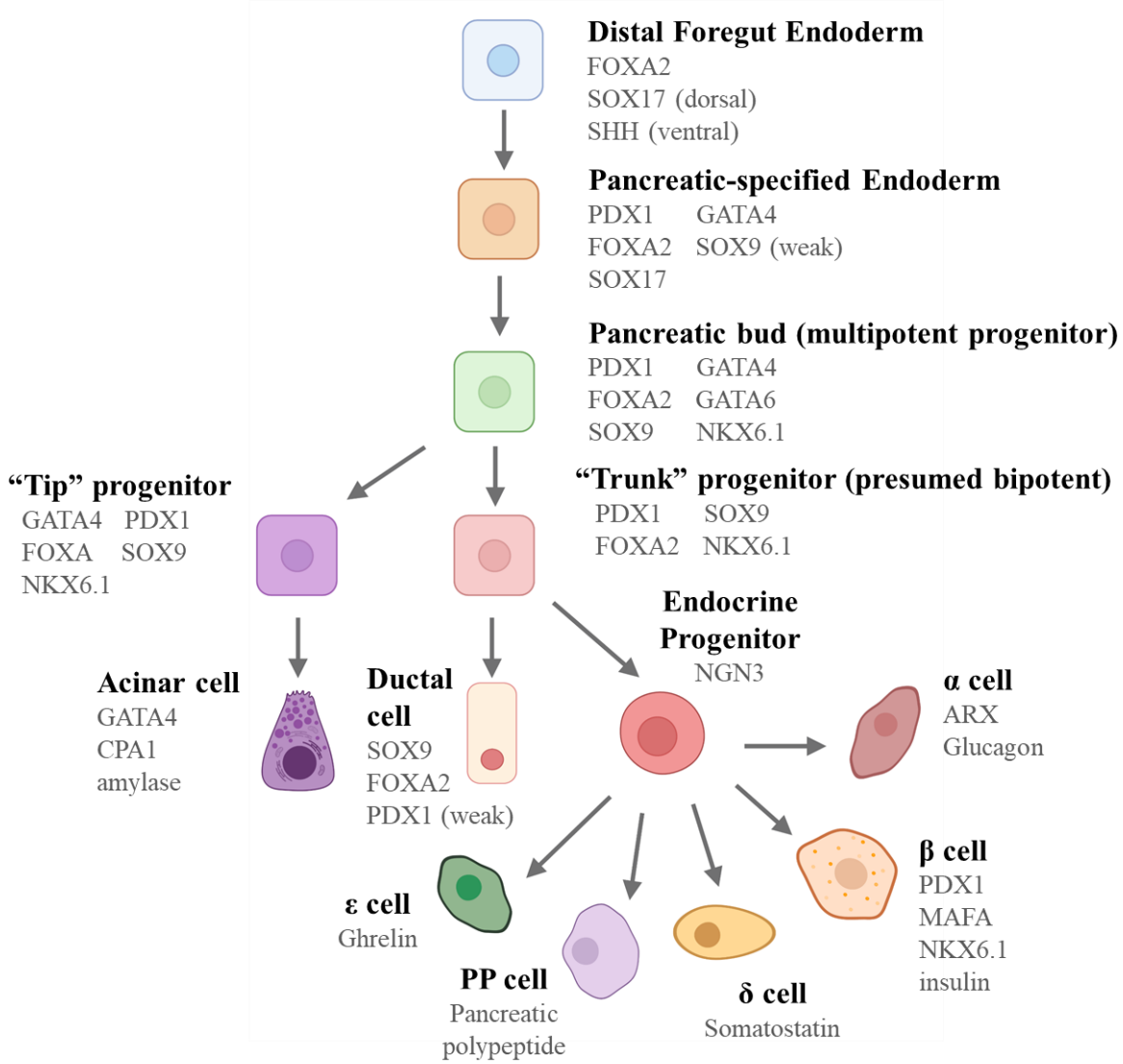

Figure 2. Stages of human pancreatic development. After W4, SHH expression is lost in the presumptive pancreatic endoderm, allowing PDX1 expression. PDX1+ multipotent progenitors at the periphery with high GATA4 expression make up the "tips" domain and will generate the acinar cells in the exocrine pancreas, while GATA4^{low} progenitors make up the pancreatic "trunk", which will give rise to the pancreatic ducts, as well as the endocrine compartment of the pancreas. At W8, NGN3 expression will push "trunk" progenitors towards an endocrine cell fate, while maintained SOX9 expression delineates ductal cells.

During W7, SOX9+/GATA4^{low}/NKX6.1+ (Homeobox protein Nkx-6.1) pancreatic progenitors within the central, duct-like structures form the “trunk” domain, which will later give rise to the ductal and endocrine cells within the pancreas. Peripheral SOX9+/GATA4+/NKX6.1+ progenitors form the “tips”, which will eventually generate the pancreatic acini (Jennings et al. 2013). Also during W7, the left bud of the ventral pancreas gradually disappears, while the right ventral bud fuses to the dorsal pancreas, after the rotation of the stomach and duodenum (Henry et al. 2019).

Starting with W8, some trunk progenitors lose SOX9 expression and gain Neurogenin 3 (NGN3) (Jennings et al. 2013), a transcription factor whose transient expression is essential for the development of the endocrine pancreas (Sheets et al. 2018; Pinney et al. 2011). NGN3 expression peaks between W10-14 (Fig. 3) and significantly decreases by W18-21, with no NGN3+ cells detected after W31 of human pancreatic development (Jennings et al. 2013; Salisbury et al. 2014). These NGN3+ endocrine progenitors generate all endocrine cell types in the pancreas, with β cells emerging first, followed by α and δ cells later in W8, and PP cells in W9 (F. C. Pan and Brissova 2014). ε cells were already present in the pancreas at W13, but at this stage were found as single cells scattered throughout the exocrine tissue (Andralojc et al. 2009). After W21, ε cells had clustered and re-localised around existing islets, forming a crescent-shaped layer at their periphery. Moreover, while immature, polyhormonal endocrine cells can be observed between W9-W15 of embryonic development, as endocrine cells mature, they become monohormonal (Bocian-Sobkowska et al. 1999). In the adult islet, transcription factors such as PDX1, MAFA and NKX6.1 co-express with insulin, marking mature β cells (Lyttle et al. 2008; Zhu et al. 2017).

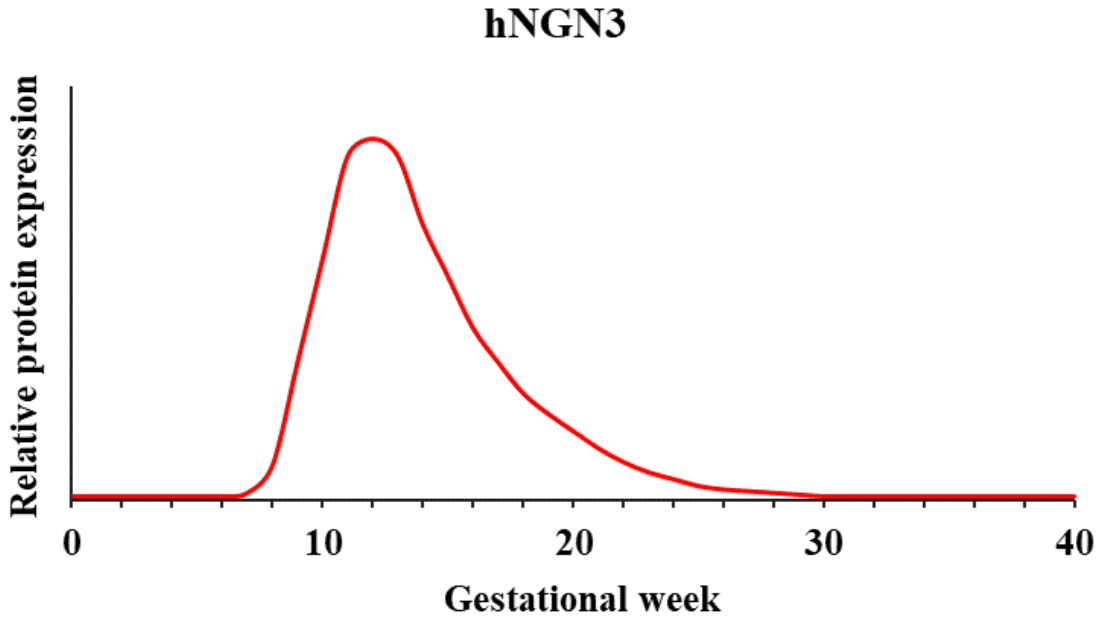

Figure 3. Relative expression of NGN3 protein during human pancreatic development (Jennings et al. 2013). NGN3 protein expression in the human developing pancreas peaks between W10-W14, with few NGN3+ cells remaining by W31.

While in the trunk endocrine progenitors emerge during W8, at the same time, tip progenitors gain carboxypeptidase A1 (CPA1) expression. They completely lose NKX6.1 and SOX9 expression by W10 and W14, respectively, giving rise to GATA4+ acinar cells, clustered around SOX9+ centroacinar and ductal cells from the trunk domain (Jennings et al. 2013). Within the trunk, definitive ductal structures, with intercalated, intralobular and interlobular ducts can be detected at W24-32 (Adda, Hannoun, and Loygue 1984), but when ductal cells become terminally differentiated, if at all, remains unknown (F. C. Pan and Brissova 2014).

1.1.2 Mouse pancreas development

The mouse pancreas comprises the same main cell types as the human one, with an exocrine compartment including the acini and ductal network, and an endocrine compartment containing islets with α, β, δ, ε and polypeptide-positive (PP) cells. However, in contrast to the human pancreas, the murine pancreas is not as well-defined organ, being diffusely distributed within the mesentery of the proximal small intestine. It is composed of three distinct lobes (duodenal,

splenic and gastric), all drained by a large interlobular duct into which the duodenal, splenic and gastric ducts converge (Dolenšek, Rupnik, and Stožer 2015).

As far as the endocrine compartment is concerned, earlier studies reported major differences between mouse and human islet architecture. Mouse islets were described as having a β-cell core, surrounded by a mantle made up of mostly α-cells, while human islets showed a seemingly random layout, with different endocrine cell types interspersed throughout the islet (Cabrera et al. 2006; A. Kim et al. 2009). However, more recent studies have suggested that while human islets are more heterogeneous in terms of endocrine cell type composition, medium-sized human islets still tend to exhibit a similar architecture to that found in rodents, with β-cell cores surrounded by a non-β-cell mantle (Bonner-Weir, Sullivan, and Weir 2015). However, large human islets containing higher percentages of α-cells seemed more likely to present a non-standard architecture, with heterogeneity higher in some donors than in others (Bonner-Weir, Sullivan, and Weir 2015).

Pancreas formation in rodents is generally split into a primary, secondary and tertiary transition. During the primary transition (E8.5–E10.5 in the mouse), pre-differentiated cells give rise to proto-differentiated cells which express pancreas-specific proteins at low levels (Jørgensen et al. 2007). In this stage, pancreatic progenitors proliferate forming a stratified epithelium characterised by expression of PDX1, HLXB9, PTF1A, NKX6-1, and NKX2.2 (Jørgensen et al. 2007; Dassaye, Naidoo, and Cerf 2016). The secondary transition (E13.5-E16 in mouse) oversees the conversion of proto-differentiated cells into fully differentiated cells (Jørgensen et al. 2007), while during the tertiary transition (E16.5-Postnatal), differentiated cells within the pancreas undergo remodelling and maturation (Dassaye, Naidoo, and Cerf 2016).

Within the primary transition, murine pancreas formation is first evident at E9.5, when the dorsal bud of the pancreas emerges, followed by the ventral bud at E10. However, PDX1 expression can be observed as early as E8.5 (Villasenor, Chong, and Cleaver 2008). At E10.5 PDX1, NKX6.1 and PTF1A are highly co-expressed in the epithelium of both pancreatic buds. By E11.5, during the secondary transition, NKX6.1 expression becomes restricted to the pancreatic "trunk", while expression of PTF1A delineates the pancreatic "tips" (Jørgensen et al. 2007; Schaffer et al. 2010). PTF1A is known to regulate transcription of genes that encode enzymes secreted by acinar cells, such as elastase and amylase (Rose et al. 2001). Research by Schaffer et al suggests that NKX6.1 could be responsible for the transcriptional repression of PTF1A in multipotent progenitors during a critical time window before E14, under the control of the Notch signalling pathway, which favours NKX6.1 expression (Schaffer et al. 2010). This, in turn, would prevent the expression of acinar-specific genes downstream of PTF1A, resulting in the commitment of the cells to a bipotent progenitor "trunk" fate. At E12.5, after gut rotation, the dorsal and ventral buds fuse, becoming one organ. After E13, during the secondary transition, "tips" cells further differentiate to form the pancreatic acini, starting to synthesise enzymes such as amylase and trypsinogen (Pictet et al. 1972).

In contrast to human pancreatic development, NGN3 expression during the development of the mouse pancreas is biphasic (Fig. 4): Ngn3 transcripts are present in a first wave of expression between E8.5 and E11 (Villasenor, Chong, and Cleaver 2008), during the primary transition. This is followed by a second wave between E12.5 and E17.5, during the secondary transition, with a peak at E15.5 (Villasenor, Chong, and Cleaver 2008; Apelqvist et al. 1999). At protein level, NGN3 expression has been observed at E10.5, after which it decreases until E11.5 (Villasenor, Chong, and Cleaver 2008). The second wave starts by E12 and peaks at E15.5, followed by decreasing NGN3 expression until only few NGN3+ cells are left at E18.5 (Villasenor, Chong, and Cleaver 2008; Mellitzer et al. 2004).

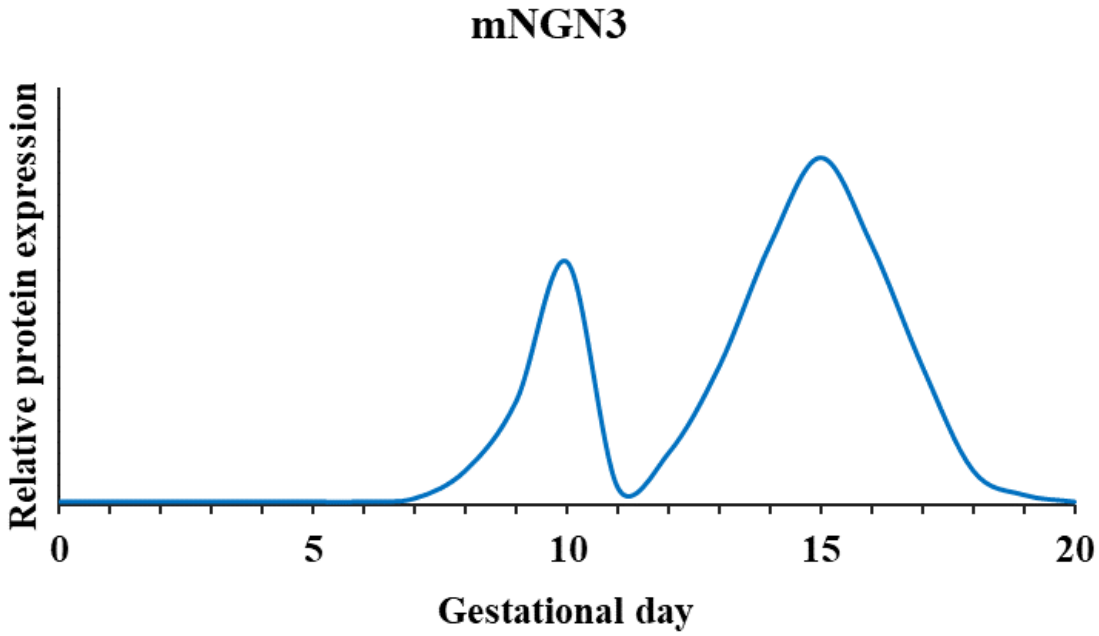

Figure 4. Relative expression of NGN3 protein during mouse pancreatic development (Villasenor, Chong, and Cleaver 2008)**.** NGN3 expression in mouse pancreatic development is biphasic, with a first wave of expression at E10-W10.5 and a second wave between E12-E18.5, peaking at E15.5.

During the secondary transition, NGN3+ endocrine precursors give rise to the majority of endocrine cells found in islets at the end of gestation. Out of the different endocrine cell types in the pancreas, α cells are believed to emerge first during mouse pancreatic development (Rall et al. 1973; F. C. Pan and Wright 2011), as opposed to the human pancreas, in which β cells can be observed before all other endocrine cell types (F. C. Pan and Brissova 2014). Multiple transcription factors with roles in endocrine lineage specification have been identified, such as ARX, whose expression promotes an α cell fate (Collombat et al. 2007), and PAX4, which is essential for β cell specification (Collombat et al. 2009). The absence of both PAX4 and ARX expression appears to boost δ cell numbers (Collombat et al. 2005). Similarly to β cell development in the human pancreas, expression of certain transcription factors, such as PDX1, MAFA and NKX6.1, is essential for β cell maturation and function (Aramata et al. 2005; F. C. Pan and Wright 2011). However, in contrast to human β cells, mouse β cells lose expression of transcription factor MAFB in order to achieve maturity (Nishimura, Takahashi, and Yasuda

2015; Artner et al. 2010), while this phenomenon is not observed in human pancreatic development (Dai et al. 2012).

During the tertiary transition, differentiated PP cells are generated and endocrine cells within the pancreas migrate to neighbouring exocrine tissues to initiate the formation of pancreatic islets. Postnatally, β cells within mouse islets can proliferate to maintain β cell mass, although this ability gradually declines between postnatal week 4 and after weaning (Teta et al. 2007; Rankin and Kushner 2009). Similarly, acinar cells continue to proliferate and mature postnatally, until weaning (Desai et al. 2007).

1.1.3 Diabetes

Diabetes constitutes a group of chronic disorders characterised by impaired glucose metabolism, resulting in high blood sugar levels. If left untreated, it can lead to serious complications such as diabetic ketoacidosis, hyperosmolar hyperglycaemic state (Kitabchi et al. 2009), cardiovascular and kidney disease, cognitive impairment (Saedi et al. 2016) and even death. The great majority of diabetes cases fall into the category of either Type 1 (T1D), or Type 2 diabetes (T2D). Despite being grouped together based on similar symptomatology, the two disorders have distinct causes, disease mechanisms and treatment options. T2D is responsible for over 90% of diabetes cases worldwide (Y. Wu et al. 2014). Although it normally occurs in patients over the age of 40, more recently it is being increasingly diagnosed in younger people, including adolescents (Viner, White, and Christie 2017). In T2D, the patient develops insulin resistance, with cells no longer able to respond adequately to normal insulin levels, resulting in dysregulated glucose homeostasis. A failure of β cells to compensate for the increasing insulin demands of the body further contributes to the development of T2D (Saisho 2015), but the exact trigger for insulin resistance onset is still unknown. In some cases, T2D

can be controlled through lifestyle changes, while metformin treatment, as well as insulin injections can also be prescribed (Turner 1998).

In T1D, insulin-producing β-cells in the pancreas are destroyed due to an autoimmune reaction (Yoon and Jun 2005), resulting in impaired insulin production, abnormal blood glucose levels and dysregulated glucose metabolism (Atkinson, Eisenbarth, and Michels 2014). T1D makes up roughly 10% of diabetes cases overall, but accounts for the majority of diabetes cases in patients under 15 years old. Most people affected being diagnosed before the age of 20 (Katsarou et al. 2017). As T1D pathology derives from insulin insufficiency, T1D requires lifelong treatment, with multiple insulin injections necessary throughout the day. In some cases, patients can benefit from other treatment options, such as continuous subcutaneous insulin infusion to regulate insulin levels (Roze et al. 2015), or transplantation of pancreatic islets aiming to replenish β-cells in the patient's pancreas (Zinger and Leibowitz 2014). Although this strategy has helped restore normoglycemia and insulin independence in many Type 1 diabetics, the effects are usually short-term, with most patients becoming insulin dependent again after 5 years (Rickels and Paul Robertson 2019). Moreover, a shortage of islets available for transplantation and the fact that the transplant must be accompanied by immunosuppression currently limit the clinical benefits of this therapy.

1.1.4 Strategies for β cell generation

To address the limitations of current T1D therapies, multiple studies have looked into the possibility of generating β cells *in vitro* (Pagliuca et al. 2014; Hogrebe et al. 2020; Pagliuca and Melton 2013). Induced pluripotent stem cells (iPSCs) have been a particularly attractive starting point, as they are pluripotent stem cells obtained through adult somatic cell reprogramming. This means that they could potentially be sourced from the patient,

reprogrammed, expanded, differentiated, and re-implanted without the need for immunosuppression. iPSC-to-β-cell differentiation protocols generally attempt to recapitulate consecutive pancreatic developmental stages, starting with the definitive endoderm (DE) and followed by the primitive gut tube (PGT), posterior foregut (PF), pancreatic progenitor, endocrine progenitor (EP) and ultimately hormone-expressing cells (Russ et al. 2015; Trott et al. 2017). This is achieved via modulation of pathways involved in pancreatic development, and by induction of characteristic markers, such as PDX1 during the PF stage, NKX6.1 during the pancreatic progenitor stage and NGN3 during the EP stage. Additional triggers, such as induction of actin cytoskeleton depolymerisation at the start of the EP stage, can further improve β cell generation and function (Hogrebe et al. 2020). However, despite several different protocols existing for the differentiation of iPSCs into β-cells, obstacles such as insufficient β-cell maturation and *in vitro* treatments unsuitable for downstream clinical applications remain (Matthias Hebrok 2012; Shahjalal et al. 2018).

A new avenue of investigation has been opened by the discovery that certain *in vivo* triggers, such as pancreatic ductal ligation, inflammation, or induced overexpression of certain transcription factors, are able to induce plasticity *in situ* (Fig. 5). This results in limited transdifferentiation between different cell types within the pancreas (Demcollari, Cujba, and Sancho 2017). For instance, β cell reconstitution through δ cell reprogramming in response to injury has been previously described in juvenile patients (Chera et al. 2014). Interestingly, overexpression of key transcription factors, NGN3, PDX1, and MAFA, was sufficient to reprogram mouse exocrine pancreatic cells to insulin+ β-like cells (Zhou et al. 2008). NGN3 overexpression on its own could induce transdifferentiation to somatostatin+ cells in 40% of infected cells, while overexpression of both NGN3 and MAFA could generate both glucagon+ and somatostatin+ cells (Weida Li et al. 2014). No transdifferentiation was observed when overexpression PDX1 or MAFA, on their own or together, in the absence of NGN3. This re-

affirms the essential role of NGN3 in the generation of endocrine cells within the pancreas, with PDX1 and MAFA required for β cell fate specification and maturation. Similarly, overexpression of PDX1, NGN3 and MAFA successfully induced insulin expression in cells from other endoderm-derived tissues, such as intestine (Y. J. Chen et al. 2014) antral stomach (Ariyachet et al. 2016), and liver (Banga et al. 2012). Due to the relative abundance of these cell types compared to β cells in both the diabetic and the healthy patient, harnessing this plasticity to generate β cells *in situ* provides a promising alternative to *in vitro* generation of β cells from iPSCs. However, the clinical use of adenoviral or lentiviral vectors such as the ones used in these studies may not be straightforward, due to safety concerns regarding immunogenicity and off-target effects.

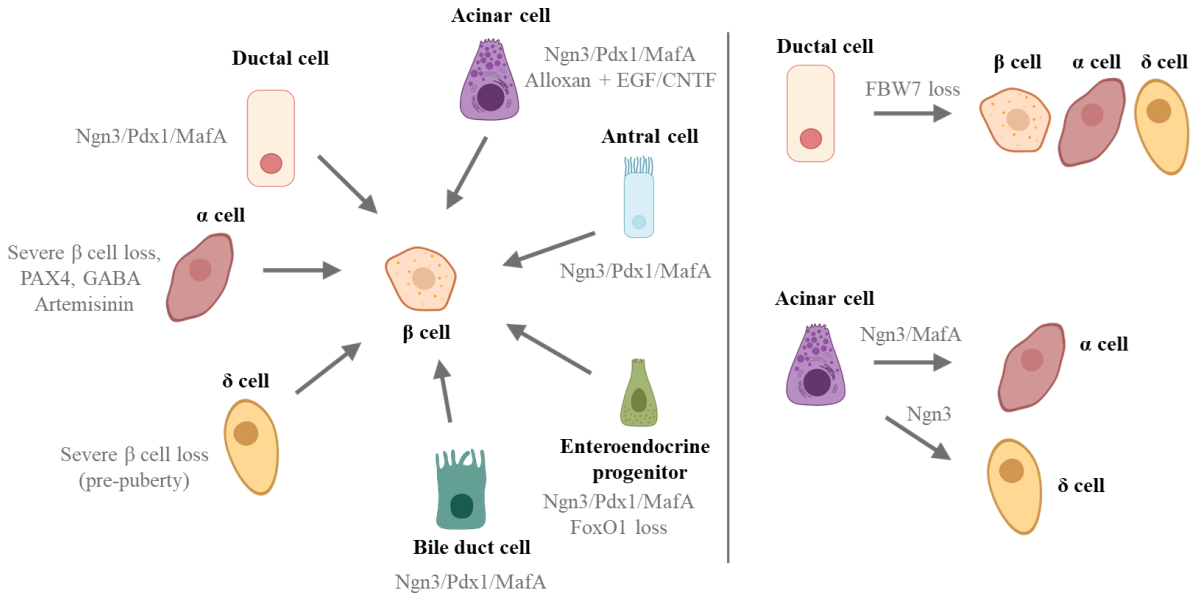

Figure 5. Diagram of cell plasticity triggers that result in transdifferentiation to endocrine pancreatic cells. Overexpression of Ngn3, Pdx1 and MafA induces transdifferentiation to β cells in exocrine cells in the pancreas, as well as non-pancreatic cells such as antral, enteroendocrine and bile duct cells. FBW7 loss induces ductal-to-endocrine cell plasticity, generating α, β, and δ cells. Schematic adapted from Demcollari et al (Demcollari, Cujba, and Sancho 2017).

Besides transcription factor overexpression, loss of E3 ubiquitin ligase FBW7 can induce ductal-to-endocrine cell plasticity in mice (Sancho et al. 2014). This is due to the fact that NGN3 is a substrate for FBW7-mediated ubiquitination. Loss of FBW7 results in decreased

NGN3 ubiquitination, decreased degradation through the ubiquitin proteasome system (UPS), and increased stability of an otherwise unstable NGN3. NGN3 accumulation then pushes the cell towards endocrine transdifferentiation, similarly to its effect during pancreatic development. However, transdifferentiation efficiency is still less than 1% (Sancho et al. 2014). Therefore, additional pathways may be responsible for the regulation of NGN3 stability and endocrine specification in the pancreas. As NGN3 expression is a key factor in the generation of endocrine pancreatic cells, both during development and in the adult pancreas, through exocrine-to-endocrine cell reprogramming, further research into its post-translational regulation could reveal new ways to improve endocrine cell generation in general, and β-cell generation in particular.

1.2 NGN3

1.2.1. NGN3 structure and function

Due to its essential role in pancreatic endocrine specification, as well as its potential use in inducing exocrine-to-endocrine plasticity in the adult pancreas, NGN3 has been widely studied. NGN3 is a basic helix–loop–helix (bHLH) 23kDa transcription factor whose transient expression during pancreatic development is essential for the emergence of the endocrine pancreas. It is encoded by the Neurog3 (Ngn3) gene with only one coding exon (Sommer, Ma, and Anderson 1996), and contains 214 amino acids, with a c-terminal activation domain and a bHLH domain located between positions 83-135 (Fig. 6A). The activation domain facilitates the interaction of NGN3 with transcription co-regulators such as CBP and p300 (Breslin et al. 2007; Vojtek et al. 2003). In particular, it has been shown that the activation domain of NGN3 is necessary for its interaction with transcription factor HNF1α, which, in turn, is required for the induction of Pax4 gene expression (Smith et al. 2003). The bHLH domain is made up of DNA-binding basic region (b) followed by two α-helices separated by a variable loop region

(HLH) (Ferré-D'Amaré et al. 1993). HLH-promoted dimerization with the same, or other bHLH transcription factors allows the basic regions of the newly formed homo- or heterodimers to bind hexanucleotide sequences (Ohsako et al. 1994; Murre et al. 1989). As a Class A bHLH transcription factor, NGN3 can bind "E-box" hexameric DNA sequences (CANNTG), such as E1 and E3, when found in a heterodimeric complex with transcription factor E47 (Breslin et al. 2007; Huang et al. 2000). The bHLH domain is entirely conserved between murine and human NGN3, while the protein itself is 75% conserved between the two species.

In mouse, NGN3 expression has been detected during embryonic development in the restricted region of the developing spinal cord, in the hypothalamic region and in pancreatic endocrine progenitors (Sommer, Ma, and Anderson 1996). Additionally, NGN3 expression is also essential for the differentiation of enteroendocrine cells in the stomach and intestine, and the maintenance of gastric epithelial cell identity (C. S. Lee et al. 2002).

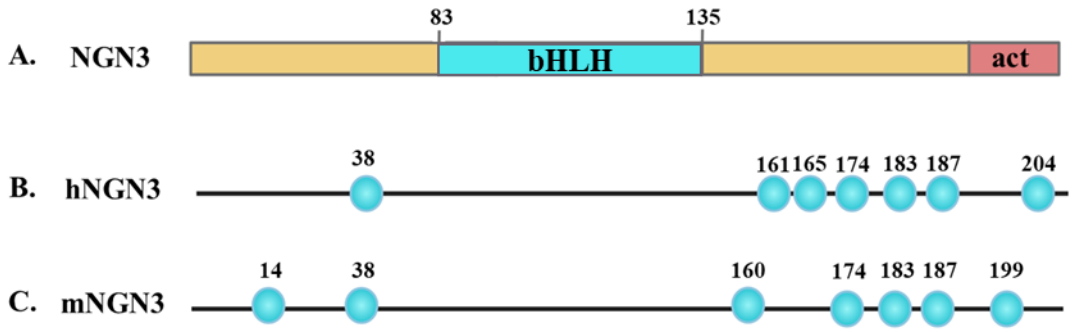

Figure 6. Schematic of NGN3 protein sequence. A. NGN3 is a 214 amino acid protein, containing a bHLH domain (residues 83-135) and an activation domain at the C-terminus. **B.** Serine residues that are part of serine-proline phosphorylation motifs within the human NGN3 sequence. **C.** Serine residues that are part of serine-proline phosphorylation motifs within the mouse NGN3 sequence.

Within pancreatic development, NGN3 activates the transcription of multiple downstream target genes whose expression is essential for endocrine specification, such as NeuroD1 (Huang et al. 2000), Insm1 (Mellitzer et al. 2006), Rfx6 (Soyer et al. 2010), Pax4 (Gasa et al. 2008) and Nkx2-2 (Gasa et al. 2008). In the case of NeuroD1, for instance, NGN3 induces expression

by forming a heterodimer with transcription factor E47 and binding to the E1 and E3 boxes within the NeuroD1 promoter (Huang et al. 2000).

The importance of NGN3 expression during pancreatic development has been highlighted by Ngn3 knockout studies in mouse (Gradwohl et al. 2000) and pig (Sheets et al. 2018) embryos. In both cases, embryos failed to develop pancreatic islets and the animals exhibited a diabetic phenotype after birth, either dying shortly after, or requiring humane euthanasia. In humans, homozygous Ngn3 mutations have been linked to cases of congenital malabsorptive diarrhoea due to a lack of enteroendocrine cells within the intestine (Jan N Jensen et al. 2007; Ünlüsoy Aksu et al. 2016). The patients had not initially presented with neonatal diabetes, as was the case in mouse and pig studies, although they did eventually develop diabetes during childhood (Sayar et al. 2013). It was hypothesised that this was due to the fact that the Ngn3 mutations in these patients were hypomorphic, rather than null, with a study in human embryonic stem cells (ESC) showing that while Ngn3 knockout prevented differentiation towards pancreatic endocrine cells, a 75-90% knockdown of Ngn3 still allowed for some endocrine cell generation (McGrath et al. 2015). Indeed, neonatal diabetes was reported in patients with more severe Ngn3 mutations (Pinney et al. 2011; Rubio-Cabezas et al. 2011). However, even in these cases, low C-peptide levels were detected in the patients' blood, indicating the existence of a small, but functional population of insulin-producing cells. This suggests that although NGN3 expression is responsible for endocrine specification in the human pancreas, there may still be an alternate way for a limited supply of endocrine cells to be generated. Nevertheless, NGN3 activity is still necessary for the formation of a fully functional endocrine compartment in the pancreas, with even hypomorphic mutations in the Ngn3 gene resulting in childhood-onset diabetes.

1.2.2. NGN3 transcriptional and post-translational regulation

Within the pancreas, transient NGN3 expression during embryonic development plays an essential role in endocrine specification. As NGN3 expression is no longer detected in the human pancreas after gestational W31, strict regulatory pathways must be in place to ensure the NGN3 expression peak subsides, allowing endocrine precursor cells to proceed towards a mature endocrine fate. Multiple transcription factors have been found to regulate Ngn3 gene expression. Firstly, a Notch-dependent mechanism for Ngn3 transcriptional regulation was identified, wherein intermediate Notch activity promotes expression of SOX9, which in turn activates Ngn3 gene expression (Shih et al. 2012). Despite SOX9 being essential for the induction of Ngn3 expression, further endocrine differentiation requires downregulation of SOX9, which is achieved via transcriptional inhibition of Sox9 by NGN3. In contrast, high Notch activity induces expression of HES1, a repressor of Ngn3 transcription (Shih et al. 2012). In addition to SOX9, other transcriptional activators of Ngn3 expression have been identified, such as HNF6 (Jacquemin et al. 2000), HNF1α (J. C. Lee et al. 2001), FOXA2 (J. C. Lee et al. 2001), PDX1 (Oliver-Krasinski et al. 2009) and GLIS3 (Y. Yang et al. 2011). Moreover, transcription factor NGN3 operates on a positive auto-feedback loop, activating its own transcription (Shih et al. 2012; Ejarque et al. 2013), so even though NGN3 may downregulate expression of some of its transcriptional activators, such as SOX9, it can still maintain its own gene expression at high levels. The end of this positive auto-feedback loop is likely facilitated by Ngn3 transcriptional repressors such as HES1, by an increase in NGN3 protein degradation, or by a combination of the two.

Once generated, NGN3 goes through an additional layer of strict post-translational regulation, with the half-life of human NGN3 being roughly 1 hour (X. Zhang et al. 2019). The half-life of mouse NGN3 has been shown to be as low as 11 minutes when exogenously expressed in

MIN6 cells (Azzarelli et al. 2017), but over 15 minutes when overexpressed in HEK293T cells (Sancho et al. 2014), suggesting that different cell types may vary in their expression of proteins necessary for NGN3 post-translational regulation.

NGN3 is degraded through the UPS system and can be ubiquitylated on lysines, the N-terminus and on non-canonical residues, such as cysteines, serines and threonines (Roark, Itzhaki, and Philpott 2012). NGN3 interacts with, and is ubiquitinated by the E3 ubiquitin ligase FBW7, and this interaction is facilitated by phosphorylation at the S183 residue on NGN3 by kinase GSK3β (Sancho et al. 2014) (Fig. 7). GSK3β consensus site (S183-S187) is conserved between mouse and human NGN3, further emphasising the importance of the GSK3β/FBW7 pathway in NGN3 post-translational regulation. Serine-to-alanine mutation of NGN3 residues S183 and S187 leads to the doubling of mouse NGN3 half-life (Azzarelli et al. 2017), as a lack of phosphorylation at those residues impairs the NGN3/FBW7 interaction, preventing NGN3 ubiquitination and proteasomal degradation. However, Azzarelli et al identified five additional predicted phosphorylation sites for mouse NGN3 containing a serine-proline (Ser-Pro) motif: S14, S38, S160, S174 and S199 (Fig. 6B). Mutating all five sites, in addition to S183, leads to further NGN3 stabilisation, with NGN3 half-life increasing from roughly 11 minutes, to over 52 minutes (Azzarelli et al. 2017). This indicates the possibility that phosphorylation at all, or at some of these sites plays a role in additional pathways for NGN3 regulation. While the human NGN3 protein does not contain serine-proline motifs at residues 14, 160, and 199, it does contain serine-proline motifs at other positions throughout the protein, with S161, S165 and S204 being possible phosphorylation sites (Fig. 6C). Some of these sites, such as S161 and S165, in addition to other serines not part of serine-proline motifs, are sequentially phosphorylated in response to phosphorylation at the S183 residue, but do not appear to undergo phosphorylation independently of S183 (Krentz et al. 2017), while mutating S204 does not appear to have any effect on NGN3 stability, activity or phosphorylation status (X. Zhang

et al. 2019). A lower number of phosphorylation sites could explain, in part, the longer half-life of human NGN3 compared to mouse, although other phosphorylation sites could still exist within the NGN3 amino acid sequence, even in the absence of a traditional serine-proline motif.

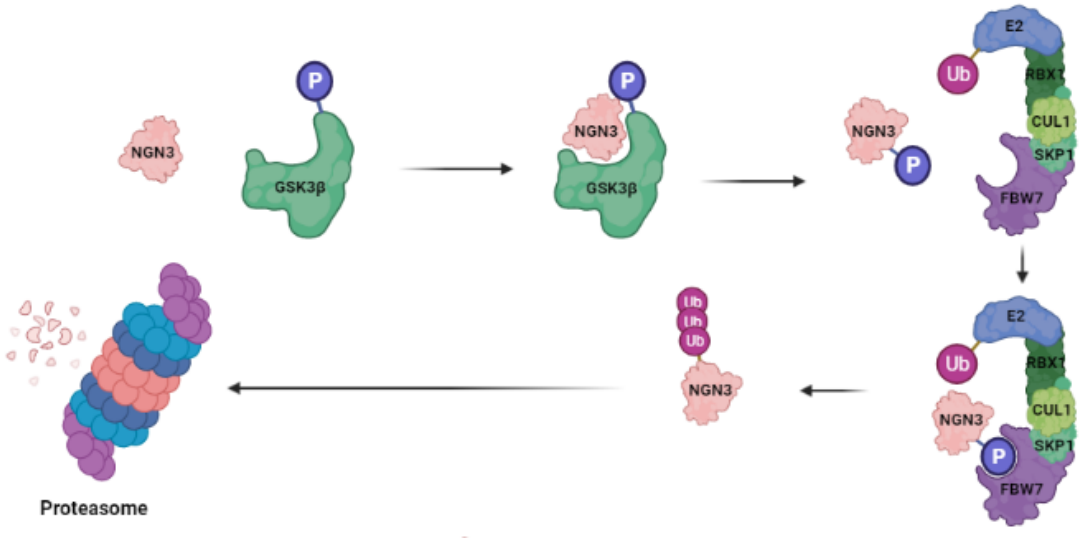

Figure 7. Schematic of the FBW7-mediated NGN3 degradation pathway via the UPS system. NGN3 phosphorylated at S183 is recognised by FBW7 and ubiquitinated. Ubiquitinated NGN3 is then targeted to the proteasome for degradation.

1.2.3. Ubiquitination and E3 ubiquitin ligases

One of the main post-translational modifications responsible for NGN3 regulation is ubiquitination. During the ubiquitination process, ubiquitin, an 8.6 kDa protein, is added to a lysine residue of a substrate, playing an important role in protein function and degradation. Protein ubiquitination requires three enzymatic steps and is initiated by a ubiquitin-activating enzyme (E1), which activates ubiquitin (Ub) in an ATP-dependent manner and forms a thioester linkage between the C-terminus of ubiquitin and the active site cysteine (Cys) of E1. Ubiquitin is then transthiolated to the active site of a ubiquitin-conjugating enzyme (E2) and generates an E2~Ub thioester (Metzger et al. 2014). Ubiquitin protein ligases (E3) transfer the ubiquitin chain from the E2~Ub thioester to lysine residues on the ubiquitination substrate, with the carboxyl group of the carboxy-terminal Gly residue of ubiquitin being covalently

conjugated to the ε-amino group of an internal Lys in the substrate. Other residues containing thiol- or hydroxyl- groups, like cysteine, serine or threonine, can also serve as ubiquitination sites, although this is less common (Cadwell and Coscoy 2005; X. Wang et al. 2007). E3s are the main contributors to ubiquitination specificity, as they are relatively diverse, with 500–1000 different enzymes encoded by the mammalian genome (Varshavsky 2017). In turn, this diversity has made them potential targets for therapeutic interventions (Nalepa, Rolfe, and Harper 2006). In contrast to ubiquitin ligases, deubiquitinases (DUB) can remove ubiquitin from their substrates.

Proteins can be ubiquitinated either at a single residue or at multiple residues. Moreover, each site can be either monoubiquitinated, when a single ubiquitin molecule is added, or polyubiquitinated, when the initial ubiquitin molecule serves as a substrate for the binding of further ubiquitin molecules, forming a ubiquitin chain. Different ubiquitination patterns can lead to different fates for the substrate (Petroski and Deshaies 2003). In the case of polyubiquitination, a ubiquitin molecule can bind to any of the seven lysine residues found in another ubiquitin molecule (K6, K11, K27, K29, K33, K48 or K63), but most commonly this binding occurs at the K48 or K63 sites. Polyubiquitination via the K48 site generally tags the substrate protein for degradation (Fig. 8), while polyubiquitination through a K63-linkage and monoubiquitination play roles in processes such as signal transduction, endocytosis and vesicular sorting (Hicke and Dunn 2003). Polyubiquitination events on less conventional lysine residues seem to also target proteins for degradation, similarly to those involving K48-linkages (P. Xu et al. 2009).

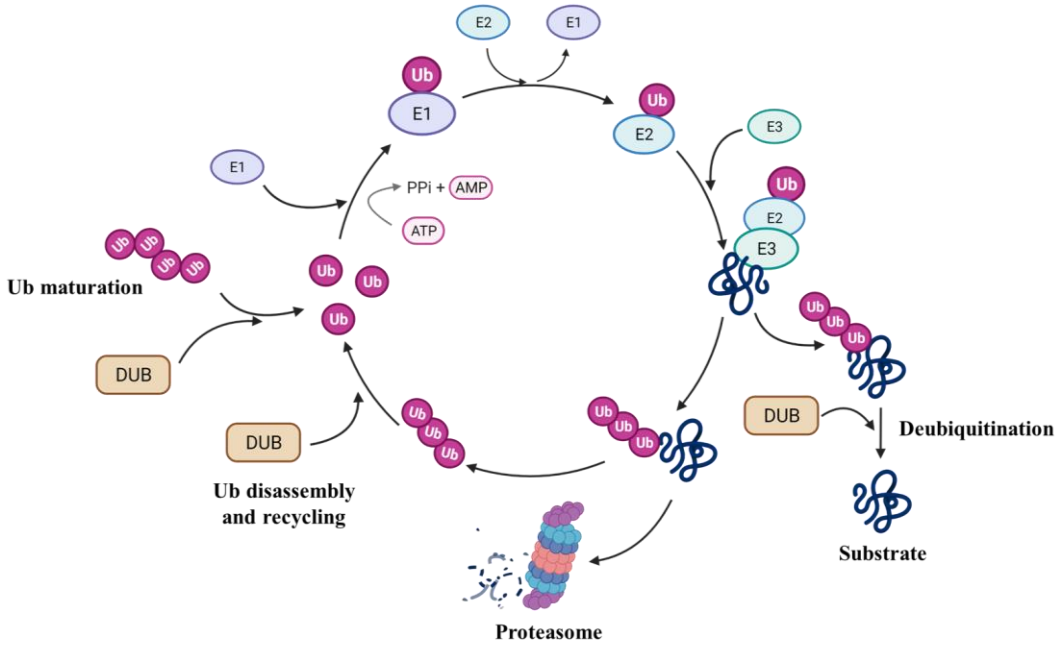

Figure 8. Schematic of the ubiquitin proteasome system in the context of degradative ubiquitination. Ubiquitin activating enzyme E1 binds free ubiquitin and transfers it to ubiquitin-conjugating enzyme E2. Ubiquitin ligase E3 can then transfer the ubiquitin onto its substrate, resulting in either mono- or polyubiquitination. The ubiquitinated substrate is then either deubiquitinated by a deubiquitinase or targeted for proteasomal degradation. While the substrate is degraded, the ubiquitin chain is disassembled and recycled.

E3 ubiquitin ligases classically act through one of two mechanisms: some act as a catalytic intermediate in ubiquitination, similarly to E1 and E2. Other E3s can act as a scaffold to mediate the transfer of ubiquitin directly from the E2~Ub thioester to the substrate. The first mechanism is used by E3s from the Homologous to E6-AP Carboxy Terminus (HECT) family, while Really Interesting New Gene (RING) E3s use the latter (Metzger et al. 2014). A third E3 family, the RING-between-RING (RBR) E3s, act through a HECT/RING hybrid mechanism: they contain an E2-binding RING domain, as well as a second domain (RING2) that forms an E3~Ub intermediate, through a Cys residue in its active site (Wenzel et al. 2011).

Genomic studies have predicted the existence of 300 different RING E3s in the human genome, while only identifying 28 potential HECT E3s (Wei Li et al. 2008). These 28 HECT E3s can recognize their substrates either directly or with the help of adaptor proteins and can be further

divided into the Nedd4 family (9 ligases), the HERC family (6 ligases) and other HECTs (13 ligases), based on the architecture of the protein's N-terminus.

1.3. HUWE1 as an E3 ubiquitin ligase

1.3.1 Structure, function and known substrates

One of the 13 ligases that makes up the "other HECTs" family is HUWE1 (HECT, UBA and WWE domain-containing protein 1), a 482 kDa E3 ubiquitin ligase encoded by the Huwe1 gene found on the X chromosome. HUWE1 contains a ~350 amino acid HECT domain at its C-terminus, made up of two lobes (N-lobe and C-lobe) connected by a hinge loop (Pandya et al. 2010). While the N-lobe contains an E2 binding region (residues 4150–4200), the C-lobe contains the catalytic cysteine (Cys-4341) essential for Huwe1's enzymatic function. The HUWE1 HECT domain also contains a conserved structural element, the α1 helix of the N-lobe, which stabilises the domain, limiting autoubiquitination (Pandya et al. 2010).

In addition to its C-terminus HECT domain, at the N-terminus HUWE1 contains two Armadillo (ARM) repeat-like domains, a WWE domain, normally associated with proteins involved in the regulation of ubiquitin-dependent proteolysis, a BH3 (Bcl-2 homology region 3) domain present in all Bcl-2 family proteins (Zhong et al. 2005), a ubiquitin-associated (UBA) domain involved in ubiquitin binding (Hofmann and Bucher 1996; Wilkinson et al. 2001) and a UBM1 domain of unknown function (Fig. 9). The BH3 domain is important in the interaction of HUWE1 with Bcl-2 family substrates, such as MCL-1, which HUWE1 normally polyubiquitinates and targets for degradation in response to DNA damage, leading to apoptosis (Zhong et al. 2005). The WWE domain likely plays a role in the recognition of specific substrates (Aravind 2001).

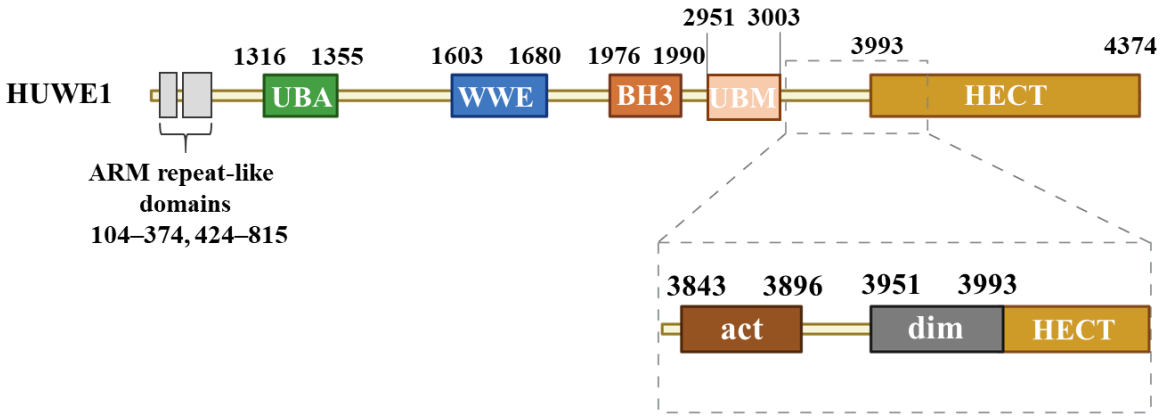

Figure 9. Diagram of HUWE1 protein structure. The HECT catalytic domain is preceded by an activation segment (act) and a dimerisation region (dim). The HECT domain contains the catalytic cysteine C4341, essential for HUWE1's enzymatic activity.

A previous study has shown that the catalytic activity of HUWE1 is down-regulated by the formation of an asymmetric dimer, held together by weak interactions (Sander et al. 2017). This suggests that the ensemble of HUWE1 is dynamic in solution and that HUWE1 has the ability to self-regulate its catalytic activity. HUWE1 is also capable of self-ubiquitination via its HECT domain, participating in its own post-translational regulation (Pandya et al. 2010). Additionally, Cullin4B-RING E3 ligase (CRL4B) ubiquitinates HUWE1, targeting it for degradation in response to DNA damage (Yi et al. 2015). Depletion of CRL4B leads to HUWE1 stabilisation, which in turn destabilises MCL-1 and facilitates apoptosis. While self-ubiquitination, or ubiquitination by other E3 ligases such as CRL4B, lead to its degradation through the ubiquitin-proteasome system, deubiquitination by USP7S, the isoform of Ubiquitin-specific-processing protease 7 (USP7) phosphorylated at Ser18, results in HUWE1 stabilisation (Khoronenkova and Dianov 2013).

HUWE1 localisation appears to vary from tissue to tissue. While in the case of brain and testis cells it is generally found in the nucleus, in other tissues, such as spleen, thymus, bone marrow, liver, kidneys and muscle, it is localised in the cytoplasm, most commonly in the cells of the epithelium (Liu et al. 2007). In the case of the Purkinje cells in the cerebellum, HUWE1 is

found in both cellular compartments, although it is present to a lesser degree in the nucleus. This is also the case for cultured cell lines, such as FR3T3 or HEK293 cells (Liu et al. 2007). In the pancreas, HUWE1 is expressed in the nucleus as well as in the cytoplasmic compartment of both endocrine and exocrine cells (Uhlén et al. 2015).

HUWE1 has been shown to ubiquitinate a vast array of different substrates (Yue Xu, Anderson, and Ye 2016), including, transcription factors involved in cell fate decisions, like ASCL1 (Urbán et al. 2016) and ATOH1 (Cheng, Tong, and Edge 2016). Both ASCL1 and ATOH1 are bHLH proneuronal transcription factors. HUWE1 ubiquitinates ASCL1 at lysine residues within its bHLH domain, promoting its degradation (Gillotin, Davies, and Philpott 2018). In the adult mouse hippocampus, this mechanism has been shown to push proliferating stem cells towards a quiescent fate, preventing the depletion of the stem cell pool and ensuring long-term neurogenesis potential (Urbán et al. 2016). While phosphorylation at serine-proline (SP) sites has been linked to the stability of both ASCL1 and ATOH1 (F. R. Ali et al. 2014; Cheng, Tong, and Edge 2016; Forget et al. 2014), a connection has not yet been drawn between ASCL1 phosphorylation and the ubiquitin-proteasome system. In contrast, it has been shown that phosphorylation at the S328 and S339 residues targets murine ATOH1 for HUWE1-mediated ubiquitination, followed by proteasomal degradation (Forget et al. 2014). As ATOH1 plays a role in the proliferation and differentiation of cerebellar granule neuron progenitors, in the absence of HUWE1, ATOH1 accumulates in the cell, leading to migratory and differentiation defects in cerebellar organotypic cultures (Forget et al. 2014). These findings further emphasise the important role HUWE1 plays in cell fate decisions, not only during embryonic development but also in adult tissues. Moreover, in addition to the role ATOH1 plays in neuronal development, it is also an important regulator of secretory cell generation in the intestine (VanDussen et al. 2012). Here, prolyl hydroxylase 3 (PHD3) competes with ATOH1 for HUWE1 binding, leading to a decrease in ATOH1 ubiquitination and an increase in its

stabilisation, which in turn pushes the cell towards a secretory Goblet cell fate (Yi ming Xu et al. 2020). Certain similarities between ATOH1 and NGN3, such as their bHLH structure, post-translational regulation mechanisms, function in neural development and role in the differentiation of enteroendocrine cells in the intestine, raise the possibility that HUWE1 may also be involved in the ubiquitination and degradation of NGN3.

Furthermore, there is precedent for HUWE1 sharing its substrates with FBW7, a previously identified interactor of NGN3, as in the case of p53 and MYC (Tripathi et al. 2019; Sato et al. 2015), both involved in tumorigenesis and cancer progression (D. Yang et al. 2018; Adhikary et al. 2005). Inactivation of HUWE1 in a human lung cancer cell line resulted in increased p53 stability due to a decrease in p53 ubiquitination, which in turn led to decreased cell proliferation (D. Yang et al. 2018). Moreover, the same study revealed that increased Huwe1 expression in lung cancer patients was associated with a worse prognosis.

While HUWE1-mediated ubiquitination of p53 leads to its degradation, in the case of MYC, the effect of its interaction with HUWE1 is two-fold. Firstly, lysine residues at the carboxy terminus of MYC serve as ubiquitination sites for K63-linked polyubiquitination by HUWE1 (Adhikary et al. 2005). Mutating these lysine residues to arginine inhibits MYC ubiquitination and leads to a decrease in the ability of MYC to activate a subset of its downstream target genes, involved in cell proliferation, cellular metabolism, and protein synthesis. Further experiments from the same study have suggested that this is due to the decreased ability of non-ubiquitinated MYC to bind co-factor p300 at the transcription site of these genes. These observations are in line with previous findings that show K63-linked polyubiquitination plays a role in processes other than the proteasomal degradation of the substrate (Hicke and Dunn 2003). Secondly, MYC has also been shown to undergo HUWE1-mediated K48-linked

polyubiquitination, with HUWE1 deficient cells showing increased MYC stability (Inoue et al. 2013).

Similarly, different studies have painted contrasting pictures of the role of HUWE1 in DNA repair. Its ubiquitination of DNA polymerase β leads to reductions in base excision repair (Parsons et al. 2009), while its interaction with PCNA and monoubiquitination of H2AX alleviates replication stress (Choe et al. 2016). The contradictory roles of HUWE1 in MYC regulation, as well as in DNA repair, suggest that the effect of HUWE1 on individual substrates may be context-dependent and differ based on cell-type. This is particularly likely as we know that the cellular localisation of HUWE1 varies between different organs and tissues.

Furthermore, there is also variation in the types of polyubiquitin chains generated from HUWE1-mediated ubiquitination. In addition to the traditional K48- and K63-linked polyubiquitination, HUWE1 has also been shown to assemble K6- and K11-linked chains onto its substrates, like in the case of mitofusin-2 (Michel et al. 2017). Although research into the functions of K11- and K6-linked ubiquitin chains is limited, it has been suggested that K11-linked chains play an important role in cell division (Wickliffe et al. 2011), while K6-linked chains may be involved in DNA damage response (Elia et al. 2015). Interestingly, K6-linked chains showed a 75% decrease in abundance in HUWE1$^{-/-}$ HeLa cells (Elia et al. 2015), suggesting that at least in some cell lines, HUWE1 may be responsible for the majority of K6-linked polyubiquitination in the cell. These studies reveal an additional level of complexity to HUWE1 function, making it even more difficult to predict the overall effect of HUWE1 activity on a given cell process of pathway.

1.3.2. HUWE1 in health and disease

Due to its virtually ubiquitous expression in the body and its role in the regulation of essential cell processes like proliferation, apoptosis and DNA repair, dysregulation of HUWE1 activity can lead to severe phenotypes, and in particular to a considerable number of X-Linked Intellectual Disabilities (XLID) (Froyen et al. 2008; Bosshard et al. 2017). Missense mutations in HUWE1 have been described as a potential cause for Juberg-Marsidi syndrome (JMS) and Brooks syndrome (Friez et al. 2016), as well Say-Meyer syndrome (Muthusamy et al. 2019), all presenting with intellectual disability, developmental delay and cranial malformations, among other symptoms. Analysis of lymphoblastoid cell transcriptomes from five XLID patients with different HUWE1 mutations has revealed a set of differentially expressed genes known to be modulated by the p53 signalling pathway (Aprigliano et al. 2021). As p53 is a known substrate for HUWE1 ubiquitination, these results suggest that the studied mutations impair HUWE1 activity, leading to a decrease in p53 ubiquitination, an increase in its stability, and p53 accumulation in the cells. The same study has shown that the upregulation of p53 signalling results in a reduced ability of JMS patient-derived induced pluripotent stem cells (iPSCs) to differentiate into neural cells, likely explaining the pathology of XLID associated with HUWE1 missense mutations (Aprigliano et al. 2021). Huwe1 is also one of 17 candidate genes linked to West Syndrome, a form of early infantile epileptic encephalopathy, in a 2018 study by Peng et al (J. Peng et al. 2018), and one of 33 candidate genes linked to autism spectrum disorders in a 2012 study by Nava et al (Nava et al. 2012).

While a lot of focus has been placed on the role HUWE1 mutations play in XLIDs, dysregulated HUWE1 expression is also a feature of other, more common pathologies. HUWE1 has been established as an essential regulator of cardiac homeostasis, with expression being reduced in left ventricular samples from end-stage heart failure patients (Dadson et al.

2017). Cardiac-specific Huwe1 knockout mice experienced cardiac hypertrophy and premature mortality, as myocardial c-MYC was stabilised due to reduced polyubiquitination, downregulating Pgc-1α, Pink1, and mitochondrial complex proteins expression (Dadson et al. 2017). Separately, HUWE1 inactivation specifically in murine pancreatic β-cells led to p53 stabilisation and β-cell death, resulting in a severe diabetic phenotype (Ning Kon et al. 2012). A similar result was observed when Huwe1 was knocked out in all pancreatic cells using a Pdx1-Cre Huwe1$^{fl/fl}$ system, leading to a decrease in β-cell mass as a result of p53 activation (L. Wang et al. 2014). Interestingly, other pancreatic cell populations, such as α cells, did not seem to be affected, with pancreas weight and architecture consistent between genotypes, suggesting that β-cells are particularly vulnerable to Huwe1 loss.

1.3.3 Role in cancer and potential as therapy target

As a regulator of multiple substrates tied to tumorigenesis, HUWE1 has been widely investigated as a potential therapeutic target. However, different tumour types exhibit sometimes opposite patterns of HUWE1 expression. A meta-analysis of HUWE1 expression in different tumour types has found that HUWE1 is overexpressed in leukaemia and lung cancer, but downregulated in brain cancer, lymphoma, sarcoma and testicular seminoma (Su et al. 2019). Indeed, Huwe1 knockout in the A549 human lung adenocarcinoma cell line led to decreased proliferation and colony formation capacity, due to an upregulation in p53 signalling (D. Yang et al. 2018). Similarly, Huwe1 knockdown significantly decreases growth of haematopoietic stem and progenitor cells (HSPC) with constitutive expression of the KRAS^{G12V} oncogene (Ruckert et al. 2020). Plasma cells from Multiple Myeloma patients showed significantly increased HUWE1 levels compared to healthy donors, while HUWE1 inhibition led to decreased viability and cell cycle arrest in the JJN3 myeloma cell line (Crawford et al. 2020).

In contrast, HUWE1 has also been suggested to act as an intestinal tumour suppressor, via the Wnt pathway (Dominguez-Brauer et al. 2016). Huwe1 deletion or mutations were detected in a significant number of uterine cervical carcinoma patients alongside c-MYC amplification, while siRNA-mediated silencing of Huwe1 resulted in c-MYC overexpression and increased proliferation of cervical cancer primary cells *in vitro* (Bonazzoli et al. 2020). Additionally, more aggressive tumour biology in Black/African-American breast cancer patients compared to White/Caucasian patients has been associated, in part, with a HUWE1 missense mutation more common in the former cohort (Andey et al. 2020). Therefore, in the context of carcinogenesis, the effect of HUWE1 on tumour growth and patient prognosis is highly unpredictable, with HUWE1 knockdown slowing down proliferation of some cancer cell types, while promoting proliferation in others.

1.4 USP7 as a deubiquitinase

1.4.1 USP7 structure, function, and known substrates

In contrast to E3 ubiquitin ligases such as HUWE1, deubiquitinases are enzymes that remove ubiquitin from their substrates. USP7 (also known as herpes-associated ubiquitin-specific protease HAUSP) is a 135 kDa member of the Ubiquitin Specific Proteases (USP) family of deubiquitinases and is encoded by the Usp7 gene, which is found on chromosome 16 and made up of 35 different exons. The protein consists of a TRAF-like (Tumour necrosis factor Receptor–Associated Factor) domain at the N-terminus, followed by a catalytic core domain and five C-terminal ubiquitin-like domains (UBL1-5) grouped in three units, in a in a 2+1+2 pattern (Holowaty et al. 2003; Faesen, Dirac, et al. 2011) (Fig. 10). The TRAF-like domain, as well as the UBL domains, recognise and interact with various USP7 substrates (Hu et al. 2006; Ashton et al. 2021). The TRAF domain has an eight-stranded, antiparallel β-sandwich fold (Saridakis et al. 2005) and is essential for USP7 nuclear localisation (Zapata et al. 2001). It

binds substrates that contain a P/A/ExxS motif using residues D164 and W165 located in a shallow groove on its surface (Sheng et al. 2006; Chavoshi et al. 2016), suggesting that substrates may have to compete for binding.

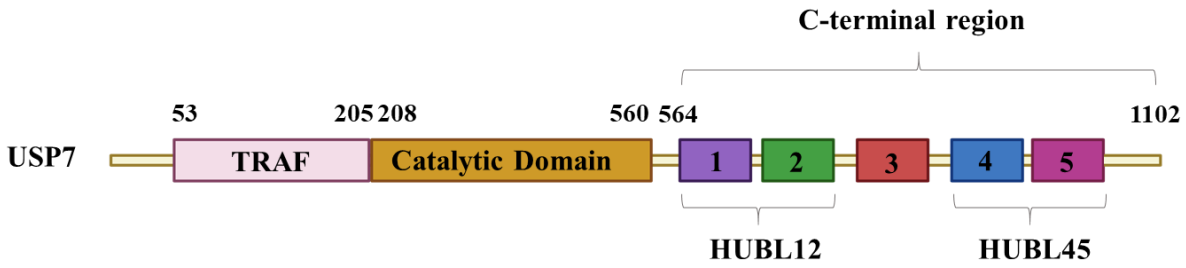

Figure 10. Diagram of USP7 protein structure. USP7 contains a TRAF-like domain at the N-terminus, followed by its catalytic domain and a C-terminal region that encompasses the five Ubiquitin-like domains (UBLs). The first two and last two UBLs are grouped into HUBL12 and HUBL45, respectively. The HUBL45 region binds to the catalytic domain to self-activate USP7, while UBLs 1, 2 and 3 serve can serve as a binding site for GMP-synthase, resulting in further USP7 activation.

Other substrates, such as DNTM1, bind to an acidic pocket in the region of the five UBL domains, through a KG-linker. The C-terminal region of USP7 includes UBL1-5, and in addition to recognising substrates, the region has proved essential for the enhancement of USP7 catalytic activity (Ma et al. 2010; Faesen, Dirac, et al. 2011). The last UBL unit in the C-terminus region, containing USP7/HAUSP UBL domains 4 and 5 (HUBL-45) helps self-activate USP7 by binding to a “switching” loop between residues W285 and F291 of the catalytic domain and organizing the active site, leading to an increased affinity for ubiquitin and a 100-fold increase in USP7 activity. This process is made possible by the linkers connecting the different domains, which allow for flexibility and interdomain arrangement. Additionally, hyperactivation of USP7 can be achieved by binding of GMP-synthase to the first three UBL domains (HUBL123), as this allosterically stabilises the HUBL45-mediated active state (Faesen, Dirac, et al. 2011).

The catalytic core domain of USP7 binds ubiquitin and cleaves the isopeptide bond between ubiquitin and a substrate (Pozhidaeva and Bezsonova 2019). It contains a catalytic triad made up of amino acids C223, H464 and D481. However, the distance between the H464 and C223 sidechains has been calculated at 9.7 Å, which is not in close enough proximity for meaningful interactions to occur (Hu et al. 2002). Substrate binding triggers a change in conformation and bring the catalytic triad residues closer together (Molland, Zhou, and Mesecar 2014; Hu et al. 2002).

USP7 has low tissue specificity, being widely expressed in most organs in the adult human (Uhlén et al. 2015), including the pancreas and other endoderm-derived organs, such as liver and intestine. Due to its ubiquitous expression, and to its important role in processes such as cell cycle, DNA repair, chromatin remodelling, and epigenetic regulation (Z. Wang et al. 2019), USP7 activity in the cell is tightly regulated. USP7 undergoes phosphorylation at residues S18 and S963 and ubiquitination at K869 (Fernández-Montalván et al. 2007), with these post-translational modifications influencing USP7 activity. For instance, CK2-mediated phosphorylation at S18 creates favourable binding conditions for substrate MDM2, while S18-dephosphorylated USP7 has higher affinity for p53 binding (Khoronenkova et al. 2012). In response to ionising radiation, phosphatase PPM1G dephosphorylates USP7 at S18, leading to USP7 deubiquitinating and stabilising p53, which accumulates in the cell and initiates the p53-dependent DNA damage response (Khoronenkova et al. 2012). Moreover, S18 dephosphorylation also leads to a destabilisation of USP7. This fact, alongside previous work showing that a catalytically inactive mutant of USP7 has decreased stability compared to wildtype (Alonso-De Vega et al. 2015), might suggest a role for USP7 in self-deubiquitination. Indeed, other members of the USP deubiquitinase family that USP7 is part of have been shown to deubiquitinate and stabilise themselves (Mei et al. 2011). However, aside from S18, not

much is known about the role of other post-translational modifications on USP7 (R. Q. Kim and Sixma 2017).

USP7 can deubiquitinate both mono- and polyubiquitinated substrates, removing K6-, K11-, K27-, K29, K33-, K48- and K63-linked chains, although doing so less efficiently in the case of K27 and K29 chains (Faesen, Luna-Vargas, et al. 2011). Additionally, different mechanisms are used for the depolymerisation of K48- and K63-linked chains by USP7, resulting in faster USP7-mediated depolymerisation for K63-linked chains than K48-linked ones (Kategaya et al. 2017). USP7 is unable to deubiquitinate M1-linked chains, which are chains formed through linkage of the C-terminal glycine of the incoming ubiquitin to the N-terminal methionine of the preceding ubiquitin, instead of to a lysine residue (Pozhidaeva and Bezsonova 2019).

Similarly to HUWE1, USP7 has been shown to interact with a large array of substrates with diverse functions within the cell, such as n-MYC, PTEN, and TRIM27 (Pozhidaeva and Bezsonova 2019). Through its effect on the MAGE-L2-TRIM27 ubiquitination complex, as well as its interaction with actin nucleating protein WASH, USP7 plays a key role in endosomal protein recycling (Hao et al. 2015). In this pathway, the MAGE-L2-TRIM27 complex adds K63-linked polyubiquitin chains onto WASH, activating it for endosomal actin assembly and protein recycling. USP7 deubiquitinates E3 ubiquitin ligase TRIM27, preventing its degradation, while also deubiquitinating WASH, inactivating it (Hao et al. 2015). Thus, USP7 plays a complex part in the fine-tuning of the pathway.

USP7 is involved in interactions with several viral proteins, such as EBNA1, ICP0, vIRF1, E1B-55K and HIV Tat (Z. Wang et al. 2019). In the case of EBNA1, a protein involved in activation of latent Epstein-Barr virus genomes, it is believed that the protein outcompetes p53 to bind to USP7, preventing apoptosis of infected cells (Saridakis et al. 2005). A similar

mechanism may be involved in the interaction of USP7 with vIRF1, a Kaposi sarcoma herpesvirus protein (Chavoshi et al. 2016). In both cases, inhibition of USP7 may decrease virulence of these viruses. Of particular interest is the interaction between USP7 and the HIV Tat protein, which is responsible for enhancing viral production after infection with Human Immunodeficiency Virus (HIV). USP7 deubiquitinates and stabilises Tat, leading to an increase in HIV production, while HIV infection stabilises USP7 (A. Ali et al. 2017), suggesting that small molecule inhibitors of USP7 may help suppress HIV viral production.

Several studies have reported that USP7 loss impairs cell cycle progression and cell proliferation (Giovinazzi et al. 2013; Reverdy et al. 2012), with multiple cell cycle proteins identified as USP7 substrates. One way in which USP7 impacts the cell cycle is by deubiquitinating histone demethylase PHF8, which in turn regulates expression of cyclin A2, an essential regulator of the cell division cycle (Q. Wang et al. 2016). PLK1, an early trigger for G2/M transition, was also found to interact with USP7 and be deubiquitinated and stabilised by it (Y. Peng et al. 2019). In contrast, USP7 inhibition destabilised PLK1, inducing cell cycle G2/M arrest and apoptosis. While such interactions have pushed USP7 to the forefront of potential cancer therapy targets, as its inhibition slows down cell proliferation, toxicity as a result of USP7 inhibition has been described. A recent study has suggested that this is caused by activation of CDK1 in response to USP7 inhibition, with USP7 involved in limiting CDK1 activity (Galarreta et al. 2021). Lowering CDK1 activity can therefore help circumvent this issue.

While the involvement of USP7 in cell cycle and proliferation make it an attractive target for research into novel cancer therapies, its contribution to other essential cellular processes, such as DNA damage repair, telomere maintenance, DNA replication (Valles et al. 2020) and the regulation of important pathways such as Wnt/β-catenin signalling (Ji et al. 2019) suggest that

impaired USP7 expression may have complex and extensive consequences in a non-cancer context. However, in comparison, relatively little research has been carried out into the role of USP7 outside of tumorigenesis and cancer progression. While previous Usp7 knockout studies have shown that USP7 is essential during embryonic development (N. Kon et al. 2010), for instance, its role in this process has not been fully elucidated.

1.4.2. USP7 loss of function in mice and human

Homozygous Usp7 knockout in mice leads to early embryonic lethality (N. Kon et al. 2010), in part due to impairment of the USP7/MDM2/p53 regulation pathway. As a p53 knockout in $Usp7^{-/-}$ only partially rescued the phenotype, it is likely that other pathways are affected by Usp7 knockout. Furthermore, conditional Usp7 knockout in the murine brain proved similarly lethal (N. Kon et al. 2011). No cases of USP7 homozygous-null mutations have ever been documented in humans (Fountain et al. 2019), likely due to early embryonic lethality, further emphasising the crucial role USP7 plays during development.

The newly named Hao-Fountain syndrome is caused by heterozygous USP7 mutations and has been first described in 2015 study. Hao et al identified seven individuals with intellectual disability, seizures and autism spectrum disorders who featured USP7 *de novo* heterozygous loss-of-function mutations (Hao et al. 2015). The same study suggested that the role of USP7 in the MAGE-L2-TRIM27/WASH pathway may explain the observed pathology, as the hypothalamus, where MAGE-L2 expression is enriched in the mouse brain, is implicated in multiple symptoms linked to USP7 and MAGE-L2 mutations, such as autism and Prader-Willi syndrome. However, this possible link has not yet been validated.

A second study provided additional information about the seven previously described cases, while also identifying an additional 16 (Fountain et al. 2019). Symptoms such as speech and

developmental delay, intellectual disability, autism spectrum disorders, eye anomalies, hypotonia and abnormal MRIs were observed in over half of the affected individuals. Out of the 15 individuals that underwent an MRI, 11 showed paucity of white matter as well as additional alterations to gross brain structure, such as a thinning of the corpus callosum, and abnormally shaped ventricular systems of the central nervous system. While these findings further support an essential role for USP7 in brain development, with even heterozygous USP7 mutations being detrimental to development, other organs, including the pancreas, remain seemingly unaffected.

1.4.3. Role of USP7 cancer and potential as therapy target

USP7 seems to be upregulated in many cancers, including some bladder, prostate, colon, liver, and lung cancers, while being downregulated in others, for example head and neck, breast and brain (Hussain, Zhang, and Galardy 2009). n-MYC, a known oncogene and driver of neuroblastoma tumorigenesis, is a substrate for USP7 (Tavana et al. 2016). USP7 deubiquitinates and stabilises n-MYC, with high USP7 levels in neuroblastoma patients being linked to poorer prognosis. Small molecule inhibition of USP7 in mice implanted with n-MYC amplified human neuroblastoma cell lines led to a significant reduction in neuroblastoma cell proliferation (Tavana et al. 2016), supporting the hypothesis that chemical inhibition of USP7 could be a workable strategy for future neuroblastoma therapies.

Another USP7 substrate, PTEN, is a tumour suppressor gene with phosphatase activity which inhibits tumour cell migration and proliferation. PTEN activation and its translocation to the nucleus is dependent on monoubiquitination, often at residues K289 or K13 (Trotman et al. 2007). USP7 can deubiquitinate PTEN, inactivating it and blocking its nuclear import (Morotti et al. 2014). This is an issue when USP7 expression is dysregulated like in the case of certain

cancers, such as chronic lymphocytic leukemia, as PTEN is prevented from reaching the nucleus and enacting its tumour-suppressing role (Carrà et al. 2017). Like in the case of neuroblastoma cells, USP7 inhibition arrests growth and induces apoptosis in chronic lymphocytic leukemia cells, this time by re-starting translocation of PTEN into the nucleus (Carrà et al. 2017).

In contrast, a 2006 study by Masuya et al found that in a cohort of 131 patients with non-small cell lung cancer, 45.0% of carcinomas showed decreased USP7 expression and 44.3% showed a reduction in p53 expression, with 71% of all carcinomas exhibiting one, the other, or both. Decreased expression of both proteins was a predictor for poor prognosis, suggesting that reduction in USP7 expression may promote tumorigenesis via a p53-dependent pathway (Masuya et al. 2006).

Finally, in the context of pancreatic ductal adenocarcinoma (PDAC), a particularly lethal type of cancer resistant to most existent therapies, chemical inhibition of USP7 slowed cell growth and induced apoptosis in some PDAC lines, while it had no significant effect in others, such as the PANC1 line (H. Chen et al. 2020). However, treatment with USP7 inhibitor P22077 did increase PANC1 sensitivity to doxycycline treatment, indicating that USP7 expression in some PDAC lines may help cells maintain chemoresistance. Furthermore, when USP7 expression in PANC1 was disrupted using CRISPR-Cas9 methods, cells showed slower growth and increased doxycycline sensitivity *in vitro*, while also generating significantly smaller tumours after implantation into nude mice (H. Chen et al. 2020). While these studies are encouraging, the contrasting effects of USP7 in different cancer types suggest that despite its low tissue specificity, its expression, regulation, function, and interactions may vary from tissue type to tissue type.

1.5. Aims of this thesis

In type 1 diabetes, patients' β-cells are destroyed by an autoimmune reaction, resulting in a lack of insulin secretion and high blood glucose levels. While symptoms can be kept under control with insulin injections, therapies that aim to help patients achieve insulin independence, such as islet transplantation, are still limited by the low supply of available islets, while iPSC-derived β-cells have not been able to achieve sufficient maturity to be a clinically viable option. Several studies have shown that overexpressing key transcription factors such as NGN3, PDX1 and MAFA in exocrine pancreatic cells can induce exocrine-to-endocrine transdifferentiation, resulting in β-cell generation. In particular, stabilisation of proendocrine transcription factor NGN3, whose expression during pancreatic development leads to the generation of all endocrine lineages in the organ, has been shown to stimulate exocrine-to-endocrine plasticity. A 2014 study by Sancho et al has shown that E3 ubiquitin ligase FBW7 ubiquitinates NGN3, targeting it for proteasomal degradation, and that FBW7 loss leads to NGN3 stabilisation, pushing a small number of cells to transdifferentiate to α, β and δ cells. However, the efficiency of this process is still under 1%, raising the question of whether there are other pathways involved in NGN3 regulation that could be targeted for further NGN3 stabilisation.

This thesis identifies new pathways involved in NGN3 regulations and investigates whether modulation of these pathways affects β cell generation. The main objectives were:

1. Identify and validate new regulators of NGN3 stability

2. Describe the mechanism through which these regulators interact and modulate NGN3 expression

3. Investigate the effect of these interactions on NGN3 stability and β cell generation in an iPSC 3D differentiation model.

The hypothesis of this study was that novel NGN3 interactors play a role in its regulation, thus impacting the differentiation of pancreatic endocrine cells. We identified E3 ubiquitin ligase HUWE1 and deubiquitinase USP7 as interactors of NGN3 from a mass-spectrometric analysis of NGN3 immunoprecipitation samples. To investigate the mechanisms of these interactions, we overexpressed NGN3 in HEK293A cells and assessed its ubiquitination status and stability in response to USP7 overexpression and HUWE1 inhibition. Finally, we inhibited HUWE1 and USP7 during iPSC-to-β-cell differentiation and analysed the effect of the inhibition on NGN3 expression and endocrine cell differentiation.

Chapter 2: Methods

2.1 Mouse lines

Mouse lines were generated by intercrossing $Usp7^{Flox/Flox}$ (N. Kon et al. 2011), Pdx1-Cre (Hingorani et al. 2003) and Rosa26-LSL-YFP (Srinivas et al. 2001) mice on a C57BL/6 background. All strains were genotyped by Transnetyx. All animal experiments were approved by the Francis Crick Institute Animal Ethics Committee and conformed to UK Home Office regulations under the Animals (Scientific Procedures) Act 1986 including Amendment Regulations 2012. The study is compliant with all relevant ethical regulations regarding animal research. With the exception of processing, cryosectioning and immunofluorescent staining of E14 mouse embryos, all animal work presented in this project was carried out by Dr Jessica Nelson, from the Behrens lab.

2.2 Cell culture

2.2.1 Expansion of cell lines

HEK293A (Thermofisher, R70507) and PANC1 cells (ATCC, CRL-1469) were grown in DMEM (Gibco, 61965026) with 10% foetal bovine serum (FBS, Sigma-Aldrich, F7524-500ml) and 1% penicillin/streptomycin. Cells were passaged weekly with TryplE (Gibco, 12604021). For experiments thar required inhibition of GSK3β or HUWE1, 24 h treatment with 10 μM CHIR99021 (Sigma Aldrich, SML1046) was used to inhibit GSK3β, while HUWE1 was inhibited with either 20 μM Heclin (Sigma Aldrich, SML1396) or 10 μM BI8622 (Generon, HY-120929) for 24 h.

The Kute-4 healthy iPSC line was kindly provided by the Human Induced Pluripotent Stem Cell Initiative (HipSci) (https://www.hipsci.org/). iPSC-derived pancreatic progenitors were

generated in the lab by Ana-Maria Cujba, using the STEMdiff™ Pancreatic Progenitor Kit (Stem Cell Technologies, 05120). The differentiation was done following manufacturer's instructions, with some modifications: cell seeding was 500,000 cells/well (in 12-well plates) and 42,000 cells/well (in black 96-well plates) and the first stage of differentiation was extended to three days, as also recommended by the manufacturer. iPSC-derived pancreatic progenitors were then cultured in Matrigel (Corning, 356230) domes as organoids, following the protocol previously established by Tuveson et al (Boj et al. 2015) (Table 1). Cells were passaged every 7-10 days by dissolving the Matrigel in TryplE (5 min, 37°C, on shaker). After organoid dissociation, organoids were resuspended in Matrigel and replated, with 10.5 µM Rho Kinase inhibitor Y-27632 (Sigma-Aldrich, Y0503-1MG) added to the media for the first two days of culture. Media was then changed every 2 days, without Y-27632.

Table 1. Culture media for iPSC-derived pancreatic progenitor organoids

Reagent	Concentration	Supplier	Catalogue no.
Advanced DMEM/F-12	0.78	ThermoFisher Scientific	12634010
1M HEPES	1X	ThermoFisher Scientific	15630049
Penicillin/Streptomycin	1X	Sigma Aldrich	P4458-100ml
GlutaMAX Supplement	1X	ThermoFisher Scientific	35050038
A83-01 (TGF Beta Inhibitor)	0.5 µM	Sigma Aldrich	SML0788-5MG
mEGF	0.05 µg/mL	Peprotech	AF-100-15-1000
FGF-10	0.1 µg/mL	Peprotech	100-26-500UG
Gastrin I	0.01 µM	Sigma Aldrich	SCP0151-1MG
mNoggin-conditioned media	10 %	Francis Crick Institute	-
N-acetylcysteine	1.25 mM	Sigma Aldrich	A9165-5G
Nicotinamide	10 mM	Sigma Aldrich	N0636-100G
B27 supplement	1X	ThermoFisher Scientific	17504-044
R-spondin-conditioned media	10%	Francis Crick Institute	-
Y-27632*	10.5 µM	Adooq Bioscience	A11001

*****Only added after splitting

2.2.2 Cell transfection

Transfection of HEK293A and PANC1 cells was carried out using the previously described Polyethylenimine (PEI) transfection protocol (Longo et al. 2013), adjusted for different plate formats and plasmid DNA concentrations. Briefly, cells were plated onto tissue culture dishes just below confluency and left to attach overnight. For transfection into a 10 cm dish, 10 µg of DNA were mixed with 250 µl of Optimem and incubated for 10 min. 30 µl of PEI were simultaneously incubated in another 250 µl of Optimem, then added to the DNA mix and further incubated at room temperature for 20 min, before being pipetted dropwise onto the tissue culture dish containing the previously plated cells.

2.2.3 Cycloheximide chase assay

HEK293A or PANC1 cells were seeded onto 12-well plates (250,000 cells/well). After 24h, cells were transfected with a total of 1 µg plasmid DNA and incubated for 48h. Cells were then treated with 100 µg/ml cycloheximide for 15, 30 or 60 min in the case of mNGN3 experiments, or 30, 60, 90 or 180 minutes in the case of hNGN3 experiments. Untreated controls were also kept. Cells were then washed with PBS, scraped off and processed for immunoblotting.

2.2.4 NGN3 transcriptional activity assay

To assess NGN3 transcriptional activity, HEK293A cells were transfected with HA-NGN3, alongside a pGL3[NeuroD1/GFP] plasmid vector able to induce GFP expression under the control of the NeuroD1 promoter (NGN3 target). The plasmid was generated in the lab by Dr Mario Alvarez, by cloning the NeuroD1 promoter into the pGL3 basic EGFP backbone (Addgene, 128053). After 48 h, cells were harvested, lysed, and processed for immunoblotting. Samples were run on a 4-20% Polyacrylamide precast gel (Biorad), transferred to a PVDF membrane and blotted for NGN3, GFP and Vinculin.

2.2.5 3D Russ pancreatic progenitor differentiation to β cells

Confluent Matrigel domes with Kute-4 iPSC-derived pancreatic organoids were detached intact from the plate and transferred to a 6-well plate (maximum 12 domes per well) for suspension culture. β-cell differentiation was then initiated from the pancreatic progenitor stage onwards using a previously described protocol (Russ et al. 2015) with the addition of adjustments made by Trott et al (Trott et al. 2017) (Table 2).

Table 2. Differentiation media for 3D Russ differentiation

Day	Reagent	Concentration	Supplier	Catalogue no.
1-2	DMEM (25 mM Glucose)	-	ThermoFisher Scientific	31966-021
	B27 50X	0.5X	ThermoFisher Scientific	A14867-01
	Retinoic acid	1 μM	Sigma Aldrich	R2625-100mg
	mEGF	50 ng/ml	Peprotech	AF-100-15-1000
3-4	DMEM (25 mM Glucose)	-	ThermoFisher Scientific	31966-021
	B27 50X	0.5X	ThermoFisher Scientific	A14867-01
	mEGF	50 ng/ml	Peprotech	AF-100-15-1000
	KGF	50 ng/ml	R&D Systems	251-KG-010
5-9	DMEM (25 mM Glucose)	-	ThermoFisher Scientific	31966-021
	B27 50X	0.5X	ThermoFisher Scientific	A14867-01
	LDN-193189	500 nM	Stemgent	04-0074
	TBP	30 nM	Millipore	565740-1MG
	ALKi II	1 μM	Axxora	ALX-270-445-M001
	KGF	25 ng/ml	R&D Systems	251-KG-010
10-20	DMEM (2.8 mM Glucose)	-	ThermoFisher Scientific	21885-025
	Glutamax 100X	1X	ThermoFisher Scientific	35050061
	NEAA 100X	1X	ThermoFisher Scientific	11140035

Domes were kept in suspension, on a shaker at 100 rpm for the duration of the differentiation, with daily media changes. Domes were treated with 20 μM Heclin for 24 h on differentiation

day 6 (D6) or 8 (D8) or remained untreated. For each timepoint (D0, 5, 7, 9, 12 and 16), one dome from each condition (untreated, early treatment, or late treatment) was harvested for RNA extraction, and another for cryosectioning and immunostaining.

2.2.6 3D Hogrebe pancreatic progenitor differentiation to β cells

Similarly to the 3D Russ differentiation protocol, Matrigel domes containing Kute-4 iPSC-derived pancreatic organoids were detached and transferred to suspension culture in a 6-well plate. Differentiation to β-cells was achieved by following the recently described protocol by Hogrebe et al (Hogrebe et al. 2020), with the media being changed daily (Table 3), and the domes kept in suspension, on a shaker at 100 rpm.

Domes were harvested at D5 for RNA extraction, after which 5 μM GNE6640 was added to the daily media for half of differentiating until D12 of the protocol. After D5, treated and untreated domes were harvested for mRNA extraction and immunostaining at D6, D9, D12 and D20. RNA extraction samples were frozen as pellets and kept at -80°C until the end of the differentiation, when all samples were processed at the same time. Domes reserved for immunostaining were fixed, equilibrated in 30% sucrose, encapsulated in OCT (ThermoFisher Scientific, 361603E), and stored at -80°C before cryosectioning.

Table 3. Differentiation media for 3D Hogrebe protocol

Day	Reagent	Concentration	Supplier	Catalogue no.
	MCDB 131 media	-	Corning	15-100-CV
1-4	Glucose	0.44 mg/ml	Sigma Aldrich	G7528
	Sodium bicarbonate	1.754 mg/ml	Sigma Aldrich	S5761
	BSA	20 mg/ml	Sigma Aldrich	A9647-100G
	ITS-X	5 µl	ThermoFisher Scientific	41400-045
	GlutaMAX	1X	ThermoFisher Scientific	35050061
	Vitamin C	0.044 µg/ml	Sigma Aldrich	A4544
	Penicillin/Streptomycin	1X	Sigma Aldrich	P4458-100ml
	KGF	50 ng/ml	R&D Systems	251-KG-010
	LDN193189	200 nM	Cambridge Bioscience	11802-1mg-CAY
	TPPB	500 nM	Tocris Bioscience	53431
	Retinoic acid	0.1 µM	Sigma Aldrich	R2625-100mg
	SANT1	0.25 µM	Sigma Aldrich	S4572-5MG
5-12	Glucose	3.6 mg/ml	Sigma Aldrich	G7528
	Sodium bicarbonate	1.754 mg/ml	Sigma Aldrich	S5761
	BSA	20 mg/ml	Sigma Aldrich	A9647-100G
	ITS-X	5 µl	ThermoFisher Scientific	41400-045
	GlutaMAX	1X	ThermoFisher Scientific	35050061
	Vitamin C	0.044 µg/ml	Sigma Aldrich	A4544
	Penicillin/Streptomycin	1X	Sigma Aldrich	P4458-100ml
	Heparin	10 µg/ml	Sigma Aldrich	H3149-100KU
	ALK5i II	10 µM	Enzo Life Sciences	ALX-270-445
	Betacellulin	20 ng/ml	R&D Systems	261-CE-050
	Retinoic acid	0.1 µM	Sigma Aldrich	R2625-100mg
	SANT1	0.25 µM	Sigma Aldrich	S4572-5MG
	T3	1 µM	Merck	64245-250MG-M
	XXI	1 µM	Merck	595790-1MG
	Latrunculin A*****	1 µM	Sigma Aldrich	L5163-100UG
13-20	Glucose	0.46 mg/ml	Sigma Aldrich	G7528
	BSA	20 mg/ml	Sigma Aldrich	A9647-100G
	GlutaMAX	1X	ThermoFisher Scientific	35050061
	Penicillin/Streptomycin	1X	Sigma Aldrich	P4458-100ml
	Heparin	10 µg/ml	Sigma Aldrich	H3149-100KU
	NEAA	1X	ThermoFisher Scientific	11140035
	ZnSO4	0.168 µg/ml	Merck	10883
	Trace Elements A	1 µ/ml	25-021-CI	Corning
	Trace Elements B	1 µl/ml	25-022-CI	Corning

* Only added on Day 5

2.3 Molecular biology techniques

2.3.1 RNA extraction

Samples were processed using the RNeasy mini kit (Qiagen, 74106) according to manufacturer's instructions. Pelleted samples were resuspended in 300 µL lysis buffer, and all samples were homogenised by being passed through syringes with 21-gauge needles. The RNA in each sample was quantified using the NanoDrop 2000 spectrophotometer (Thermo Fisher Scientific) and maintained at -80°C or used for complementary DNA (cDNA) preparation.

2.3.2 cDNA reverse transcription

cDNA was prepared from extracted RNA using the QuantiTect Reverse transcription kit (Qiagen, 205314) according to manufacturer's instructions. Generally, reactions of 300-1000 ng RNA were set up, keeping the quantity of RNA reverse transcribed the same for all samples within the same experiment. After cDNA reverse transcription, cDNA was diluted in nuclease-free water to a concentration of 10 ng/µl, then stored at -20°C.

2.3.3 Quantitative reverse transcription PCR (RT-qPCR)

Triplicate reactions were set up for each sample, each in a 10 µl volume, within a 384-well plate (Biorad, HSP3841 or Applied Biosystems, 4309849). For each reaction, 5 µl SYBRGreen Master Mix (ThermoFisher Scientific, 4385614), 1.75 µl of nuclease-free water and 1.25 µl of 2.5 µM forward and 2.5 µM reverse primer mix (1:1 ratio) (Table 4) were added to 15-20 ng of cDNA. Negative controls were also set up for each primer pair, replacing cDNA with 2 µl of nuclease-free water. The plate was sealed and centrifuged at 1000 g for 5 minutes, then loaded into either a CFX 384 Touch RT-qPCR machine (Bio-Rad), or a 7900HT Fast Real-Time PCR System (Applied Biosystems). Run conditions can be found in Table 5. For each

sample, triplicate Ct values were averaged and only samples with Ct values lower than the negative control were taken into account. The average Ct for each sample was then normalised by the average Ct of housekeeping gene Gapdh, yielding ΔCt. The relative expression for each gene of interest was then determined by calculating $2^{-\Delta Ct}$.

Table 4. Sequences of human RT-qPCR primers

Gene	Forward Primer (5' to 3')	Reverse Primer (5' to 3')
AMY2B	TCGCAAGTGGAATGGAGAG	GCTCTGTCAGAAGGCATGAA
CK19	GCCACTACTACACGACCATGG	CAAACTTGGTTCGGAAGTCAT
FBW7	GTTTGGTCAGCAGTCACAGG	TGATGTTGTCTCTCATTTGT
GAPDH	TTGCTTGTAGCCAAATTCGTTG	ATTGCCCTCAACGACCACTTT
GCG	TTCCCAGAAGAGGTCGCCATTGTT	CAACCAGTTTATAAAGTCCCTGGCGG
HUWE1	TCCTCGTGGGATTCGTTG	CTCTGGATCACTAACCCAC
INS	AGGCTTCTTCTACACACCCAAG	CACAATGCCACGCTTCTG
MAFA	GCTTCAGCAAGGAGGAGGTCAT	TCTGGAGTTGGCACTTCTCGCT
NEUROD1	GGTGCCTTGCTATTCTAAGACGC	GCAAAGCGTCTGAACGAAGGAG
NGN3	CTCGGACCCCATTCTCTCTT	CTTCTGGTCGCCAAGTTCA
NKX2-2	GGGACTTGGAGCTTGAGTCCT	GGCCTTCAGTACTCCCTGCA
NKX6-1	CACACGAGACCCACTTTTTC	CCGCCAAGTATTTTGTTTGT
PDX1	CACATCCCTGCCCTCCTAC	GAAGAGCCGGCTTCTCTAAAC
SST	GAGAATGATGCCCTGGAACCTGAAGA	ATTCTTGCAGCCAGCTTTGCGT
USP7	ACCCTCAGACGGACCAAAAT	TACACCATTTGCCATCCCCT

Table 5. Settings for RT-qPCR reactions.

Step	Cycles	Time (s)	Temperature (°C)
1	x1	180	95
2	x40	3	95
		25	60
3	x1	15	60
		-	60-95 (0.5°C step)

2.3.4 Immunoblotting

Cells were washed with PBS, pelleted, and lysed in 50 µl NP40 lysis buffer (containing 20 mM Tris pH 7.5, 150 mM NaCl, 1 mM EDTA, 0.2% IGEPAL, 10% Glycerol) supplemented with 0.1 M Sodium Fluoride (NEB, P0759), 10 mM Phenylmethylsulfonyl fluoride (Sigma-Aldrich,

PMSF-RO), 10 mM Orthovanadate (NEB, P0758) and Protease inhibitor cocktail (Sigma-Aldrich, P8340-5ML). Lysis was carried out on ice, for 15 minutes. Samples were then centrifuged at 13000 rpm, 4°C, for 5 minutes, the supernatant was isolated and the protein concentration in each sample quantified using a Bradford assay kit (BioRad, 5000006), with bovine serum albumin (BSA) standards. Lysate corresponding to 50 µg of protein was then added to 8 µl of 4x Laemli Buffer (Genetex, GTX16355) and made up to 32 µl with NP40 lysis buffer. Samples were boiled at 95°C for 10 min, then stored at -20°C.

Samples were resolved on homemade 10% SDS-PAGE gels (Table 6) alongside Colour Prestained Protein ladder (NEB, P7719S) for 1-1.5 h, at 120V, in 1x Tris/Glycine/SDS running buffer (BioRad, 1610732).

Table 6. Reagents and volumes necessary for 10 ml of 10% SDS-PAGE resolving gel and 2 ml of stacking gel

Reagent	Volume (for resolving gel)	Volume (for stacking gel)	Company	Catalogue no.
Water	4 ml	1.4 ml	-	-
30% Protogel	3.3 ml	0.33 ml	Geneflow	A2-0072
1.5M Tris HCL (pH 8.8)	2.5 ml	0.25 ml	Sigma Aldrich	10812846001
10% SDS	0.1 ml	0.02 ml	Sigma Aldrich	L3771
10% Ammonium persulfate	0.1 ml	0.02 ml	Sigma Aldrich	A3678-100G
TEMED	0.004 ml	0.002 ml	Sigma Aldrich	T9281

Gels were transferred to Trans-Blot Turbo Mini 0.2 µm PVDF Transfer Packs (BioRad, 1704156) using the Turbo Transfer system (BioRad), at 13V for 7 min. Membranes were blocked with 5% non-fat dry milk diluted in 1x TBS-Tween (TBS-T) buffer (Severn Biotech, 20-7310-10) for 1 h at room temperature (RT), then blotted with primary antibody diluted in blocking buffer (Table 7) for 1.5 h at RT, or overnight (O/N) at 4°C. Membranes were washed with 1x TBS-T buffer for 3 x 5 min, then blotted with HRP-conjugated secondary antibodies

(Table 7) diluted in blocking buffer for 1 h, at RT. No blotting with secondary antibodies was carried out in the case of HRP-conjugated primary antibodies. After 3 x 5 min washes with 1x TBS-T buffer, membranes were incubated with Clarity Western ECL Substrate kit reagents (BioRad, #1705061) for 3-5 min and developed in a ChemiDoc Touch imaging system (BioRad). All blotting and washing steps were carried out on a shaker.

Table 7. Primary and secondary antibodies used for immunoblotting.

Antibody	Species	Company	Catalogue no.	Dilution
Anti-GFP	rabbit	Cell Signalling	2956S	1:1000
Anti-HA-Tag	rabbit	Santa Cruz	sc-804	1:1000
Anti-HA-Tag	mouse	Cell Signalling	2367S	1:1000
Anti-HUWE1	rabbit	Atlas Antibodies	HPA002548	1:1000
Anti-MDM2	rabbit	GeneTex	GTX100531-S	1:1000
Anti-Mouse IgG (H+L)-HRP	goat	Jackson ImmunoResearch	115-035-146-JIR	1:5000
Anti-Myc-Tag	mouse	DSHB	9e10c	1:1000
Anti-NGN3	mouse	DSHB	F25A1B3	1:1000
Anti-p53	mouse	CellSignalling	2524S	1:1000
Anti-Rabbit IgG (H+L)-HRP	goat	Jackson ImmunoResearch	111-035-144-JIR	1:10000
Anti-USP7	rabbit	Abcam	ab4080	1:1000
Anti-Vinculin-HRP	mouse	Santa Cruz	SC-73614-HRP	1:1000
Anti-β-Catenin	mouse	BD Transduction Laboratories	610153	1:1000

Protein expression was calculated in ImageJ, by quantifying the mean gray value of protein expression bands, subtracting the background and normalising protein of interest bands by housekeeping protein Vinculin.

2.3.5 Immunoprecipitation

HEK293A cells were plated onto 10 cm tissue culture dishes (Corning) and transfected with a 1:3 DNA:PEI ratio. After 24-48h, samples were treated with 1 µM proteasomal inhibitor MG132 (Alfa Aesar, J63250.MA) for 6h. Samples were then centrifuged at 13000 rpm, 4°C, for 5 minutes, the supernatant was isolated and the protein concentration in each sample quantified using a Bradford assay kit (Biorad, 5000006), with bovine serum albumin (BSA) standards. Input control samples were processed as previously described in the immunoblotting protocol, with lysate (50 µg of protein) being boiled in 1x Laemli Buffer, at 95°C for 10 min, then stored at -20°C. For immunoprecipitation, a lysate volume corresponding to roughly 1 mg of protein was made up to 500 µl with lysis buffer and incubated with 25 µl of washed Pierce™ Anti-HA Magnetic Beads (ThermoFisher Scientific, 88837) or 50 µl of anti-FLAG-Magnetic beads (Sigma-Aldrich, M8823-1ml) on a vertical shaker, O/N, at 4°C. The beads were washed 5 times with lysis buffer, then resuspended in 1x Laemli Buffer in NP-40 buffer and boiled at 95°C for 10 min.

Both input control and immunoprecipitated samples were resolved on homemade 10% SDS-PAGE gels, or 4–20% Mini-PROTEAN® TGX^{TM} Precast Protein Gels (BioRad, 4561096) in the case of NGN3/HUWE1 immunoprecipitation experiments, for 1-1.5 h, at 120V. Gels were transferred to Trans-Blot Turbo Mini 0.2 µm PVDF Transfer Packs (BioRad, 1704156) using the Turbo Transfer system (BioRad), at 13V for 7 min. For NGN3/HUWE1 immunoprecipitation experiments, the top part of the gel, containing HUWE1, was cut and transferred separately, for 10 min at 13V, followed by incubation of the transfer cassette at 4°C for 10 minutes, and another 10 min transfer at 13V. The lower section of the gel was transferred as normal. The membranes were then processed as described in the Immunoblotting section.

The relative amount of co-immunoprecipitated protein was quantified in ImageJ, by subtracting the background from the mean gray value of each band, then normalising the resulting mean grey value of the output co-immunoprecipitated protein band by the resulting mean grey value of the immunoprecipitated NGN3 band in the same sample.

2.3.6 Ubiquitination assay

HEK293A cells were plated into 10 cm tissue culture dishes (Corning) at a seeding density of 2.5-3 x 10^6 cells/dish. After 24h, for HUWE1 inhibition assays, cells were transfected with 2.5 µg HA-NGN3 plasmid DNA and 2.5 µg ubiquitin (Ub-His) plasmid DNA, with a 1:3 DNA:PEI transfection mix. An empty pcDNA3 vector was used for co-transfection with either Ub-His or NGN3, as a control. 24 h post-transfection, half of NGN3/Ub-His co-transfected cells were treated with 20 µM Heclin or 10 µM BI8622. After 18 h, all samples were treated with 1 µM proteasomal inhibitor MG132 (Alfa Aesar, J63250.MA) for a further 6h, then cells were harvested, lysed, and processed for immunoprecipitation, as previously described. For immunoprecipitation, 350 µg of protein from each sample were made up to 500 µl and incubated with 10 µl of washed anti-ubiquitin TUBE 2 beads (LifeSensors, UM402). After incubating for 2.5 h at RT on a vertical shaker, beads were washed as per manufacturer's protocol. Both input controls and immunoprecipitation samples were then boiled and resolved on a 10% SDS-PAGE gel, as described in the Immunoblotting section.

For USP7 overexpression assays, cells were transfected with 2.5 µg HA-NGN3 plasmid DNA, 3.5 µg Ub-His (wildtype, K48R or K63R) plasmid DNA and 2.5 µg Flag-USP7 or Flag-USP7^{C223A}. In the case of USP7 titration experiments, varying amounts of Flag-USP7 plasmid DNA were used for transfection, from 0.5 to 2.5 µg. Empty pcDNA3 vector was used to make up the total amount of DNA added to each sample to 10 µg. After 42 h, cells were treated with

1 µM MG132 for 6 h, then harvested, lysed and the amount of protein quantified. For immunoprecipitation, 350 µg of protein from each sample were made up to 500 µl with lysis buffer and incubated with 14 µl of washed TUBE2 magnetic beads (LifeSensors, UM402M) for 2.5 h at RT, on a vertical shaker. Beads were then washed as per manufacturer's instructions and samples were processed for immunoblotting as previously described, alongside input controls.

2.3.7 DNA cloning

HA-NGN3 mutants (S14A, S38A, S160A, S174A and S199A) and the Flag-USP7^{C223A} mutant were generated through site-directed mutagenesis PCR, from the original pcDNA3.HA-NGN3 vector and pcDNA.FLAG-USP7 vector respectively (Table 8).

Table 8. Sequences of forward (F) and reverse (R) primers used for cloning.

Primer	Sequence (5' to 3')
NGN3-S199A F	AGGTGCCCAGCGCCCCATCC
NGN3-S199A R	GGATGGGGCGCTGGGCACCT
NGN3-S174A F	GCTCTATCTACGCCCCAGTCTCCCAA
NGN3-S174A R	TTGGGAGACTGGGGCGTAGATAGAGC
NGN3-S160A F	GAGCTGGGGGCCCCCGGAGG
NGN3-S160A R	CCTCCGGGGGCCCCCAGCTC
NGN3-S38A F	CCCCACCTGCCCCCACTCTC
NGN3-S38A R	GAGAGTGGGGGCAGGTGGGG
NGN3-S14A F	CCATCCAAGTGGCCCCAGAGACACAAC
NGN3-S14A R	GTTGTGTCTCTGGGGCCACTTGGATGG
BamHI-hNGN3	ATTAAGGATCCATGACGCCTCAACCCTCG
hNGN3-XbaI	GCGGATCTAGATCACAGAAAATCTGAGAAAGC
hNGN3-S199F F	GGCCACCTTTTCCGCCTGCTTG
hNGN3-S199F R	CCGGTGGAAAAGGCGGACGAAC
USP7-C223A F	AGGGAGCGACTGCTTACATGAACAG
USP7-C223A R	GTCCCTCGCTGACGAATGTACTTGT

The human version of the pcDNA3.HA-NGN3 plasmid was generated by amplifying the hNGN3 sequence from the Hygro-iNGN3 plasmid (Addgene, 75340), adding BamHI and XbaI

cutting sites at the 5' end and 3' end respectively (Table 8). Both the pcDNA3.HA-NGN3 backbone, and the PCR-amplified insert were then digested with BamHI (NEB #R0136) and XbaI (NEB #R0145), according to NEB instructions, excising the mouse NGN3 sequence from the backbone. Samples were then purified from a 1.5% agarose gel using the Monarch DNA Gel Extraction Kit (NEB, #T1020) and the pcDNA.HA backbone was ligated to the hNGN3 insert according to the T4 ligase NEB protocol. The pcDNA3.HA-hNGN3-S199F mutant plasmid was generated through site-directed mutagenesis, with pcDNA3.HA-hNGN3 as a template. Plasmids were expanded in One Shot® TOP10 competent cells and successful introduction of desired mutations or inserts was validated through sequencing by Source Bioscience. All PCR reactions were set up using the Q5® High-Fidelity PCR Kit (NEB, E0555), following manufacturer's instructions.

The USP7-Flag, Ub-K48R-His and Ub-K63R-His constructs were kindly provided by the Behrens Lab, at the Institute of Cancer Research.

2.3.8 Bacterial transformation and plasmid preparation

One Shot® TOP10 competent cells were thawed and incubated with plasmid DNA for 15 min on ice, then heated to 42°C for 90 s and cooled for a further 2 min on ice. 1000 µl liquid broth (LB) media without antibiotics were added to the cells, and the sample was incubated at 37°C for an hour. Cells were pelleted, resuspended in 50 µl LB and spread onto 1:1000 Ampicillin agar plates, which were then incubated at 37°C O/N.

Colonies were then picked, expanded in LB with 1:1000 Ampicillin O/N at 37°C, and mini-prepped using the Monarch® Plasmid Miniprep Kit (NEB, #T1010), or midi-prepped with the QIAGEN® Plasmid MIDI Kit (Qiagen, 12145). DNA quantification was carried out on a NanoDrop 2000 spectrophotometer (Thermo Fisher Scientific).

2.3 Histology and imaging

2.3.1 Immunofluorescent staining of cell monolayers

For immunofluorescent imaging, cells were plated onto µClear PS F-bottom 96 well plates (Greiner, 655090) at a seeding density of 25,000 cells/well. After transfection and/or treatment, cells were washed with PBS and fixed for 20 min in 4% paraformaldehyde (PFA) at RT, then further washed for 3 x 5 min with PBS. Cells were permeabilised with 0.3% Triton-X (Sigma Aldrich, T8787) in PBS for 5 min at RT, then blocked for 1 h, covered, on the shaker, at RT, in 5% donkey serum in PBS. After blocking, primary antibodies (Table 9) diluted in blocking buffer were added onto the cells and left to incubate O/N at 4°C, in the dark.

Cells were then washed 3 x 5 min with PBS and incubated with secondary antibodies (Table 10) diluted in PBS and 2.5 µg/ml DAPI for 1 h, at RT, covered. After 3 x 5 min washes in PBS, cells were imaged with a Leica SP8 Confocal microscope.

Table 9. Primary antibodies used for immunofluorescent staining.

Antibody	Species	Company	Catalogue no.	Dilution
Anti-CK19	rat	DSHB	TROMAIII	1:200
Anti-glucagon	mouse	Sigma	G2654-100UL	1:200
Anti-HUWE1	rabbit	Atlas Antibodies	HPA002548	1:200
Anti-insulin	guinea pig	Dako	A0564	1:300
Anti-NGN3	mouse	DSHB	F25A1B3	1:100
Anti-NGN3	sheep	R&D	AF3444	1:50
Anti-PDX1	rabbit	Cell Signalling	5679	1:200
Anti-PDX1	guinea pig	abcam	ab47308	1:200
Anti-somatostatin	rabbit	Dako	A0566	1:300
Anti-USP7	rabbit	Abcam	ab4080	1:200
Anti-α amylase	rabbit	Sigma	A8273	1:200

Table 10. Secondary antibodies used for immunofluorescent staining.

Antibody	Company	Catalogue no.	Dilution
Donkey anti-Rat 647	Jackson ImmunoResearch	712-605-150-JIR	1:500
Donkey anti-Rabbit 488	Jackson ImmunoResearch	711-545-152-JIR	1:500
Donkey anti-Mouse RR-X	Jackson ImmunoResearch	715-295-151-JIR	1:500
Donkey anti-Mouse 488	Jackson ImmunoResearch	715-545-151-JIR	1:500
Donkey anti Rabbit RR-X	Jackson ImmunoResearch	711-295-152-JIR	1:500
Donkey anti-Mouse 647	Jackson ImmunoResearch	715-605-151-JIR	1:500
Donkey anti-Rabbit 647	Jackson ImmunoResearch	711-605-152-JIR	1:500
Goat anti-Guinea Pig RR-X	Jackson ImmunoResearch	706-295-148-JIR	1:500
Goat anti-Guinea Pig 647	Jackson ImmunoResearch	706-605-148-JIR	1:500
Donkey anti Sheep RR-X	Jackson ImmunoResearch	713-295-147-JIR	1:500

2.4.2 Immunofluorescent staining of Matrigel dome sections

Pancreatic organoid domes collected throughout the differentiation (Russ and Hogrebe protocols) were fixed in 4% PFA for 20 min at RT, washed for 3 x 10 min with PBS and equilibrated in 30% sucrose in PBS, O/N at 4°C. Domes were then embedded into OCT (ThermoFisher Scientific, 361603E) and cryosectioned into 10 µm-thick frozen sections, which were then permeabilised, blocked and stained (Table 9,10) as previously described for immunofluorescent staining of cell monolayers. Slides were washed 3 times with PBS, mounted with ProLong™ Gold Antifade Mountant (ThermoFisher Scientific, P36934) and imaged on a Leica SP8 confocal microscope.

2.4.3 Immunofluorescent staining of E14 mouse embryo sections

E14 wildtype and Pdx1-Cre; Usp7-/- mouse embryos were generously provided by the Behrens Lab, at the Institute of Cancer Research. Embryos were fixed in 4% paraformaldehyde (PFA) at 4°C, O/N, on a shaker, washed for 3 x 10 min in PBS, equilibrated in 20% sucrose for 24h at 4°C, and embedded into OCT. The blocks were then sectioned longitudinally, and frozen sections (10 µm thickness) containing the embryonic pancreas were collected.

Section slides underwent heat-mediated antigen retrieval in 10 mM sodium citrate buffer (pH 6.2). The buffer was pre-warmed in a microwave until gently bubbling before slides were submerged and heated for 5 minutes in the microwave on 50% power. Slides were then allowed to sit in the buffer to cool for 30 min, followed by 3 x 5 min washes in PBS and permeabilization in 0.03% Triton X-100 for 5 min. After another set of 3 x 5 min washes in PBS, slides were blocked for 1h at RT in PBS with 10% foetal bovine serum (FBS), 3% bovine serum albumin (BSA), 0,05% Triton X-100, 0,05% Tween 20 and 0.25% fish gelatin. The sections were then stained with primary antibodies (Table 9) diluted in blocking buffer, in the dark, at 4°C, O/N, washed in PBS, then stained with secondary antibodies (Table 10) and DAPI (2.5 µg/ml) diluted in PBS, in the dark, for 1 h at RT. Slides were washed 3 times with PBS, mounted with ProLong™ Gold Antifade Mountant (ThermoFisher Scientific, P36934) and imaged on a Leica SP8 confocal microscope.

2.4.4 Image analysis

Image analysis was carried out in ImageJ, with cells counted manually using the Cell Counter function. For images of Matrigel dome sections, the percentage of NGN3+, INS+, GCG+ and SST+ cells was calculated, out of total cell numbers within the same frame, with at least 7 frames quantified for each sample.

For images of E14 mouse embryo sections, the proportion of endocrine progenitor cells within the pancreas was assessed by calculating the percentage of NGN3+ cells out of all pancreatic cells in the frame, delineated by PDX1 expression. For each embryo, 5 different frames were quantified.

2.4.5 Haematoxylin and eosin staining of tissue sections

Slides with frozen E14 mouse embryo sections were incubated in Haematoxylin for 1 min to stain the cell nuclei, then washed under running tap water before immersion into 1% acid alcohol for 5 s, to remove cytoplasmic staining. Slides were then left to wash under running water for 2 min for bluing, followed by a 20 s incubation in 1% Eosin, prompt rinsing with cold water and dehydration in 70% ethanol for 3-5 s. The sections then underwent two sequential 1 min incubations in absolute ethanol and two sequential 2 min incubations in xylene. Slides were mounted with ProLong™ Gold Antifade Mountant (ThermoFisher Scientific, P36934) and scanned on a Nanozoomer 2.0RS slide scanner (Hamamatsu).

2.5 Bioinformatics techniques

2.5.1 scRNA-seq dataset analysis

The human foetal pancreas dataset was initially published by Yu et al (Yu et al. 2021) and accessed from OMIX (https://bigd.big.ac.cn/omix/; identifier OMIX236). Dataset processing was carried out in R by Cristina Garrone, a PhD student in our lab, using the Seurat package: cells were subset based on the percentage of mitochondrial genes (<15%) and feature counts (>500, <4000), data was normalised using the SCTransform() function with a Gamma-Poisson Generalized Linear Model and the top 3000 variable genes were selected. Dimensionality reduction was performed via Principal-component analysis (PCA) and cells were clustered with the FindClusters() function, with a resolution of 0.2. The FindMarkers() function was used to analyse differential gene expression and the top differentially expressed genes were used to determine identity of each cluster. Epithelial cell clusters were then subset, re-clustered at a resolution of 0.5, and labelled according to the top differentially expressed genes.

2.5.2 Filtering of mass spectrometry hits

HEK293A cells were transfected with either the HA-NGN3 construct (pcDNA3.HA-NGN3) or an empty pcDNA3 control vector and immunoprecipitation of the HA-tag was carried out. Duplicate HA-NGN3 immunoprecipitated samples, alongside a pcDNA3 control, were then sent for Mass Spectrometry analysis at the Centre of Excellence for Mass Spectrometry, within King's College London. The resulting list of hits was filtered with the help of Scaffold Viewer software, at 95% protein threshold, 1 minimum peptide and 95% peptide threshold. A hit was deemed a potential interactor of NGN3 if it appeared in the HA-NGN3 transfected samples at a Protein Identification Probability higher than 0%, but not in the empty pcDNA3 transfected control.

2.6 Statistical analysis

Statistical analysis was carried out on all experiments with at least three biological replicates. All graphs show mean values per group, with error bars representing the standard error of the mean (S.E.M). Unpaired Two-tailed Student's t-test and one-way Analysis Of Variance (ANOVA) statistical tests were performed accordingly for comparison between groups and are described in each figure legend, alongside corresponding P-values and sample sizes. Within datasets analysed by ANOVA, multiple comparisons between a control group (wildtype or untreated, as mentioned in figure legends) and each of the other groups were done using Dunnett's correction, unless otherwise specified.

Chapter 3: Multiple interactors may contribute to Ngn3 post-translational regulation

3.1 Introduction

NGN3 is a transcription factor whose transient expression during pancreatic development is essential for the generation of the endocrine pancreatic compartment. Its importance is emphasised by *in vivo* studies in mice and pigs, in which loss of NGN3 in the embryonic pancreas leads to an absence of islets and a diabetic phenotype post-partum (Gradwohl et al. 2000; Sheets et al. 2018). Moreover, null NGN3 mutations in humans have been shown to cause neonatal diabetes, while less severe mutations can still lead to the onset of diabetes during childhood (Pinney et al. 2011; Rubio-Cabezas et al. 2011; Sayar et al. 2013). NGN3 overexpression, alongside other transcription factors such as PDX1 and MAFA, has been shown to induce exocrine-to-endocrine transdifferentiation in acinar and ductal pancreatic cells (Zhou et al. 2008; Demcollari, Cujba, and Sancho 2017). Moreover, currently available protocols aiming to differentiate embryonic stem cells (ESCs) or iPSCs towards β cells consistently include steps that recapitulate embryonic NGN3 expression patterns during the differentiation process (Hogrebe et al. 2020; Russ et al. 2015; Trott et al. 2017). Therefore, the ability of NGN3 to act as a driver for pancreatic cell fate plasticity and its essential role in β cell differentiation points at it as a potential target to improve *in vitro* and *in situ* β cell generation protocols.

One way to indirectly modulate NGN3 expression is to take advantage of pathways that play a role in its post-translational regulation. NGN3 undergoes phosphorylation at multiple sites, some of which are known to target it for ubiquitination and degradation through the ubiquitin-proteasome system. For instance, FBW7, an E3 ubiquitin ligase, recognises NGN3

phosphorylated at the S183 residue by kinase GSK3β and facilitates its ubiquitination and degradation (Sancho et al. 2014). In turn, FBW7 loss stabilises NGN3 and induces ductal-to-endocrine cell transdifferentiation (Sancho et al. 2014), an outcome similar to that of direct NGN3 overexpression. However, efficiency of transdifferentiation as a result of FBW7 loss is still relatively low. Identifying additional pathways that play a role in the regulation of NGN3 could open new avenues for the optimisation of endocrine cell generation protocols, either as a result of exocrine-to-endocrine plasticity, or of iPSC-to-β-cell differentiation. Moreover, a more detailed investigation of NGN3 post-translational modifications, in particular phosphorylation, and how it affects protein stability and function, could provide insight into the complex mechanisms involved in NGN3 regulation and function during pancreatic development. Therefore, we set out to analyse the effect of individual Ser-Pro motif phosphorylation sites on the mouse NGN3 protein, mutating them one by one and assessing the ability of the protein to induce gene expression of NGN3 downstream targets, as well as cellular localisation of the protein and changes to its molecular weight. One of the generated mutants, NGN3-S199A, exhibited markedly different characteristics to the wildtype protein, prompting us to investigate it further in the context of the human NGN3 protein, particularly as this site had been linked to T2D progression (Jackson et al. 2004; J. Li et al. 2008).

To uncover new NGN3 regulatory pathways, we carried out an immunoprecipitation-mass spectrometry (IP-MS) assay in which we pulled down HA-tagged NGN3 and analysed its co-immunoprecipitated interactors. In particular, we focused on possible interactors with known functions in the ubiquitin-proteasome system, such as HUWE1 and USP7. We further validated these interactions through immunoprecipitation of HA-NGN3, followed by immunoblotting. Finally, as these experiments were carried out in a HEK293A NGN3 overexpression model, we analysed a publicly available single cell RNAseq (scRNAseq) dataset containing gene

expression data from different developmental timepoints of the human foetal pancreas, to assess the expression pattern of HUWE1 and USP7 during the NGN3 expression window.

3.2 Generation and characterisation of NGN3 phosphomutant plasmid constructs

Murine NGN3 contains several serine and threonine amino acid residues that could be targeted for phosphorylation. Concurrent mutation of six of these serines, S14, S38, S160, S174, S183, and S199 was shown to stabilise NGN3 (Azzarelli et al. 2017). However, as the individual role of each site in NGN3 post-translational regulation has not been previously investigated, with the exception of S183 (Sancho et al. 2014), it is not yet known which of these sites contribute to this stabilisation. Therefore, we generated single-mutant NGN3 constructs based on the wildtype pcDNA3.HA-mNGN3 plasmid vector through site-directed mutagenesis PCR (Fig. 11A). Despite not being part of a Ser-Pro motif site, S187 has been shown to be a phosphorylation site for NGN3 (Sancho et al. 2014). Therefore, an NGN3-S187A phosphomutant construct was also included in further experiments, alongside the NGN3-2SA (mutations at S183/S187) and NGN3-6SA mutants. In addition to plasmid sequencing, the plasmids were validated by transfection into HEK293A cells which then underwent fixation and staining for NGN3. All samples showed distinct NGN3 signal except for the untransfected control, indicating that all mutant plasmids could successfully induce NGN3 expression (Fig. 11B). Interestingly, although NGN3 expression is generally nuclear, some cytoplasmic expression could be observed in all mutants, as well as in the wildtype (WT) NGN3 transfected sample. This is likely due to the high levels of exogenous NGN3 protein in the HEK293A overexpression system, as it is not routinely observed in endocrine progenitors during pancreatic development.

As NGN3 can promote its own transcriptional activation, we set out to investigate whether phosphorylation at any of the mutated sites is required for NGN3 transcriptional activity. We overexpressed each mutant in HEK293A cells and analysed their ability to activate the transcription of the known NGN3 downstream target NKX2.2. Additionally, a previously described transcriptionally inactive NGN3 mutant, NGN3-T120A, was also tested, as a negative control. After normalisation to housekeeping gene GAPDH, NKX2.2 gene expression was significantly increased by NGN3 WT overexpression (Fig. 11C) compared to both the non-transfected (NT) control ($p=0.0004$) and the sample transfected with the NGN3-T120 transcriptionally inactive mutant ($p=0.0002$). Moreover, NKX2.2 expression was significantly lower in samples transfected with the NGN3-S160A ($p=0.0195$), NGN3-2SA ($p=0.0277$) or NGN3-6SA ($p=0.0084$) mutants compared to NGN3 WT, suggesting that some phosphorylation events may promote NGN3 transcriptional activity. Interestingly, despite the fact that NGN3-2SA appears to be less transcriptionally active than NGN3 WT, the NGN3-S183A and NGN3-S187A single mutants do not appear to show a similar trend. As these are the two sites mutated within the NGN3-2SA construct, this could indicate that aside from phosphorylation events at a particular site (e.g. S160), a lower level of overall protein phosphorylation could also impair NGN3 transcriptional activity.

Although residues S14, S38, S160, S174, S183 and S199 are all part of Ser-Pro motifs within the mouse NGN3 protein, and therefore predicted phosphorylation sites, whether or not they are actually phosphorylated has not yet been determined. To further analyse the phosphorylation status of these mutants, we expressed each construct in HEK293A cells and investigated protein weight through immunoblotting (Fig. 11D).

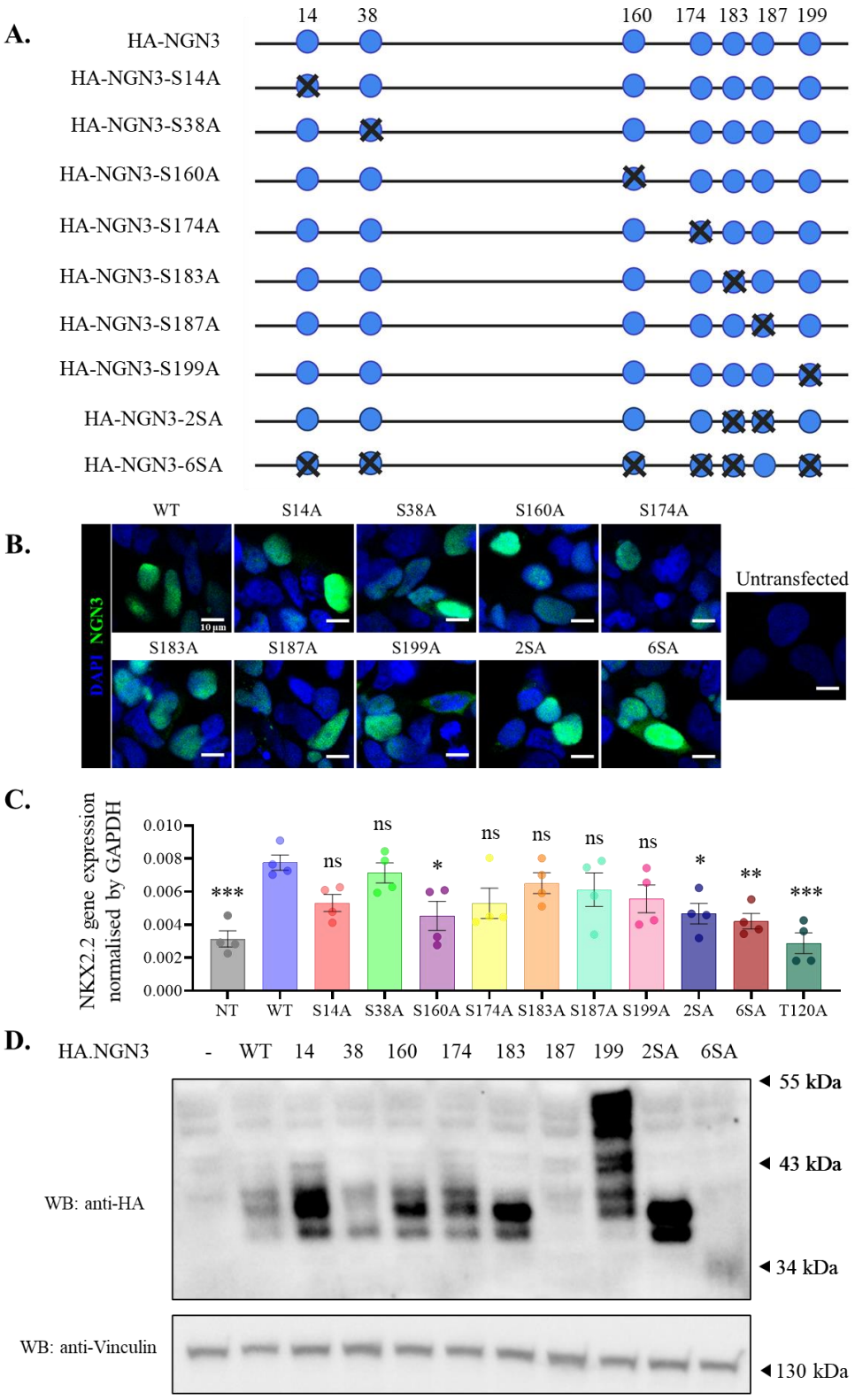

Figure 11. Generation and validation of single-site NGN3 phosphorylation mutants. A) Map of phosphorylation sites on newly generated single-site NGN3 phosphomutants, alongside the NGN3-6SA and NGN3-2SA mutants. B) Immunofluorescent staining of exogenous WT or mutant NGN3 (green) after transfection into HEK293A cells. C) Gene expression of Nkx2.2 normalised by Gapdh in HEK293A cells transfected with either wildtype of mutant NGN3. Error Bars = S.E.M, n=4, * $p<0.05$, ** $p<0.01$, *** $p<0.001$, Ordinary One-Way ANOVA, Dunnett's Multiple Comparisons Test against NGN3 WT sample. D) Immunoblot of NGN3 WT alongside newly generated mutants.

Wildtype NGN3 protein runs at 36 kDa, with two additional higher bands between 36-43 kDa as a result of phosphorylation. Complete or partial depletion of the higher of the two phosphorylation bands is observed in the NGN3-S183A and NGN3-S160S mutants, respectively. This is indicative of a decrease in phosphorylation levels due to their impaired phosphorylation site. However, none of the other single mutants show these modifications. It is likely that the lack of a phosphorylation event at a single site will not alter the molecular weight and charge of the protein by a sufficient amount to result in a visible difference in an immunoblotting assay. In the case of NGN3-S183A, previous research has shown that phosphorylation at this site can trigger additional phosphorylation events at other sites within the NGN3 protein (Krentz et al. 2017). This suggests that impairment of this site may result in the loss of multiple phosphorylation events at other sites, leading to the noticeably lower molecular weight. The partial depletion of the top NGN3-S160A band compared to the bands that correspond to less phosphorylated protein forms suggests that impairment of the S160 site could similarly affect total NGN3 phosphorylation levels, albeit to a less severe degree than impairment of S183.

Surprisingly, mutation of the S199 site seems to lead to a major alteration in NGN3 molecular weight, with additional bands detected at around 43 kDa, 50 kDa and above 55 kDa. When we inhibited protein synthesis in cells overexpressing either NGN3 WT or NGN3-S199A (Fig. 12A), NGN3 WT protein expression half-life was around 15 minutes, in line with previous reports (Sancho et al. 2014). However, in the case of the S199A mutant, while the band corresponding to the normal molecular weight of NGN3 WT did not show improved stability ($p = 0.0644$ at 15 mins and $p = 0.2147$), the upper expression bands were significantly more stable than wildtype NGN3 at the 15 min ($p=0.0064$) and 30 min ($p=0.0013$) timepoints, with protein levels even slightly rising throughout the experiment (Fig. 12B). As protein synthesis was inhibited, the source of the rise is likely due to the normal molecular weight NGN3 protein

already in the cell being modified, leading to an increase in its molecular weight. This may suggest that the S199A mutant starts out at a similar molecular weight as WT NGN3, but that unlike WT NGN3, it undergoes post-translational modifications that lead to an increase in molecular weight, impaired degradation, and accumulation in the cell.

To our knowledge, this phenomenon has not been previously described, as the role of the S199 site in mouse NGN3 function and regulation has not been extensively studied. While in the murine protein the S199 residue is part of a Ser-Pro motif, this is not the case for the human protein. In humans, NGN3 contains either a serine or a phenylalanine residue at position 199, with allele responsible for the Phe being present in 57% of the global population, compared to 43% for the Ser allele (Auton et al. 2015). The Phe residue is more common at position 199 in African, East Asian and South Asian populations, while the Ser allele is the majority allele in European and American populations (Auton et al. 2015). Although multiple studies have investigated the effect of this polymorphism on diseases such as T1D and T2D, their findings have varied. On its own, S199F has not been identified as a major indicator of predisposition to T1D or T2D in Danish or Japanese cohorts (J N Jensen et al. 2001; Okada et al. 2001). However, it may contribute to an increase in fasting blood glucose levels, 2-hour blood glucose levels and T2D risk when coupled with additional risk alleles in genes such as NEUROD1 and HNF1A (Jackson et al. 2004). Moreover, in a cohort of T2D patients, S199F was linked to increased proinsulin levels and disease progression (J. Li et al. 2008). An association between S199F and hyperglycaemia was also identified in a cohort of patients with ketosis-prone diabetes, a phenotypically defined type of diabetes common in male patients of West African ancestry (Louet et al. 2008). The same study showed that the S199F mutation did not majorly affect NGN3 transcriptional activity, indicating that a different mechanism might be responsible for the observed link between the polymorphism and hyperglycaemia in these patients. This fact, coupled with the noticeable change in molecular weight of mouse NGN3

after introduction of the S199A mutation, raises the question of whether dysregulated NGN3 post-translational modifications in the S199F variant could be responsible for the observed phenotypes.

To investigate this, we generated a human NGN3 plasmid vector (pcDNA3.HA-hNGN3) as well as a plasmid containing the sequence for the NGN3-S199F mutant (pcDNA3.HA-NGN3-S199F) and performed preliminary immunoblotting experiments to assess their stability, molecular weight, and transcriptional activity. Surprisingly, the human NGN3-S199F mutant does not show a similar molecular weight pattern to the murine NGN3-S199A (Fig. 12C). Instead, it can be observed as a single band, at the same height as wildtype hNGN3. An additional higher band found below 43 kDa in the wildtype hNGN3 is absent in the S199F mutant, suggesting that in humans, this polymorphism may generate an NGN3 phosphomutant. In a cycloheximide chase experiment, both the wildtype hNGN3 and the hNGN3-S199F mutant appear to be relatively stable, with slightly increased stability observed in the mutant (Fig. 12D,E).

To determine whether the S199F mutant is transcriptionally active, we overexpressed either NGN3 WT or NGN3-S199F in HEK293A cells, alongside a pGL3 vector that induces EGFP expression under the control of the NeuroD1 promoter. Both NGN3 WT and NGN3-S199F were able to induce EGFP expression (Fig. 12F), with EGFP protein levels being over four times higher in the S199F transfected cells (Fig. 12G). This could indicate that the S199F form of the protein has enhanced transcriptional activity. To definitively assess whether the differences identified between the two protein forms are significant, further repeats of these experiments will need to be performed. However, these preliminary results are promising, as they may help inform future research into the effect of this polymorphism on T2D progression.

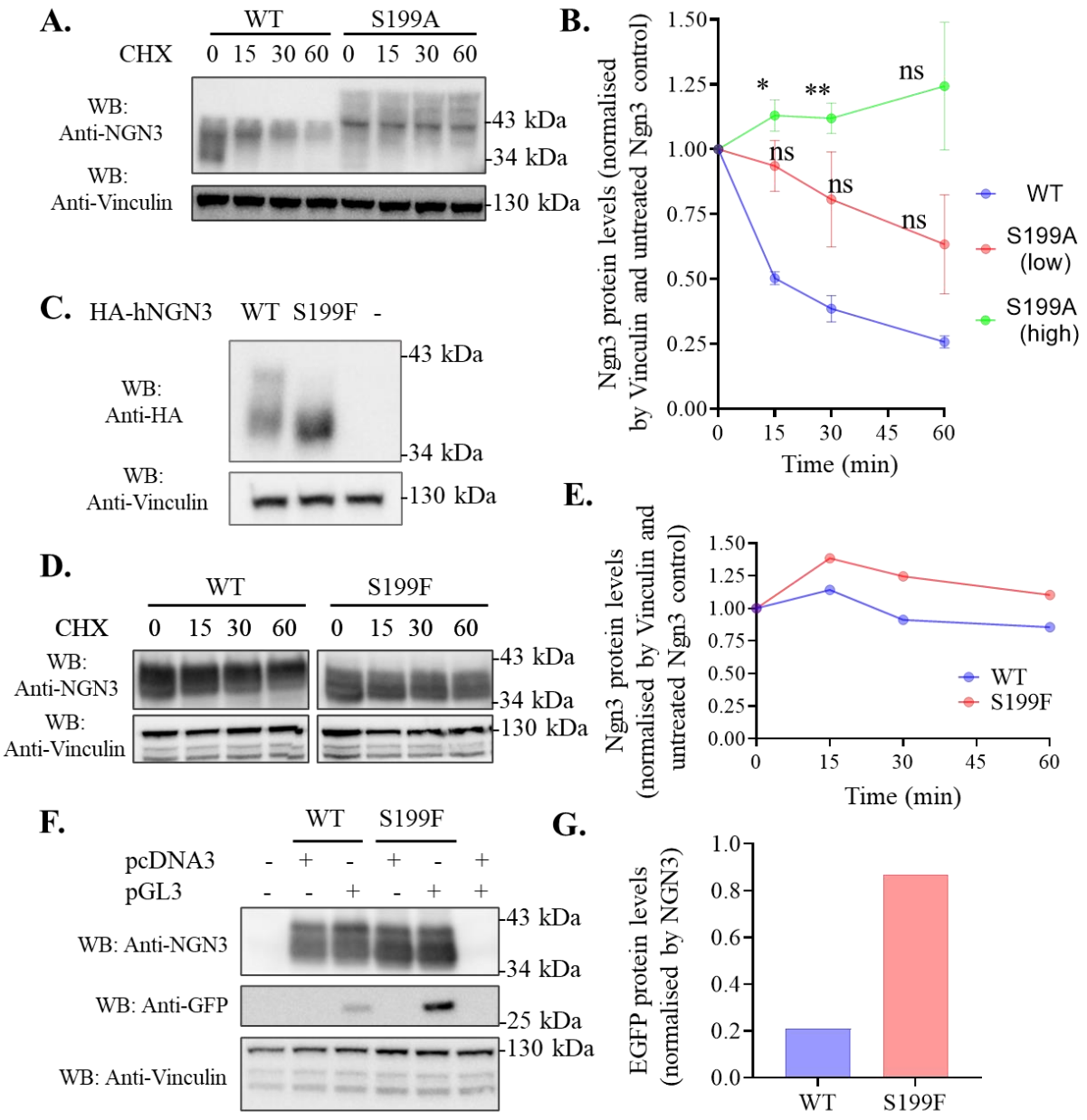

Figure 12. Characterisation of the mouse and human NGN3-S199A/F mutant. A) Immunoblotting for exogenous NGN3 (WT and S199A) in HEK293A samples from cycloheximide chase experiments. B) Quantification of NGN3 WT and NGN3-S199A protein levels normalised by vinculin in cycloheximide chase experiments. S199A (low) represents the band at normal wildtype height, while S199A (high) represents the band above normal wildtype height. Error bars = S.E.M, n=3, *: $p<0.05$, **: $p<0.01$, Two Way ANOVA, Sidak's Multiple Comparison Test against WT sample for each timepoint. C) Immunoblotting for the HA tag in samples transfected with the newly generated human HA-NGN3 WT and HA-NGN3-S199F mutant. D) Immunoblotting for exogenous hNGN3 (WT and S199F) in HEK293A samples from a cycloheximide chase experiment. E) Preliminary quantification of NGN3 WT and NGN3-S199F protein levels normalised by vinculin in a cycloheximide chase experiment, n=1. F) Immunoblotting for NGN3 and GFP in NGN3 transcriptional activity assay samples. HEK293A cells were transfected with NGN3 WT or NGN3-S199F and a pGL3 plasmid inducing GFP expression under regulation from the NeuroD1 promoter. GFP protein levels were used as an output for NGN3 transcriptional activity. G) Preliminary quantification of GFP protein levels from NGN3 transcriptional activity assay, normalised by exogenous NGN3 protein levels, n=1.

3.3 IP-MS assay reveals NGN3 interactors with roles in ubiquitination

Published research (Azzarelli et al. 2017; Sancho et al. 2014), as well as our previous results emphasise the role of post-translational modifications in NGN3 stability and function. Therefore, we wanted to investigate whether additional, unexplored pathways may be involved in the post-translational modification of NGN3, thus contributing to its regulation. To identify new interactors of NGN3, we transfected HEK293A cells with either the HA-NGN3 construct (pcDNA3.HA-NGN3) or an empty pcDNA3 control vector and carried out immunoprecipitation of the HA tag (Fig. 13A). Two HA-NGN3-immunoprecipitated sample, as well as a pcDNA3 control were then sent for mass spectrometry analysis. The resulting interactors are involved in pathways such as RNA binding and ubiquitin protein ligase binding, among others (Fig. 13B).

Of particular interest were interactors such as E3 ubiquitin ligase HUWE1 and deubiquitinase USP7, as it has been previously shown that ubiquitination plays an essential role in NGN3 post-translational regulation (Sancho et al. 2014). However, while HUWE1 was identified with a Protein Identification Possibility of 99% and 100% in each of the two HA-NGN3 samples, respectively, USP7 had a Protein Identification Possibility of 100% in one of the samples and only 9% in the other (Fig. 13C). Therefore, we further validated these interactions through additional HA-NGN3 immunoprecipitation experiments, followed by immunoblotting for both HUWE1 and USP7. Bands could be detected for both endogenous HUWE1 and USP7 in the immunoprecipitated HA-NGN3 sample, but not in the pcDNA3 control (Fig. 13D), confirming that both USP7 and HUWE1 interact with NGN3 within the HEK293A NGN3 overexpression system.

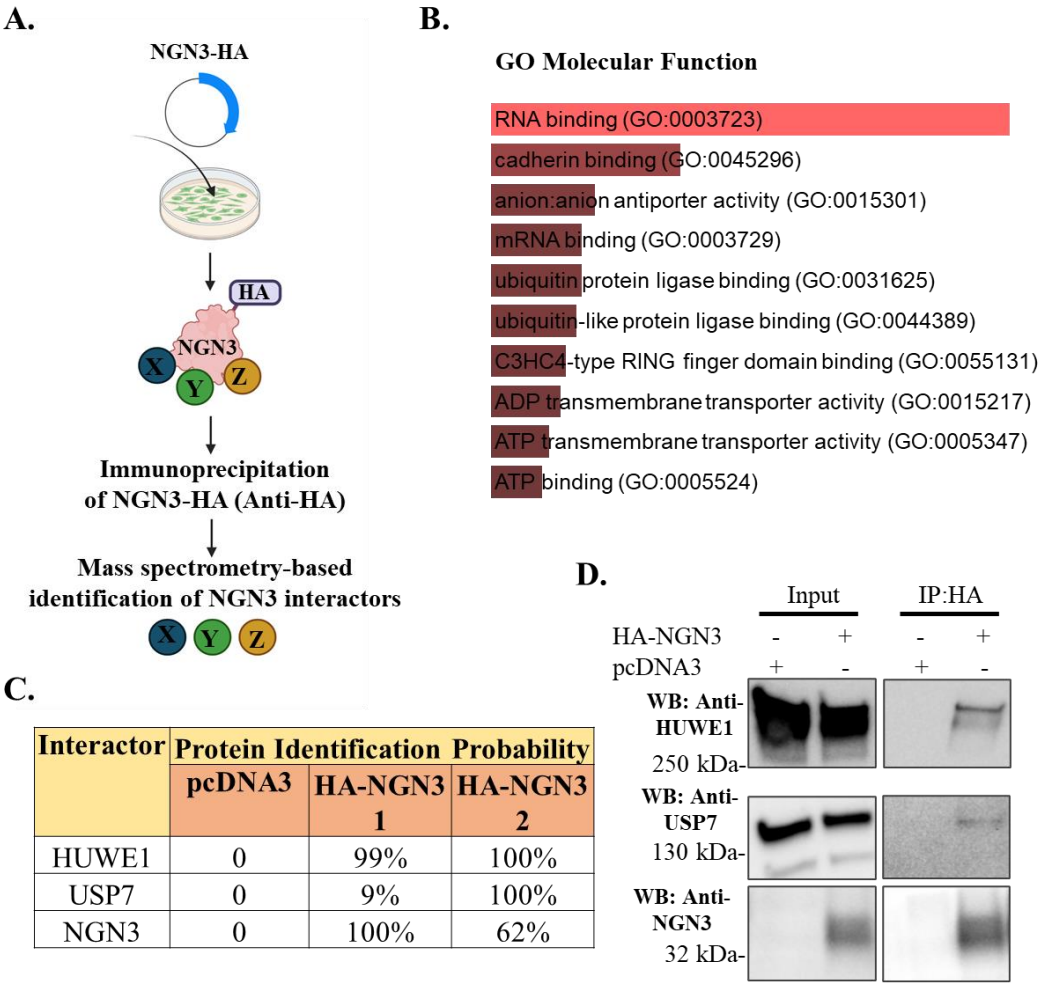

Interactor	Protein Identification Probability		
	pcDNA3	HA-NGN3 1	HA-NGN3 2
HUWE1	0	99%	100%
USP7	0	9%	100%
NGN3	0	100%	62%

Figure 13. Identification and validation of NGN3 interactors Huwe1 and Usp7 through an IP-MS experimental pipeline. A) Diagram of IP-MS strategy for NGN3 interactor identification. B) Main GO Molecular Function terms for NGN3 interactors identified through IP-MS, based on EnrichR GO Molecular Function 2021 database. C) Mass spectrometry Protein identification probabilities of NGN3 interactors involved in ubiquitin-related post-translational modifications in duplicate NGN3 pulldown samples and pcDNA3 control. D) Immunoblotting for endogenous HUWE1 and USP7 in NGN3 immunoprecipitation sample and pcDNA3 control.

3.4 Gene expression patterns of Ngn3, Huwe1 and Usp7 during pancreatic development

Both HUWE1 and USP7 are expressed at protein level in the adult pancreas (Uhlén et al. 2015). Our previous results show that exogenous NGN3 can interact with endogenous HUWE1 and USP7 in an *in vitro*, HEK293A system. However, this does not necessarily mean that the interaction routinely takes place *in vivo*, as it is still unknown whether Usp7 and Huwe1 are expressed in the developing pancreas during the Ngn3 expression window. To further investigate Huwe1 and Usp7 expression patterns, we decided to reanalyse a publicly available

scRNAseq dataset generated from human pancreatic tissue harvested at different gestational weeks (W8 to W19) throughout embryonic development (OMIX236). Epithelial cell clusters in the dataset, such as ductal, acinar and endocrine cells, were used for the analysis (Fig. 14A,B). As expected, Ngn3 gene expression was found in endocrine progenitor cells (Fig. C). However, it was also present in some cells in the Beta, Alpha and Delta Cell clusters. These are likely immature β, α, or δ cells that have not yet lost Ngn3 expression completely. Indeed, these cells were primarily found in the W16 sample, with much fewer present by W18-19 (Fig. 14B).

Huwe1 expression was detected in all clusters, including the Endocrine Progenitor cluster which also exhibited Ngn3 expression (Fig. 14D). Usp7 expression could also be observed in all clusters, similarly to that of Huwe1 (Fig. 14E). Surprisingly, while Fbw7 expression was present, it seemed to be less abundant than Huwe1 or Usp7 (Fig. 14F), despite the fact that it is a known regulator of NGN3. As the FBW7/NGN3 interaction was mostly described in the adult mouse pancreas, it is unknown whether FBW7 plays a role in NGN3 regulation during pancreatic development, or if its limited expression during this time prevents the activity of the pathway. Alternatively, while Huwe1 and Usp7 show more widespread gene expression in the dataset, this is not always indicative of higher expression at protein level. Hes1, a transcriptional repressor of Ngn3 (Shih et al. 2012), is highly expressed at early developmental timepoints (W8-10) (Fig. 14G). As expected, as its expression decreases, Ngn3 expression starts to increase. Interestingly, Hes1 expression does not recover later in development, despite Ngn3 levels plummeting after W16. This suggests that Hes1-mediated transcriptional repression of Ngn3 is not responsible for the loss of Ngn3 expression observed after its W10-W14 peak during normal pancreatic development. As NGN3 operates on a positive auto-feedback loop, activating its own transcription, one way to downregulate Ngn3 gene expression could be by destabilising NGN3 at protein level.

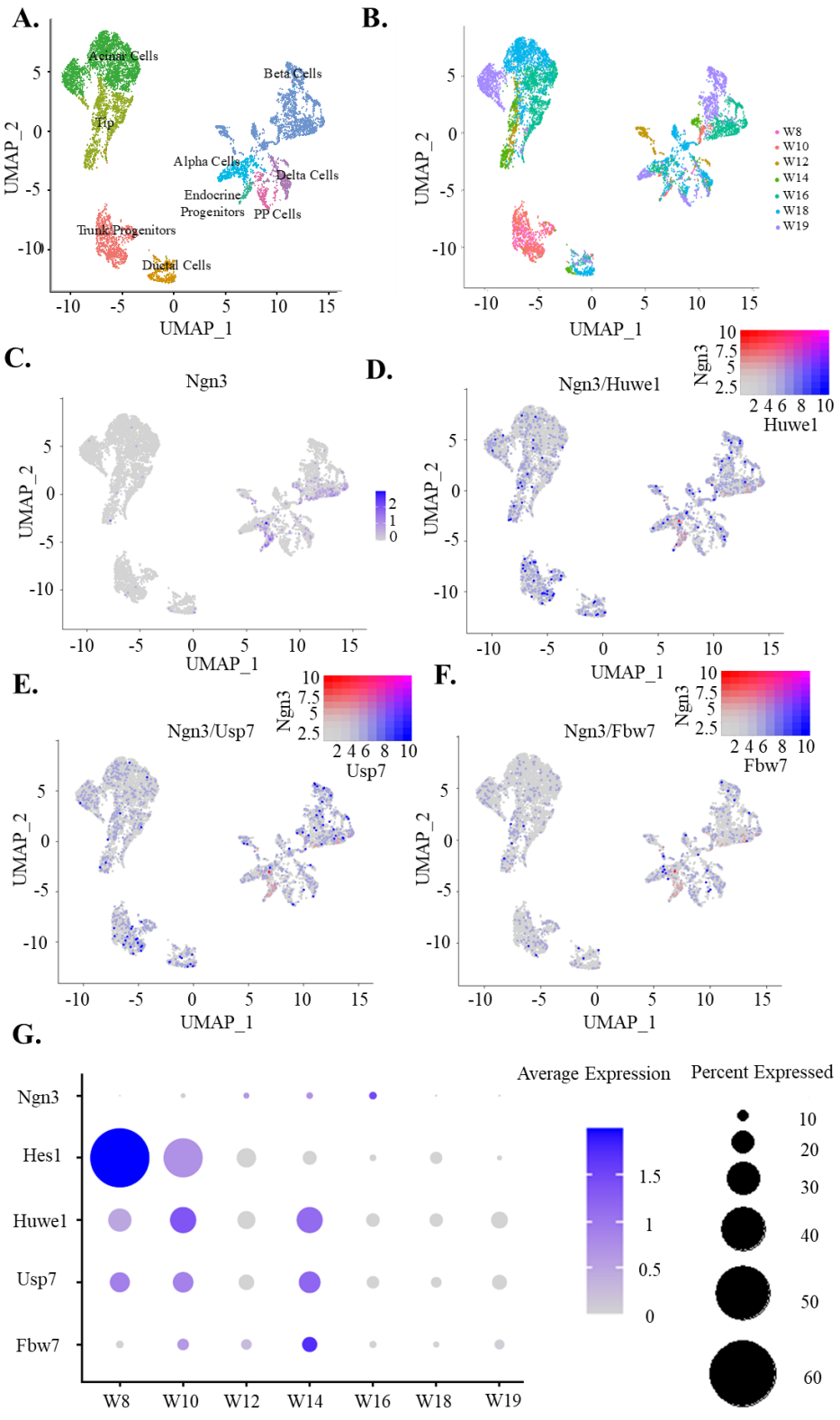

Figure 14. Huwe1 and Usp7 are expressed in the developing human pancreas. A) UMAP projection of pancreatic epithelial cells. Cells are coloured by assigned cluster. B) UMAP projection of pancreatic epithelial cells. Cells are coloured by developmental timepoint. C) Expression of Ngn3 across the scRNA-seq dataset. D) Co-expression of Ngn3 (red) and Huwe1 (blue) across the scRNA-seq dataset. E) Co-expression of Ngn3 (red) and Usp7 (blue) across the scRNA-seq dataset. F) Co-expression of Ngn3 (red) and Fbw7 (blue) across the scRNA-seq dataset. G) Expression of Ngn3, Hes1, Huwe1, Usp7 and Fbw7 across developmental timepoints in the scRNA-seq dataset.

Both Huwe1 and Usp7 show similar expression patterns throughout development, being more widely expressed during the earlier timepoints (W8, W10, W14) and preceding the start of Ngn3 gene expression (Fig. 14G). Expression of Huwe1, Usp7 and Fbw7 declines after W14, this time preceding the end of the Ngn3 expression window at W16. Like FBW7, the main function of HUWE1 and USP7 is the post-translational modification of their substrates. This, combined with the fact that we have observed their interaction with NGN3 at protein level, suggests that they may play a role in the post-translational regulation of NGN3. Additionally, NGN3 protein stability can impact its gene expression, as NGN3 is capable of activating its own transcription. Therefore, it is possible that changes in Huwe1 and Usp7 gene expression, if reflected at protein level, could have an indirect impact on Ngn3 gene expression. However, while the results from this dataset analysis are promising, further experiments will need to be carried out into the NGN3/HUWE1 and NGN3/USP7 protein-protein interactions and how they affect NGN3 stability in order to fully elucidate their effect on pancreatic development.

3.5 Discussion

In this chapter, we have identified potential pathways involved in NGN3 post-translational modifications and degradation. Firstly, we generated overexpression vectors for five predicted mouse NGN3 phosphorylation sites and characterised them alongside previously described phosphomutants, such as NGN3-S183A, NGN3-S187A, NGN3-2SA and NGN3-6SA. We have shown that while exhibiting similar cellular localisation, primarily in the nucleus, some mutants, such as NGN3-S160A, NGN3-2SA and NGN3-6SA, are less able to induce the transcription of NGN3 downstream targets such as Nkx2.2. In the case of NGN3-6SA, this is surprising, as in a previous study, NGN3-6SA was shown to be more transcriptionally active than wildtype when overexpressed in a ductal organoid system (Azzarelli et al. 2017). However, in this study, NGN3 overexpression was constitutive after lentiviral transduction,

rather than transient like in the case of transfected cells. The same study described a significantly higher stability of the NGN3-6SA mutant compared to wildtype. Therefore, depending on how long after infection the cells were harvested, the accumulation of NGN3-6SA in the cells could be orders of magnitude higher than that of wildtype NGN3. Thus, the increased expression of NGN3 target genes could be due to an increased amount of NGN3 protein accumulating in the cell, rather than an increase in NGN3 transcriptional activity. However, this cannot be confirmed without normalisation by NGN3 protein levels in the infected cells at the time of RNA extraction. Among the six sites mutated within the NGN3-6SA mutant, S160A was the only one whose impairment caused a decrease in NGN3 transcriptional activity, pointing towards a potential role of this site in NGN3 function. Separately, NGN3-2SA, which includes mutations at the S183 and S187 residues, also showed a decreased ability to induce Nkx2.2 expression, suggesting that decreases in total phosphorylation levels could also inhibit NGN3 transcriptional activity.

The Western blot analysis demonstrated that S199A exhibits multiple bands at higher molecular weight in addition to the normal molecular weight band (~36 kDa) shown by wildtype NGN3. These could be indicative of post-translational modifications incurred by NGN3 in the absence of S199 phosphorylation. As these bands have not been described in the NGN3-6SA mutant (Azzarelli et al. 2017), it is possible that the particular post-translational modifications responsible for the bands in the NGN3-S199A mutant are facilitated by phosphorylation at one of the other sites mutated within the NGN3-6SA protein. While modified NGN3-S199A is more stable than NGN3 WT (Fig. 12A), the S199A mutant does not appear to be more transcriptionally active (Fig. 11C), suggesting that either these modifications impair NGN3 transcriptional activity due to conformational changes of the protein, or that the protein may be sequestered in other cellular compartments such as the cytoplasm, and thus prevented from activating its downstream targets. However, cellular localisation of NGN3-

S199A showed no noticeable differences compared to the wildtype protein or to other mutants, suggesting that the post-translational modifications are most likely responsible for the increased stability and decreased transcriptional activity of NGN3-S199A.

While the Ser-Pro motif at the S199 site is not conserved in human NGN3, S199F is a widely described polymorphism in humans, with roughly 57% of the global population exhibiting a phenylalanine residue at NGN3 position 199. As the mouse S199A mutant showed striking differences compared to the wildtype protein, and the S199F polymorphism had been weakly linked to T2D progression in humans, we wanted to investigate whether the human version of the protein showed similar alterations to the murine NGN3-S199A mutant. We therefore generated overexpression plasmids for either wildtype human NGN3 or of the S199F mutant. The human S199F mutant did not recapitulate the alterations observed in the mouse mutant, instead being a likely phosphomutant. While one preliminary experiment has suggested S199F may be slightly more stable, and up to 4x more transcriptionally active than the wildtype protein, further replicates would need to be performed in order to determine whether these observations are statistically significant.

In addition to characterising the effect of phosphorylation at different NGN3 sites on protein function, we identified new NGN3 interactors that may play a role in regulating its stability. Both HUWE1 and USP7 co-immunoprecipitated with exogenous NGN3. As the former is an E3 ubiquitin ligase, and the latter a deubiquitinase, this finding opens up the possibility that pathways other than FBW7-mediated ubiquitination may contribute to NGN3 proteasomal degradation.

At the transcriptional level of Ngn3 regulation, Hes1, a transcriptional repressor of Ngn3, is likely not responsible for the decrease in Ngn3 expression at later developmental timepoints,

as it is not highly expressed after W12 (Fig. 14G). While this could mean that other repressors of Ngn3 transcription fulfil this role later in development, another possibility is that rapid NGN3 protein degradation prevents it from propagating the positive auto-feedback loop by which NGN3 activates its own transcription, leading to a decrease in Ngn3 gene expression. Therefore, validation of new interactors with roles in ubiquitination and deubiquitination, such as HUWE1 and USP7, could help elucidate the mechanisms for NGN3 regulation in the developing pancreas. Both Huwe1 and Usp7 are expressed at higher levels than Fbw7 during pancreatic development (Fig. 14 D-G). While this is only reflective of Huwe1 and Usp7 mRNA levels, and could differ at protein level, it is encouraging that expression of both potential interactors can be detected within the Ngn3 expression window. Therefore, as we have shown that HUWE1 and USP7 interact with NGN3 at protein level in an NGN3 overexpression system, and that expression of both genes is present in the pancreas during normal embryonic development, further chapters will characterise these interactions and investigate their effect on exogenous and endogenous NGN3 stability, as well as on endocrine cell generation.

Chapter 4: Characterisation of the HUWE1/NGN3 interaction

4.1 Introduction

Phosphorylation plays a key role in NGN3 regulation. Specifically, phosphorylation at the S183-S187 motif is essential for the interaction of NGN3 with FBW7, an E3 ubiquitin ligase. Impairment of this site leads to a decrease in NGN3 ubiquitination and a subsequent stabilisation of the protein, due to decreased degradation (Sancho et al. 2014). However, concurrent impairment of five other NGN3 phosphorylation sites leads to further stabilisation, indicating that other pathways may also play a role in NGN3 post-translational regulation (Azzarelli et al. 2017). As NGN3 expression is an essential part of pancreatic endocrine differentiation, identifying and describing these pathways could allow for a more finely tuned regulation of NGN3 in the process of β cell generation, both *in vitro*, in the case of iPSC-to-β-cell differentiation protocols, and *in situ*, when attempting to trigger exocrine-to-endocrine cell plasticity.

One of the potential NGN3 interactors we have identified in our IP-MS assay was HUWE1, a HECT E3 ubiquitin ligase. Huwe1 is expressed during human pancreatic development in the Ngn3 expression window, allowing for the possibility that the two proteins could interact in an *in vivo* setting during embryonic development. HUWE1 also shares certain substrates, such as p53 and MYC (Tripathi et al. 2019; Sato et al. 2015; D. Yang et al. 2018; Adhikary et al. 2005), with FBW7, which is also expressed during the NGN3 expression window in the developing pancreas and is a known NGN3 interactor. Furthermore, HUWE1 is involved in the regulation of other bHLH transcription factors, such as ASCL1 and ATOH1(Cheng, Tong, and Edge 2016; Gillotin, Davies, and Philpott 2018). It is therefore not excluded that bHLH transcription

factor and FBW7 substrate NGN3 could also be a substrate for HUWE1-mediated ubiquitination.

In a preliminary experiment, we showed that endogenous HUWE1 co-immunoprecipitates with exogenous NGN3 in HEK293A cells. While this is promising, this finding on its own may not necessarily translate into an important role for HUWE1 in NGN3 post-translational regulation. Therefore, we wanted to analyse the mechanism behind this interaction and determine whether HUWE1 ubiquitinates NGN3, whether this ubiquitination leads to its degradation and whether this interaction can be modulated in order to stabilise NGN3 and boost β cell differentiation. Additionally, as phosphorylation plays an important role in the interaction of NGN3 with FBW7, we wondered whether the NGN3/HUWE1 interaction is also dependent on NGN3 phosphorylation, and if so, whether any particular phosphorylation sites were especially important. In this chapter, we set out to address these questions in a HEK293A NGN3 overexpression system, as well as in an endogenous NGN3 expression model during iPSC-to-β-cell-differentiation.

4.2 NGN3 phosphorylation at the C-terminus promotes its interaction with Huwe1

The interaction between NGN3 and E3 ubiquitin ligase FBW7 is promoted by GSK3β-mediated phosphorylation at residue S183 of NGN3 (Sancho et al. 2014). Therefore, we wanted to investigate whether a similar mechanism is involved in the interaction between NGN3 and HUWE1, another E3 ubiquitin ligase we recently identified as a possible NGN3 interactor. To first determine if NGN3 phosphorylation plays a role in the interaction, we transfected HEK293A cells with either HA-NGN3 WT, HA-NGN3-2SA or HA-NGN3-6SA and carried out immunoprecipitation assays using anti-HA beads. Western blotting confirmed the presence

of HUWE1 in the immunoprecipitated samples, supporting our initial identification of HUWE1 as an interactor (Fig. 15A). Interestingly, NGN3-2SA and NGN3-6SA were significantly less able to pull down HUWE1 compared to NGN3 WT ($p=0.0116$ and $p=0.0002$, respectively, One-Way ANOVA with Dunnett's multiple comparisons test), with a 2x reduction in HUWE1 levels in the NGN3-2SA pulldown sample, and a more than 6x reduction in the NGN3-6SA pulldown sample (Fig. 15B). This suggests that phosphorylation plays a role in the NGN3/HUWE1 interaction, as it is the case for the NGN3/FBW7 interaction. However, while both NGN3-2SA and NGN3-6SA contain the S183A mutation, NGN3-6SA appears to be more severely affected in its ability to interact with HUWE1 than NGN3-2SA. It is therefore likely that sites other than S183 also facilitate the NGN3/HUWE1 interaction.

To identify which particular phosphorylation sites may contribute to the interaction, we repeated the experiment with the single-site phosphorylation mutants (S14A, S38A, S160A, S174A, S183A, S187A, S199A). While all the NGN3 phosphomutants were able to pull down endogenous HUWE1 (Fig. 15C), the S174A, S183A, S187A and S199A mutants were significantly less capable of doing so compared to NGN3 WT ($p=0.0226$, $p=0.0016$, $p=0.0226$, $p=0.0005$, respectively, One-Way ANOVA with Dunnett's multiple comparisons test) (Fig. 15D). This seems to indicate that phosphorylation towards the C-terminus of NGN3 promotes its interaction with HUWE1. However, in order to assess the ability of each mutant to pull down HUWE1, we normalised the amount of HUWE1 in the immunoprecipitated sample by the amount of NGN3 in the same sample. This was done to account for increased NGN3 stability in some of the mutants, or transfection efficiency.

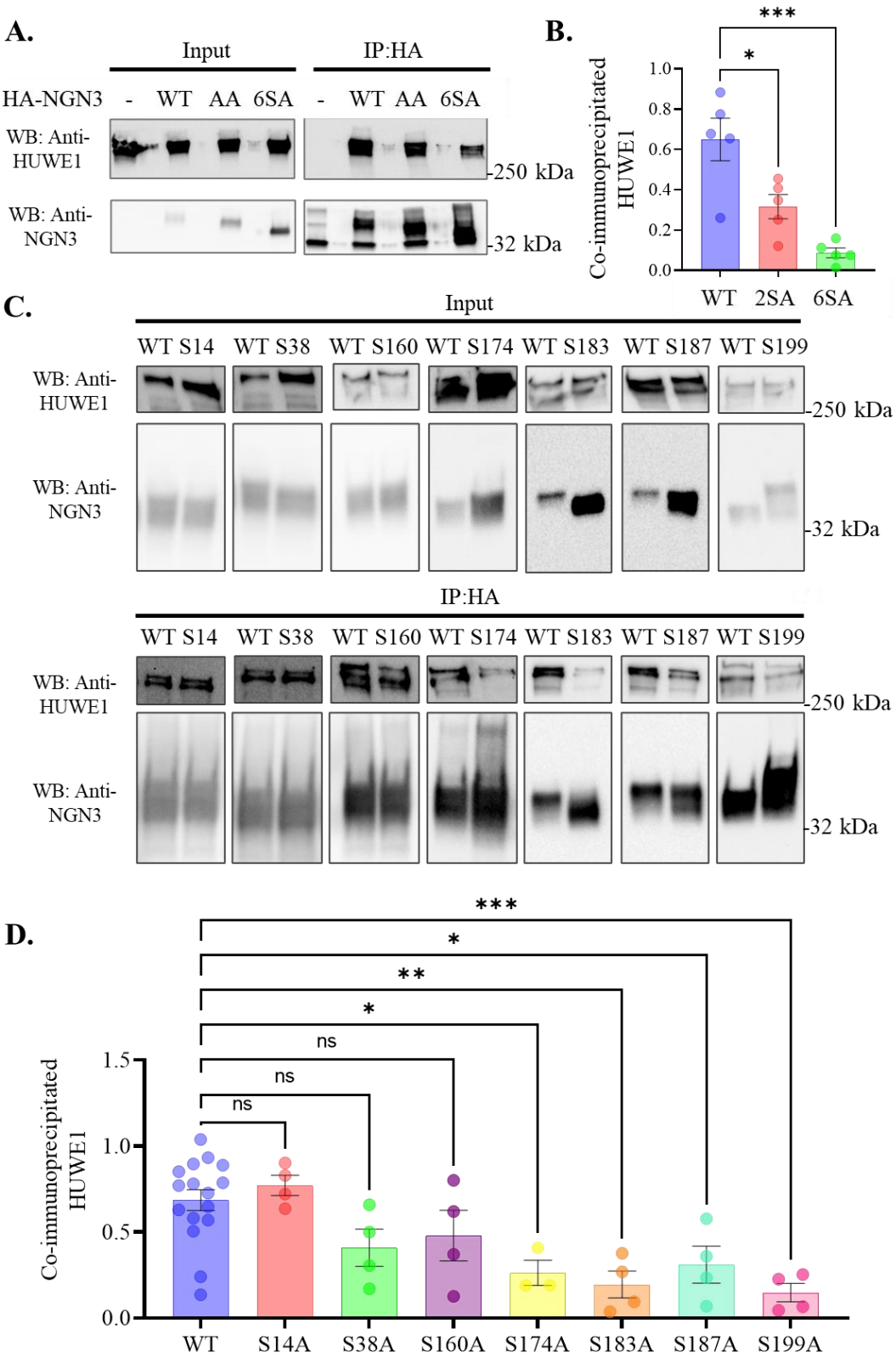

Figure 15. NGN3 phosphorylation facilitates NGN3/HUWE1 interaction. A) Immunoblotting for endogenous HUWE1 in immunoprecipitation samples for NGN3 WT, NGN3-2SA or NGN3-6SA. B) Quantification of HUWE1 protein levels co-immunoprecipitated with NGN3 WT, NGN3-2SA or NGN3-6SA normalised by NGN3 levels in the same sample; n=5 C) Immunoblotting for endogenous HUWE1 in immunoprecipitation samples for NGN3 WT or mutants S14A, S38A, S160A, S174A, S183A, S187A and S199A. D) Quantification of HUWE1 protein levels co-immunoprecipitated with NGN3 WT or mutants, normalised by NGN3 levels in the same sample; n=3-16. Error Bars = S.E.M, * p<0.05, ** p<0.01, *** p<0.001, Ordinary One-Way ANOVA, Dunnett's Multiple Comparisons Test against NGN3 WT sample.

As we have shown that the S199A mutant has substantial post-translational modifications that may impact its conformation and function, its increased stability in the cell may not be an accurate reflection of the amount of protein available to interact with HUWE1. Therefore, in the case of S199A, the significant reduction in co-immunoprecipitated HUWE1 may not occur due to a lack of phosphorylation at the S199 site, but due to the other post-translational modifications the mutant suffers as a result of this mutation.

4.3 Heclin treatment decreases NGN3 ubiquitination but does not stabilise exogenous NGN3 in HEK293A cells

As HUWE1 is an E3 ubiquitin ligase, we wanted to investigate whether the HUWE1/NGN3 interaction leads to HUWE1-mediated ubiquitination of NGN3. We transfected HEK293A cells with NGN3 WT alongside a His-tagged ubiquitin overexpression plasmid obtained from the Behrens Lab, at the Institute of Cancer Research. To inhibit HUWE1 activity, we treated cells with 20 μM of Heclin, a HECT E3 ubiquitin ligase inhibitor, for 24 h, before processing the samples for ubiquitin immunoprecipitation assays. While ubiquitinated NGN3 is detected in both Heclin-treated and untreated samples (Fig. 16A), there is a small, but significant ($p = 0.0099$, Student t-test) decrease in NGN3 ubiquitination after Heclin treatment (Fig. 16B), indicating that HUWE1, may play a role in NGN3 ubiquitination.

As ubiquitination events, especially K48-linked polyubiquitin chains, are a hallmark of the proteasomal degradation pathway, it is possible that HUWE1-mediated ubiquitination of NGN3 targets it for degradation, similarly to its interaction with FBW7. Moreover, as we have previously determined that the NGN3/HUWE1 interaction is promoted by phosphorylation near the NGN3 C-terminus, a lack of phosphorylation at these sites may stabilise the protein, by circumventing the interaction with HUWE1. We therefore used Heclin to chemically inhibit

HUWE1 in HEK293A cells transfected with either NGN3 WT, NGN3-2SA or NGN3-6SA (Fig. 16C).

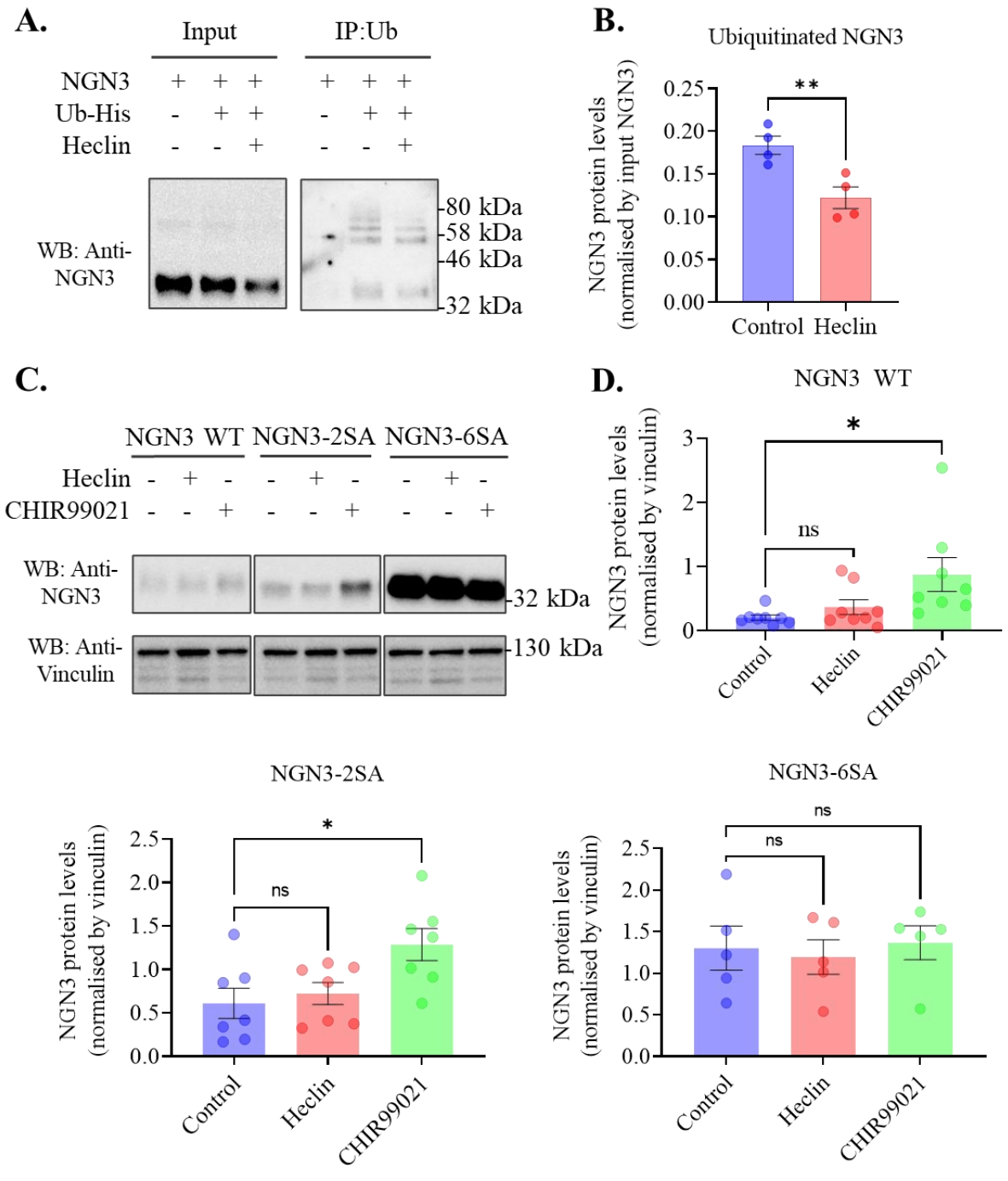

Figure 16. Heclin treatment decreases NGN3 ubiquitination but does not contribute to its stabilisation. A) Immunoblotting for exogenous NGN3 in Ub-His pulldown assay with and without Heclin treatment (20 μM, 24 h). B) Quantification of ubiquitinated NGN3 with or without Heclin-mediated HUWE1 inhibition; Error bars = S.E.M, n=3, Student t-test, **p<0.01 C) Immunoblotting for exogenous NGN3 WT, 2SA and 6SA with or without 20 μM Heclin or 10 μM CHIR99021 treatment (24 h). D) Quantification of exogenous NGN3 WT, 2SA and 6SA after HUWE1 or GSK3β inhibition; Error bars = SEM, n=5-7, Ordinary One-Way ANOVA, Dunnett's Multiple Comparisons Test against Control sample, *p<0.05.

As a positive control for NGN3 stabilisation, we also included experimental conditions where GSK3β, the kinase that targets NGN3 for FBW7-mediated ubiquitination, is inhibited with 10 μM CHIR99021. Surprisingly, despite Heclin treatment leading to a decrease in NGN3 ubiquitination, it did not stabilise either NGN3 WT or the 2SA and 6SA phosphorylation mutants (Fig. 16D). While the small decrease in ubiquitination seen in previous experiments may not be sufficient for NGN3 stabilisation, it is also possible that HUWE1-mediated ubiquitination of NGN3 is non-degradative, with different types of polyubiquitin chains playing different roles in regulating the stability, localisation and function of the substrate. Indeed, HUWE1 can add K6- and K11-linked polyubiquitin chains to its substrates (Michel et al. 2017), aside from the more common K48- and K63-linked chains.

GSK3β inhibition significantly ($p= 0.0195$) stabilised NGN3 WT (Fig. 16D), consistent with previous findings (Sancho et al. 2014). There was no change in the stability of the NGN3-6SA mutant. This could be explained by the impairment of the S183 site in this mutant, which is part of the phosphodegron motif targeted by GSK3β. However, despite containing mutations at the S183 and S187 residues, both part of the GSK3β-targeted motif, the NGN3-2SA mutant still exhibited significant stabilisation after CHIR99021 treatment, compared to untreated NGN3 ($p= 0.0135$). This suggests that other sites among the six mutated residues within the NGN3-6SA mutant may routinely be recognised and phosphorylated by GSK3β, contributing to NGN3 degradation. The difference in stability between the NGN3-6SA and NGN3-2SA mutant may be explained by this phenomenon, even in the absence of other pathways for NGN3 degradation.

4.4 Heclin treatment does not increase NGN3 stability during iPSC differentiation

We previously investigated whether Heclin-mediated HUWE1 inhibition could stabilise NGN3 in a HEK293A NGN3 overexpression system. To address this question in an endogenous expression model, we carried out pancreatic-progenitor-to-β-cells differentiation assays, adapting a protocol from Russ et al (Russ et al. 2015; Trott et al. 2017) (Fig. 17A). Ngn3 gene expression could be detected by D7, two days after the initiation of the endocrine progenitor differentiation stage (Fig. 17B). On D8, we treated half of our organoid domes with 20 μM Heclin for 24 h. No significant differences in Ngn3 gene expression were detected between the treated and untreated samples on D9, at the end of the treatment, or on D12, during the peak of Ngn3 expression. This is, however, not surprising, as the expected effect of HUWE1 on NGN3 regulation would occur at the post-translational level. After D12, when cells are transferred to low glucose maturation media, Ngn3 expression decreases, allowing for the maturation of endocrine cells. These Ngn3 expression patterns confirm the successful induction of endocrine differentiation in our pancreatic progenitors.

As we had previously found fluctuations in Fbw7, Usp7 and Huwe1 gene expression during human pancreatic development (Fig. 14G), we wanted to further analyse the expression patterns of these genes during *in vitro* endocrine differentiation. We identified expression of all three genes at the start of the endocrine progenitor stage (D5). All three showed a dip in expression on D9, then increased again at D12 (Fig. 17C). This could reflect the corresponding decrease in expression at W12 of foetal pancreas development (Fig. 14G). However, this change in gene expression *in vitro* was not statistically significant due to high variability in differentiation efficiency between experimental replicates.

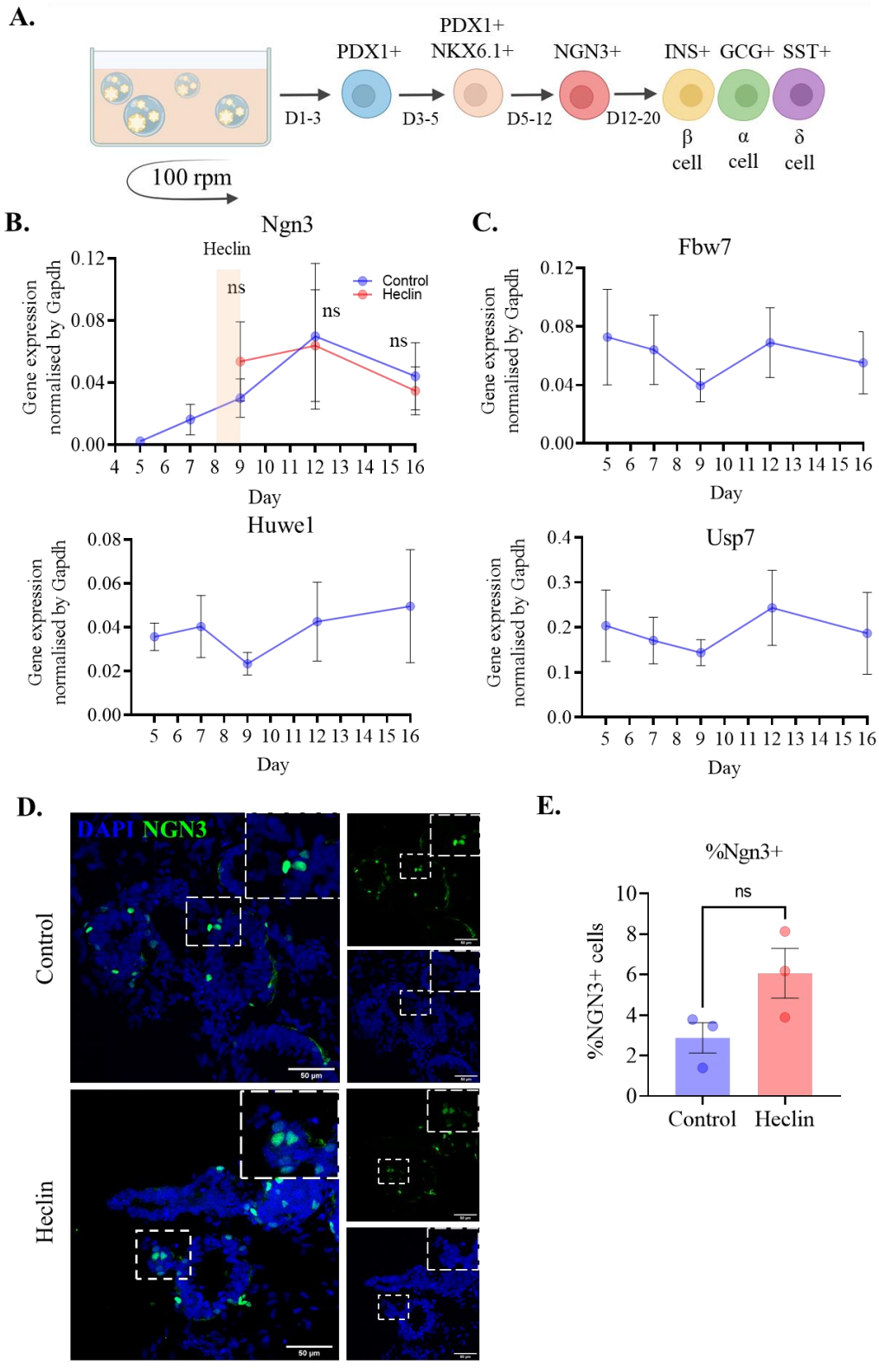

Figure 17. Heclin-mediated inhibition of HUWE1 does not stabilise NGN3 during endocrine differentiation. A) Simplified diagram of the adapted Russ differentiation protocol. B) Ngn3 gene expression normalised by Gapdh in Heclin-treated and control samples. Error bars = S.E.M, n=3, Student t-test against control sample from the same timepoint. C) Gene expression levels for Fbw7, Huwe1 and Usp7 across differentiation timepoints, normalised by Gapdh. D) NGN3 immunofluorescent staining in control and Heclin-treated samples at D9. E) Percentage of NGN3+ cells in control and Heclin-treated samples. Datapoints represent triplicate experiments, with five immunostaining images quantified per experiment. Error bars = S.E.M, n=3, Student t-test.

To investigate whether Heclin treatment affected NGN3 protein stability, we carried out immunofluorescent staining for NGN3 on frozen sections of D9 samples, after Heclin treatment. We could confirm the presence of NGN3 in the cells at protein level (Fig. 17D). However, there was no significant difference in the percentage of NGN3+ cells between Heclin-treated and control samples. This is consistent with previous results obtained from the HEK293A NGN3 overexpression system, where Heclin treatment did not stabilise NGN3. It is therefore likely that HUWE1 does not play a part in NGN3 stabilisation.

Finally, while Heclin-mediated HUWE1 inhibition did not affect NGN3 stability, it could still have an effect on NGN3 function if ubiquitination of NGN3 by HUWE1 is mostly non-degradative. Therefore, we wanted to assess whether the Heclin treatment had any effects downstream of NGN3, particularly on the generation of β-like cells. We carried out immunofluorescent staining for insulin (INS), glucagon (GCG) and somatostatin (SST) on frozen sections from D16 samples and could successfully identify cells positive for each of the three hormones. This indicates the presence of β-like, α-like and δ-like cells at the end of the differentiation (Fig. 18A). However, no significant differences between the treated and non-treated samples were identified in the percentage of INS+ cells (Fig. 18B), or in gene expression levels (Fig. 18C), suggesting that NGN3 function and its ability to activate genes that push cells towards an endocrine fate are not affected by HUWE1 inhibition.

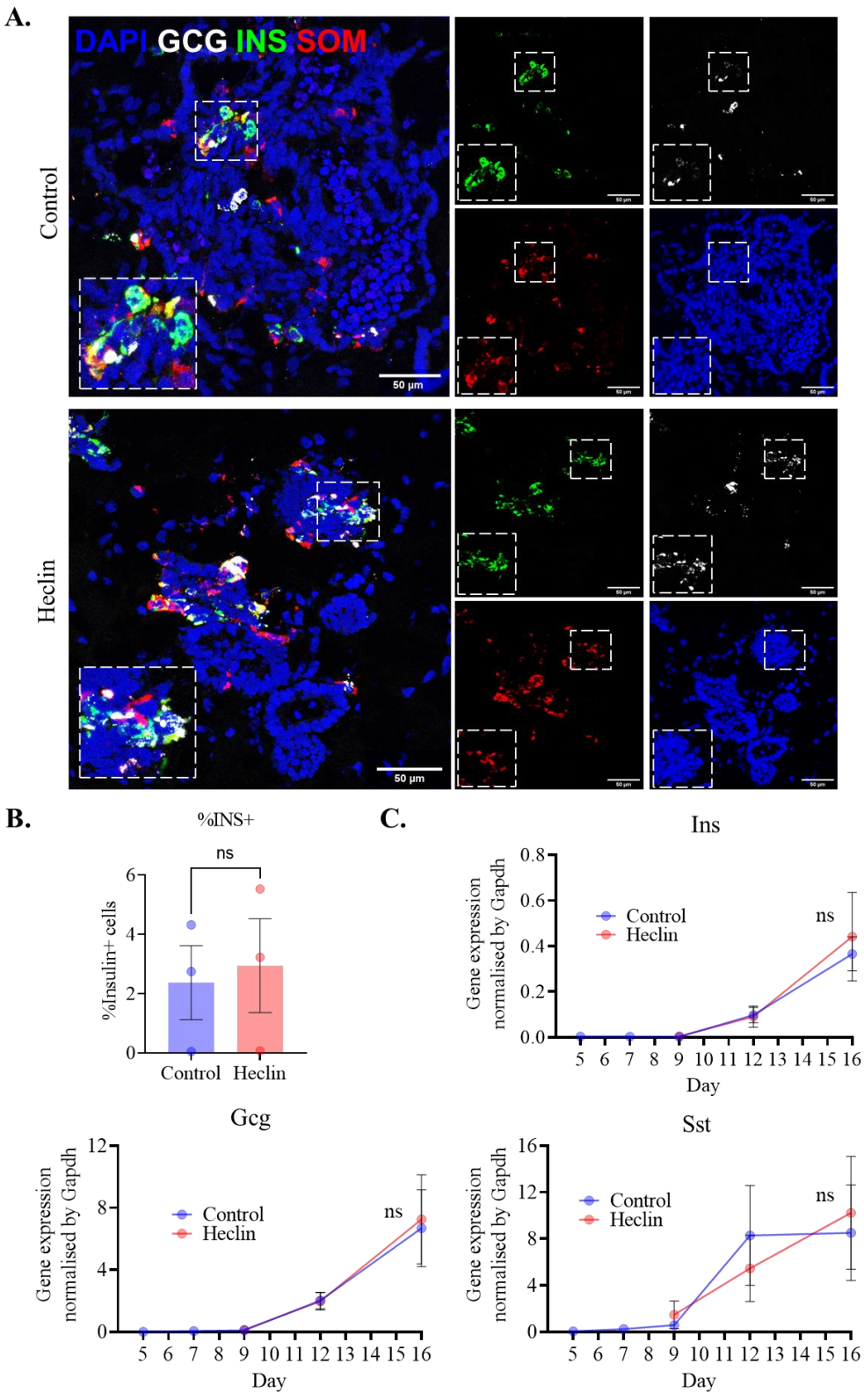

Figure 18. Heclin-mediated inhibition of HUWE1 does not boost β-like cell generation. A) Immunofluorescent staining for INS, GCG and SST in control and Heclin-treated D20 differentiation samples B) Percentage of INS+ cells in control and Heclin-treated samples. Datapoints represent triplicate experiments, with five immunostaining images quantified per experiment. Error bars = S.E.M, n=3, Student t-test. C) Ins, Gcg and Sst gene expression normalised by Gapdh in Heclin-treated and control samples. Error bars = S.E.M, n=3, Student t-test against for D20 against control sample from the same timepoint.

4.5 BI8622 treatment does not stabilise exogenous NGN3 or decrease its ubiquitination

As Heclin is an inhibitor of HECT E3 ubiquitin ligases in general, we wanted to determine whether a specific HUWE1 inhibitor would affect NGN3 ubiquitination and stability differently to Heclin. We therefore repeated the ubiquitination and stability assays in our HEK293A NGN3 overexpression system, this time treating cells with 10 μM BI8622, a specific HUWE1 inhibitor, for 24 h (Fig. 19A-D).

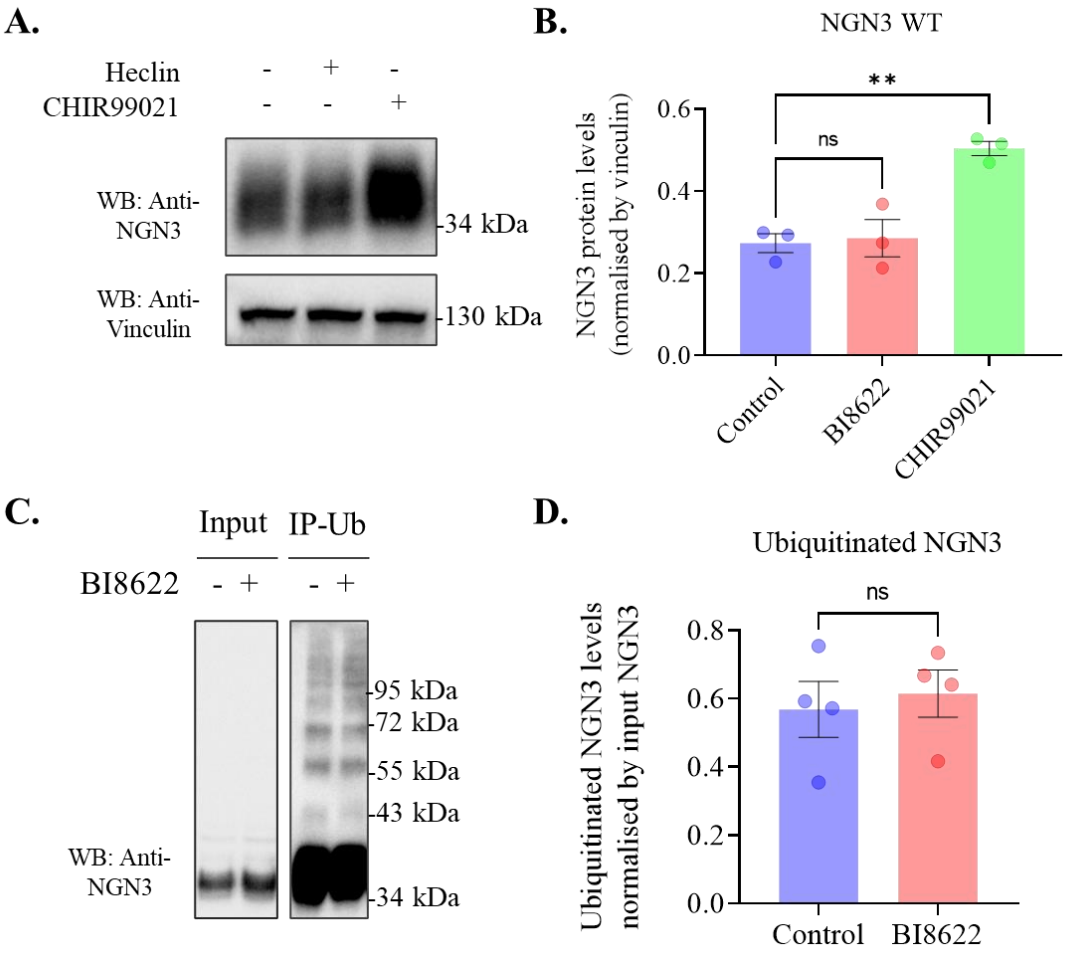

Figure 19. BI8622-mediated HUWE1 inhibition does not stabilise NGN3 or prevent its ubiquitination. A) Immunoblotting for NGN3 in BI8622-treated, CHIR99021-treated, or untreated samples. B) Quantification of NGN3 in samples treated with 10 μM BI8622, 10 μM CHIR99021 or untreated normalised by Vinculin. Error bars = S.E.M, n=3, **p<0.01, One-Way ANOVA, Dunnett's Multiple Comparisons Test against Control sample. C) Immunoblotting of ubiquitin pulldown assay in samples transfected with NGN3 and ubiquitin and treated with BI8622. D) Quantification of NGN3 protein expression in ubiquitin pulldown assays with or without BI8622 treatment. Error bars = S.E.M, n=4, Student t-test.

Similarly to Heclin, BI8622 treatment did not stabilise NGN3 (Fig. 19A). In contrast, CHIR99021 treatment successfully stabilised NGN3 ($p=0.034$), consistent with results from previous experiments (Fig. 16D). Surprisingly, despite the fact that Heclin treatment significantly decreased NGN3 ubiquitination (Fig. 16B), BI8622 treatment did not affect NGN3 ubiquitination (Fig. 19D). This suggests that the effect of Heclin on NGN3 ubiquitination may not be a direct effect of Huwe1 inhibition, but instead a consequence of Heclin inhibiting other HECT E3 ligases that could be involved in NGN3 regulation.

4.6 Discussion

In this chapter, we characterised the NGN3/HUWE1 interaction, its dependence on NGN3 phosphorylation and its effect on NGN3 ubiquitination and stability. Firstly, we investigated whether the interaction was affected by mutations in different NGN3 phosphorylation sites. Immunoprecipitation experiments for NGN3 WT, NGN3-2SA and NGN3-6SA showed that NGN3-2SA and NGN3-6SA were significantly less able to pull down HUWE1, with NGN3-6SA being more severely affected (Fig. 15A,B). This finding indicates not only that the S183-S187 phosphorylation motif promotes the NGN3/HUWE1 interaction, like in the case of FBW7, but also that other phosphorylation sites impaired in the 6SA mutant may be involved. Therefore, we repeated the experiment using the previously generated single-site mutants, to determine which sites in particular facilitate the interaction between NGN3 and HUWE1. NGN3-S174A, S183A, S187A and S199A, all including mutations at sites close to the C-terminus of NGN3, showed a significantly reduced ability to pull down HUWE1 compared to wildtype (Fig. 15C,D). However, in the case of NGN3-S199A, it is uncertain whether the lower amount of HUWE1 pulled down is due to a lack of phosphorylation at the S199 site, or due to the dramatic post-translational modifications the protein undergoes, as a result of the mutation.

We proceeded to investigate the effect of HUWE1 inhibition on NGN3 ubiquitination and stability. We transfected HEK293A cells with NGN3 and Ub-His and proceeded to chemically inhibit HUWE1, either with 20 μM Heclin, or 10 μM BI8622, for 24 h. Ubiquitin pulldown assays showed that while Heclin treatment significantly decreased NGN3 ubiquitination (Fig. 16A,B), BI8622 treatment had no effect (Fig. 19C,D). As Heclin generally inhibits HECT E3 ubiquitin ligases and BI8622 is specific to HUWE1, one possibility for this difference could be that the decrease in ubiquitination after Heclin treatment is not due to HUWE1 inhibition, but instead due to inhibition of another HECT E3 ubiquitin ligase that is involved in NGN3 ubiquitination. However, despite this decrease in ubiquitination, NGN3 is not significantly stabilised by either treatment (Fig. 16B,C, Fig. 19A,B). This suggests that the decrease in NGN3 ubiquitination seen after Heclin treatment may reflect a decrease in non-degradative ubiquitination, regardless of whether this is due to inhibition of HUWE1 activity or inhibition of another HECT E3 ubiquitin ligase.

As these experiments were carried out in an exogenous NGN3 overexpression system, we wanted to determine whether our findings would be recapitulated in an endogenous NGN3 expression model, during iPSC-to-β-cell differentiation. We adapted the previously described Russ protocol (Russ et al. 2015; Trott et al. 2017) to induce endocrine differentiation in iPSC-derived pancreatic organoids encapsulated in Matrigel domes. We then subjected the cells to Heclin treatment for 24 h, between D8 and D9, in the middle of the NGN3 expression window, to investigate whether HUWE1 inhibition would affect NGN3 stability and β-cell generation. However, no significant differences were found between treated and untreated samples in the percentage of NGN3+ cells at D9 (Fig. 17D,E), of INS+ β-like cells at D16 (Fig. 18A,B), or in overall Ngn3 (Fig. 17B), Ins, Gcg or Sst (Fig. 18C) gene expression levels throughout the differentiation.

These findings indicate that targeting HUWE1 activity would most likely not be a suitable option when trying to modulate NGN3 stability and boost endocrine differentiation. Despite interacting with NGN3 in a phosphorylation-dependent manner, HUWE1 does not seem to play a significant role in NGN3 degradation, at least under the tested conditions. While it is possible that the role of HUWE1 on NGN3 ubiquitination and stability is limited to specific developmental timepoints, or that additional components of the ubiquitination machinery are needed in order to enable HUWE1-mediated NGN3 ubiquitination, further experiments would need to be carry out to investigate these possibilities.

Lastly, during our experiments we used CHIR99021 treatment as a positive control for NGN3 stabilisation, as it inhibits GSK3β, preventing phosphorylation at NGN3 residues S183-S187 and impairing NGN3 ubiquitination and degradation. Surprisingly, we found that the NGN3-2SA mutant, in which both the S183 and S187 sites are impaired, was still stabilised by CHIR99021 treatment (Fig. 16D). One explanation could be that GSK3β exerts other, indirect, effects on NGN3 stability that are independent of its phosphorylation of S183-S187. However, if this was the case, the NGN3-6SA mutant would likely also be stabilised by GSK3β inhibition. The fact that the NGN3-6SA mutant is not stabilised by CHIR99021 treatment suggests that the stabilisation of NGN3-2SA is likely due to one or more of the other sites mutated in NGN3-6SA being targets for GSK3β-mediated phosphorylation. Future research could investigate which of the five sites (S14, S38, S160, S174, S199) are targeted by GSK3β for phosphorylation, and whether phosphorylation at these sites contributes to the recognition of NGN3 by FBW7, or other interactors involved in its post-translational regulation.

Chapter 5: USP7 deubiquitinates and stabilises NGN3

5.1 Introduction

NGN3 expression is essential for the development of the endocrine pancreas. Mouse (Gradwohl et al. 2000) and pig (Sheets et al. 2018) Ngn3 knock out embryos fail to develop pancreatic islets, leading to a diabetic phenotype soon after birth. In humans, homozygous missense Ngn3 mutations such as R107S and R93L affect the ability of NGN3 to activate transcription of downstream targets such as NEUROD1 and have been linked to congenital malabsorptive diarrhoea (Jan N Jensen et al. 2007; Ünlüsoy Aksu et al. 2016), with patients eventually developing diabetes neonatally (Pinney et al. 2011; Rubio-Cabezas et al. 2011) or during childhood (Sayar et al. 2013). While NGN3 is only expressed transiently during pancreatic development and is typically not present in the adult pancreas, NGN3 overexpression in exocrine pancreatic cells from adult mice, alongside key transcription factors PDX1 and MAFA, can induce reprogramming towards INS+ β-like cells (Zhou et al. 2008). These studies emphasise the importance of NGN3 expression for the *in vitro* and *in situ* generation of endocrine cells, including β cells, which are depleted in T1D patients. Therefore, a deeper understanding of the NGN3 regulatory pathway and of how it can be modulated could help improve the efficiency of *in vitro* β-cell differentiation protocols, as well as contribute to new T1D therapies aiming to address β-cell loss.

While previous studies have shown that at the transcriptional level, Ngn3 expression can be repressed by HES1 (Shih et al. 2012) and activated by factors such as HNF6 (Jacquemin et al. 2000), HNF1α (J. C. Lee et al. 2001), FOXA2 (J. C. Lee et al. 2001), PDX1 (Oliver-Krasinski et al. 2009) and GLIS3 (Y. Yang et al. 2011), NGN3 is heavily regulated at the post-translational level. Phosphorylation at specific sites on NGN3 promote its interaction with E3

ubiquitin ligase FBW7, which ubiquitinates NGN3 and targets it for proteasomal degradation (Sancho et al. 2014). However, in our IP-MS experiment, we identified additional possible NGN3 interactors that could play a role in its regulation, such as deubiquitinase USP7. To our knowledge, no interactions between NGN3 and a deubiquitinase have previously been described, despite the existence of ample research on the topic of NGN3 post-translational regulation and its degradation through the ubiquitin-proteasome system (Sancho et al. 2014; Azzarelli et al. 2017; X. Zhang et al. 2019).

As ubiquitination contributes to NGN3 degradation, the interaction of NGN3 with a deubiquitinase could provide new methods for NGN3 stabilisation and *in vitro* β-cell generation. Therefore, we first aimed to validate and characterise the NGN3/USP7 interaction in an exogenous expression HEK293A system, through NGN3 immunoprecipitation experiments. We then carried out ubiquitination assays, to investigate whether USP7 deubiquitinates NGN3, followed by USP7 titration experiments and cycloheximide chase assays, to assess whether USP7-mediated deubiquitination stabilises NGN3. Finally, as phosphorylation was shown to play a role in the interaction of NGN3 with both FBW7 and HUWE1, we compared the ability of the wildtype (WT) NGN3 protein and the previously generated NGN3 phosphorylation mutants to interact with, and be stabilised by, USP7.

5.2 USP7 overexpression deubiquitinates NGN3 in HEK293A cells

We previously identified USP7 as a potential NGN3 interactor in our IP-MS experiment and showed that endogenous USP7 can co-immunoprecipitate with exogenous NGN3 in our HEK293A system. USP7 can stabilise its substrates by cleaving off their ubiquitin chains, thus preventing their proteasomal degradation. Therefore, it is possible that USP7 could play a role in NGN3 post-translational regulation, stabilising it during pancreatic development. To

investigate the effect of this interaction on NGN3 ubiquitination and regulation, we used an USP7 overexpression plasmid vector (pcDNA3.Flag-USP7) obtained from the Behrens Lab, at the Institute of Cancer Research. We generated a catalytically inactive USP7 mutant (Flag-USP7^{C223A}) plasmid through site-directed mutagenesis PCR on pcDNA3.Flag-USP7 (Fig. 20A). Including the Flag-USP7^{C223A} catalytically inactive mutant alongside Flag-USP7 WT in future experiments ensured that any observed effects of USP7 on NGN3 stabilisation were due to the catalytic activity of USP7. After co-transfection of HEK293A cells with HA-NGN3 and either Flag-USP7 or Flag-USP7^{C223A}, we immunoprecipitated NGN3 by its HA tag and analysed the ability of Flag-USP7 and Flag-USP7^{C223A} to co-immunoprecipitate with NGN3 through immunoblotting (Fig. 20B). NGN3 successfully pulled down both forms of USP7, with no significant differences detected between the output protein levels of Flag-USP7 and Flag-USP7^{C223A} (Fig. 20C). This was expected, as the C223A mutation should only affect the catalytic site of USP7 and should not impair its ability to bind substrates.

Once we confirmed that both Flag-USP7 and Flag-USP7^{C223A} interact with exogenous NGN3, we set up ubiquitination assays to investigate the effect of USP7 on NGN3 ubiquitination. Firstly, we transfected HEK293A cells with HA-NGN3, His-Ub and increasing concentrations of Flag-USP7 (0, 0.5, 1, 2.5 μg). Cells were treated with MG132, to prevent the proteasomal degradation of ubiquitinated NGN3. Ubiquitinated proteins in the cell lysate were immunoprecipitated using TUBE2 anti-ubiquitin beads. Western blotting revealed decreasing NGN3 ubiquitination levels with increasing USP7 levels (Fig. 21A). Quantification of polyubiquitinated (55 kDA and above) NGN3 revealed a significant decrease in NGN3 ubiquitination upon co-transfection with 1 μg ($p=0.0085$) or 2.5 μg ($p=0.0101$) of USP7 plasmid DNA, while the decrease in NGN3 monoubiquitination (band visible above 43 kDA) was not significant. These results show that USP7 overexpression leads to NGN3 deubiquitination in a dose-dependent manner.

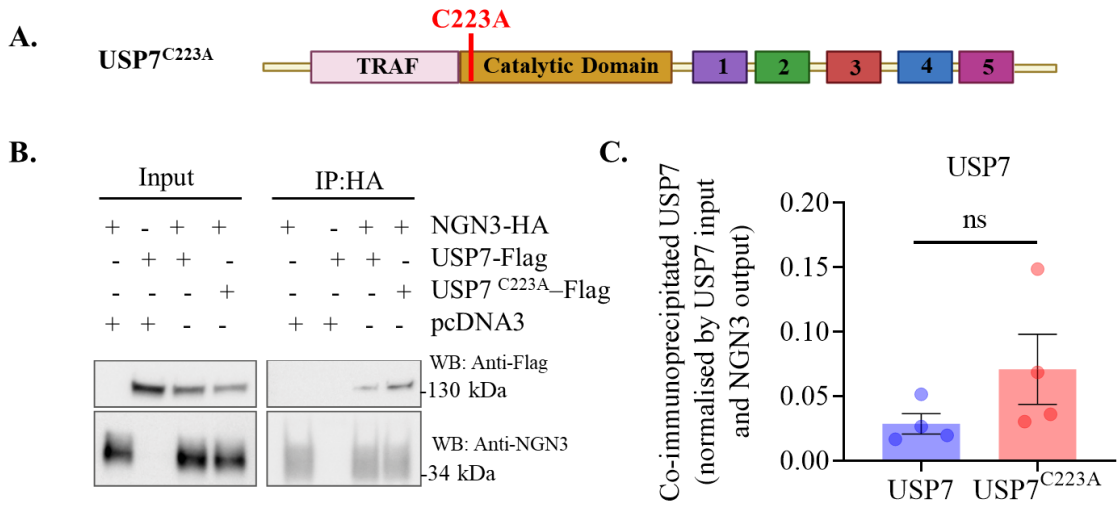

Figure 20. Exogenous USP7 and USP7-C223A interact with NGN3 in a HEK293A overexpression system. A) Diagram of C223A mutation within the structure of the USP7 protein. B) Immunoblotting for NGN3 and Flag in an HA-NGN3 immunoprecipitation experiment. Both Flag-USP7 and Flag-USP7-C223A were detected in the immunoprecipitation output. Image is representative of n=4 experiments C) Quantification of USP7 and USP7-C223A in the output of HA-NGN3 immunoprecipitation experiments, normalised by immunoprecipitated NGN3 levels and USP7 input levels in each sample. Error bars = S.E.M, n=4, Student t-test.

To confirm that the decrease in NGN3 ubiquitination after USP7 overexpression is due to the catalytic activity of USP7, we repeated the experiment, co-transfecting cells with NGN3 and 2.5 µg of either Flag-USP7 or Flag-USP7^{C223A} (Fig. 21C). Flag-USP7 overexpression resulted in a significant decrease in NGN3 polyubiquitination (p=0.0432), while overexpression of the Flag-USP7^{C223A} mutant had no significant effect (Fig. 21D) on NGN3 ubiquitination. NGN3 monoubiquitination levels were not significantly affected by co-transfection with either wildtype or mutant USP7, consistent with previous findings (Fig. 21D).

Different types of polyubiquitin chains have distinct regulatory effects on their substrate, with K48- and K63-linked polyubiquitin chains being the most commonly described. K48-linked chains generally target their substrate for proteasomal degradation, while K63-linked chains play a role in processes like signal transduction, endocytosis (Hicke and Dunn 2003). While we have shown that USP7 can deubiquitinate NGN3, whether this process affects all ubiquitination events, or whether it is specific to a certain type of polyubiquitin linkage is still unknown.

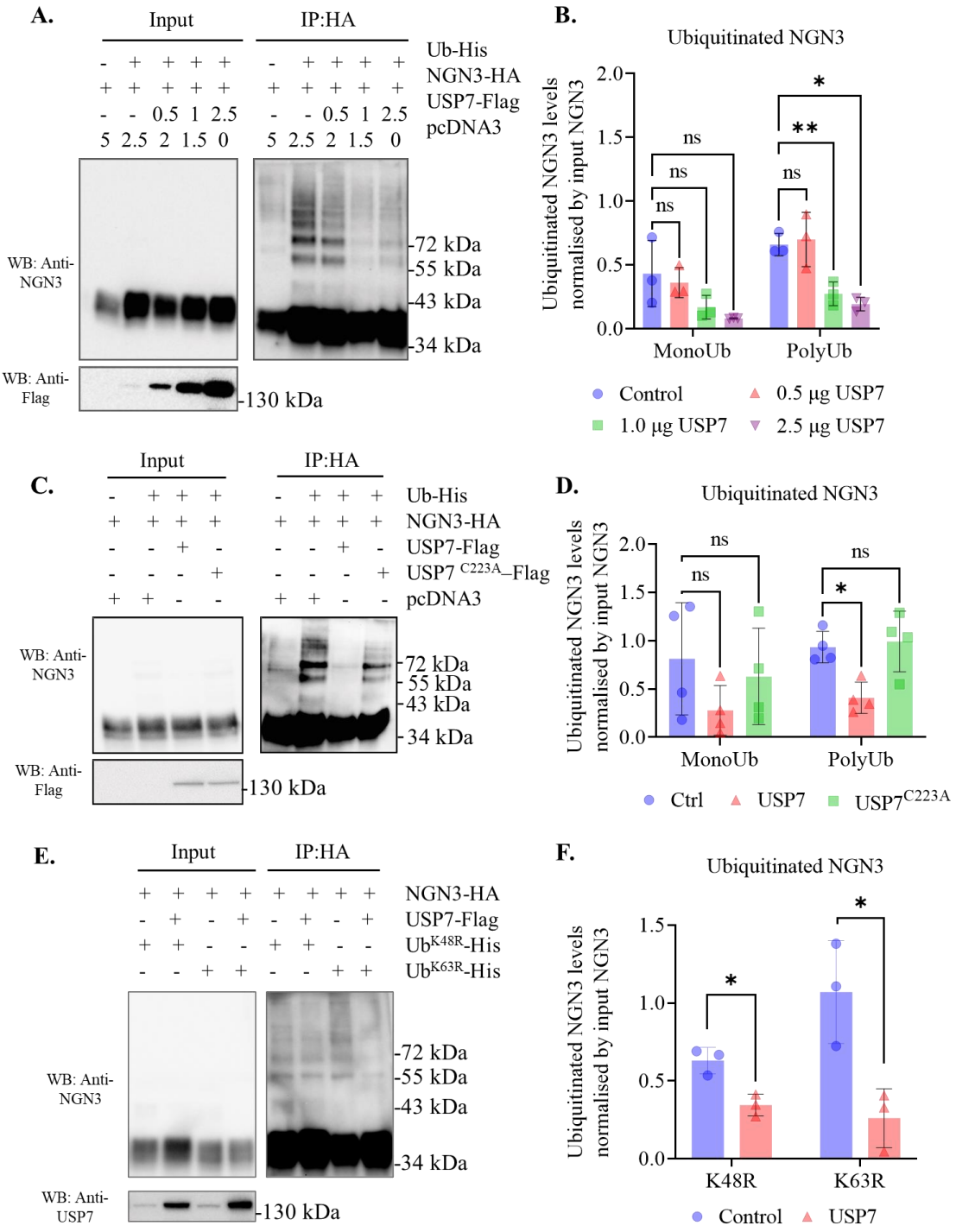

Figure 21. Exogenous USP7 deubiquitinates NGN3 in a HEK293A overexpression model. A) Immunoblotting for exogenous NGN3 in Ub-His pulldown assay with or without USP7 co-transfection (0, 0.5, 1, 2.5 µg DNA). B) Quantification of mono- (band at 43 kDa) and polyubiquitinated (bands above 55 kDa) NGN3 with or without USP7 co-transfection, normalised by input NGN3, n=3. Error bars = S.E.M, **p<0.01, *p<0.05, Two-way ANOVA with Dunnett's multiple comparison correction against corresponding Control sample. C) Immunoblotting for exogenous NGN3 in Ub-His pulldown assay after co-transfection with 2.5 µg Flag-USP7 or Flag-USP7^{C223A}. D) Quantification of mono- and polyubiquitinated NGN3 after co-transfection with either Flag-USP7 or Flag-USP7^{C223A}, normalised by input NGN3, n=4. Error bars = S.E.M, *p<0.05, Two-way ANOVA with Dunnett's multiple comparison correction against corresponding Control sample. E) Immunoblotting for exogenous NGN3 in Ub-His pulldown assay with overexpression of either His-Ub^{K48R} or His-Ub^{K63R}, and with or without USP7 overexpression. F) Quantification of ubiquitinated NGN3 with or without USP7 co-transfection, after overexpression of either His-Ub^{K48R} or His-Ub^{K63R}, normalised by input NGN3, n=3. Error bars = S.E.M, *p<0.05, Student t-test.

To answer this question, we repeated the experiment, replacing the His-Ub overexpression construct with two different ubiquitin mutants, His-Ub^{K48R} and His-Ub^{K63R}. In these mutants, the lysine residue at position 48 or 63, respectively, was mutated to arginine, preventing the use of the site in the formation of polyubiquitin chains. Therefore, NGN3 polyubiquitination in samples where the K48R mutant is overexpressed would be limited to mostly K63-linked chains, while in samples where K63R is overexpressed, these would be mostly K48-linked chains. Co-transfection of K48R or K63R mutant Ub and USP7 decreased NGN3 ubiquitination by 45.5 ± 6.5% in K48R-transfected samples (p=0.0107) and by 71.9 ± 26.2% in K63R-transfected samples (p=0.0211), suggesting that USP7 is able to remove both K63 and K48-linked polyubiquitin chains from NGN3. As K48-linked chains typically target their substrate for degradation, it is possible that the interaction with USP7 could have a stabilising effect on NGN3, as it results in the cleavage of its K48-linked polyubiquitin chains and prevents it from being targeted to the proteasome.

5.3 USP7 overexpression stabilises NGN3 in HEK293A cells

We have previously shown that USP7 can interact with, and deubiquitinate, exogenous NGN3 in a HEK293A overexpression system. Furthermore, K48-linked polyubiquitin chains, which generally target the substrate for proteasomal degradation, are likely among the types of ubiquitin chains removed from NGN3 by USP7. To investigate whether USP7 overexpression could stabilise NGN3, we transfected HEK293A cells with HA-NGN3, alongside increasing concentrations of USP7 plasmid DNA (Fig. 22A). Co-transfection with USP7 at a 1:2 USP7:NGN3 ratio (0.25 μg USP7 : 0.5 μg NGN3) was sufficient to significantly stabilise NGN3 (p=0.0398), resulting in a more than 2x increase in NGN3 protein levels (Fig. 22B). Co-transfection with 0.375 μg and 0.5 μg USP7 similarly led to NGN3 stabilisation (p=0.0218 and p=0.0098, respectively). No change in NGN3 stability was observed upon co-transfection with

the USP7^{C223A} mutant, indicating that the stabilising effect of USP7 is dependent on its catalytic activity (Fig. 22B).

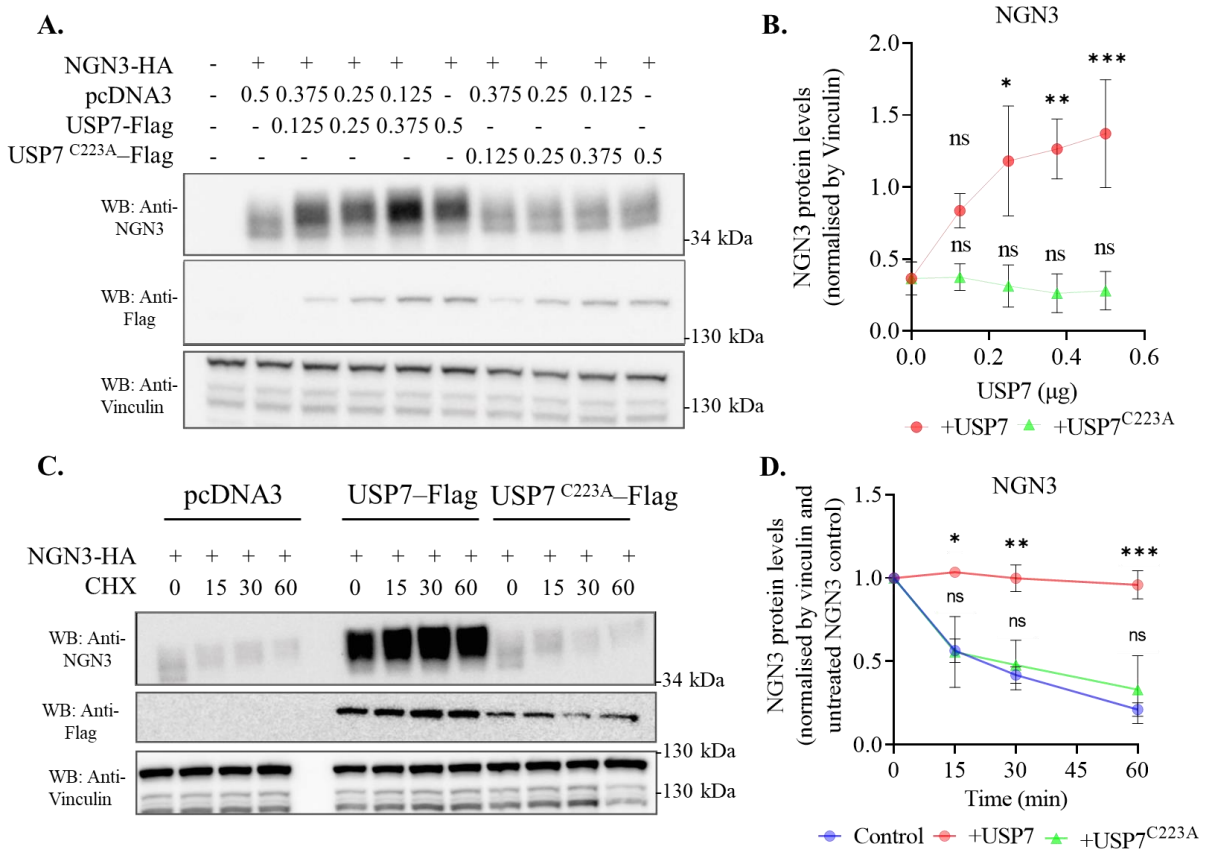

Figure 22. USP7 overexpression stabilises exogenous NGN3 in HEK293A cells. A) Immunoblotting of NGN3 in samples co-transfected with Flag-USP7 or the Flag-USP7^{C223A} catalytically inactive mutant. B) Quantification of NGN3 immunoblotting in samples co-transfected with either Flag-USP7 or Flag-USP7^{C223A}, normalised by Vinculin, n=3. Error Bars = S.E.M, *p<0.05, **p<0.01, ***p<0.001, Two-way ANOVA with Dunnett's multiple comparison test against Control sample (NGN3 co-transfected with empty pcDNA3 vector). C) Immunoblotting of NGN3 in cycloheximide chase assay co-transfected with either Flag-USP7, Flag-USP7^{C223A} or empty pcDNA3 vector. Samples were collected at 0, 15, 30 and 60 minutes after the initiation of cycloheximide treatment. D) Quantification of NGN3 protein levels throughout cycloheximide chase experiments after co-transfection with Flag-USP7, Flag-USP7^{C223A} or empty pcDNA3, normalised by Vinculin and by the untreated control (0 min) for each condition, n=4. Error Bars = S.E.M, *p<0.05, **p<0.01, ***p<0.001, Two-way ANOVA with Dunnett's multiple comparison test against pcDNA3 co-transfected sample from the corresponding timepoint.

To confirm that the stabilisation of NGN3 by USP7 takes place at the post-translational level, we carried out cycloheximide (CHX) chase assays, inhibiting protein synthesis and analysing the stability of NGN3 with or without Flag-USP7 co-transfection (Fig. 22C). While in the absence of exogenous USP7, the half-life of NGN3 is below 30 minutes, upon co-transfection with USP7 NGN3 degradation is blocked, with NGN3 levels remaining relatively constant

until the end of the experiment (Fig. 22D). USP7 overexpression achieves significant NGN3 stabilisation 15 ($p=0.044$), 30 ($p=0.0019$) and 60 ($p=0.0006$) minutes after the start of CHX treatment, while no significant changes in stability are observed upon co-transfection with $USP7^{C223A}$. These results indicate that USP7 stabilises NGN3 at the post-translational level by deubiquitinating it and preventing its proteasomal degradation.

To validate our findings in a human NGN3 overexpression system, we repeated these experiments with the pcDNA3.hNGN3-HA construct (Fig. 23A-D). USP7 overexpression successfully stabilises exogenous hNGN3 (Fig. 23A,B). However, this requires a higher USP7:NGN3 DNA co-transfection ratio (3:4 as opposed to 1:2 for the murine NGN3 experiments) in order to achieve significant NGN3 stabilisation ($p=0.1398$, $p=0.1386$, $p=0.0440$, $p=0.0236$ for 0.125, 0.25, 0.375 and 0.5 μg USP7, respectively). CHX chase experiments in HEK293A cells in which HA-hNGN3 is overexpressed revealed a much longer half-life for hNGN3 compared to the murine protein (Fig. 23C,D). However, co-transfection with USP7 still stabilises hNGN3 significantly at 60, 90 and 180 min after the beginning of CHX treatment ($p=0.1885$, $p=0.0009$, $p=0.0091$, $p=0.0022$ at the 30, 60, 90 and 180 min timepoints, respectively).

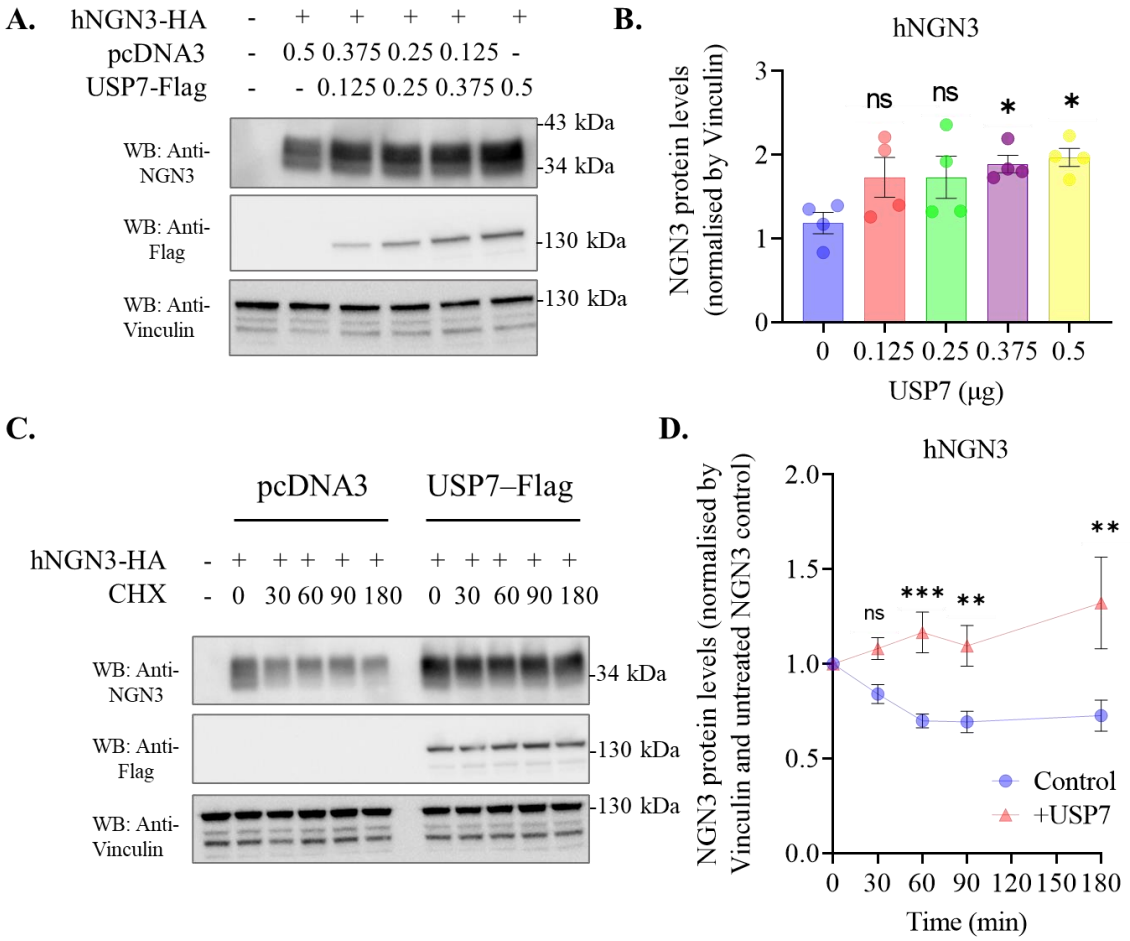

Figure 23. USP7 overexpression stabilises exogenous hNGN3 in HEK293A cells. A) Immunoblotting of hNGN3 in samples co-transfected with Flag-USP7. B) Quantification of NGN3 immunoblotting in samples co-transfected with either Flag-USP7, normalised by Vinculin, n=4. Error Bars = S.E.M, *p<0.05, One-way ANOVA with Dunnett's multiple comparison test against Control sample (hNGN3 co-transfected with empty pcDNA3 vector). C) Immunoblotting of NGN3 in cycloheximide chase assay co-transfected with either Flag-USP7 or empty pcDNA3 vector. Samples were collected at 0, 30, 60, 90 and 180 minutes after the initiation of cycloheximide treatment. D) Quantification of NGN3 protein levels throughout cycloheximide chase experiments after co-transfection with Flag-USP7 or empty pcDNA3, normalised by Vinculin and by the untreated control (0 min) for each condition, n=3-5. Error Bars = S.E.M, *p<0.05, **p<0.01, ***p<0.001, Two-way ANOVA with Sidak's multiple comparison test against pcDNA3 co-transfected sample from the corresponding timepoint.

5.4 NGN3 phosphorylation levels play a role in interaction with USP7

Phosphorylation plays an essential role in NGN3 post-translational regulation (Azzarelli et al. 2017), mediating the interaction between NGN3 and FBW7, an E3 ubiquitin ligase which ubiquitinates it and targets it for proteasomal degradation (Sancho et al. 2014). Our own experiments have indicated that phosphorylation at the C-terminus of exogenous NGN3 promotes its interaction with E3 ubiquitin ligase HUWE1 (Fig. 15D) in HEK293A cells. As

we have previously shown that USP7 can interact with, and deubiquitinate, NGN3, we set off to investigate whether NGN3 phosphorylation also played a role in the USP7/NGN3 interaction (Fig. 24).

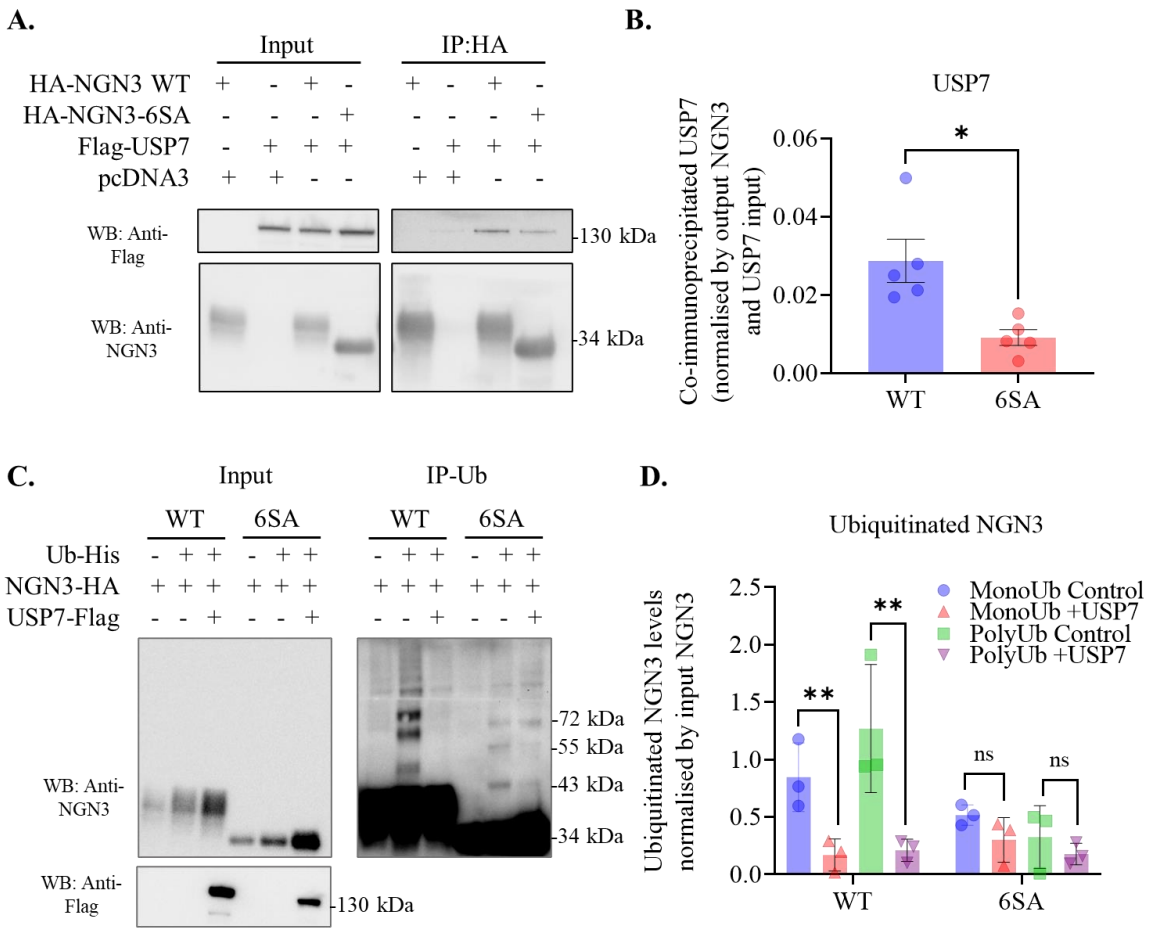

Figure 24. Lower levels of NGN3 phosphorylation lead to a reduction in the NGN3/USP7 interaction. A) Immunoblotting for NGN3 and Flag in an HA-NGN3 immunoprecipitation experiment. Flag-USP7 was detected in the immunoprecipitation output for both HA-NGN3 and HA-NGN3-6SA. Image is representative of n=5 experiments. B) Quantification of Flag-USP7 co-immunoprecipitated with either HA-NGN3 or HA-NGN3-6SA, normalised by NGN3 output and USP7 input from the corresponding sample, n=5. Error Bars = S.E.M, *p<0.05, Student t-test. C) Immunoblotting for exogenous NGN3 (HA-NGN3 and HA-NGN3-6SA) in Ub-His pulldown assay after co-transfection with Flag-USP7. D) Quantification of mono- and polyubiquitinated NGN3 after co-transfection with Flag-USP7, normalised by input NGN3, n=3. Error bars = S.E.M, **p<0.01, Two-way ANOVA with Tukey's multiple comparison correction against corresponding Control sample.

We first co-transfected HEK293A cells with Flag-USP7 and either HA-NGN3 or HA-NGN3-6SA, an NGN3 mutant containing mutations at six different predicted phosphorylation sites. Immunoprecipitation of HA-tagged NGN3 and NGN3-6SA showed significantly less co-immunoprecipitation of USP7 with the NGN3-6SA mutant (p=0.0102) (Fig. 24A,B),

suggesting that lower NGN3 phosphorylation levels may impact its ability to interact with USP7. However, as we know NGN3 phosphorylation at sites such as S183 promotes its ubiquitination, it is also possible that the effect of phosphorylation on the NGN3/USP7 interaction is indirect, through its effect on ubiquitination.

To investigate this, we carried out ubiquitin pulldown assays in samples transfected with USP7 and either HA-NGN3 or HA-NGN3-6SA (Fig. 24C). As expected, USP7 overexpression resulted in significant deubiquitination of HA-NGN3 ($p=0.0058$, $p=0.0070$ for monoubiquitination and polyubiquitination, respectively), while no significant decreases in ubiquitination were observed for the 6SA mutant. However, the 6SA mutant shows limited ubiquitination, even in the absence of USP7 overexpression, likely due to its reduced phosphorylation levels. Therefore, it is possible that impaired phosphorylation leads to lower ubiquitination of NGN3-6SA, which in turn results in its decreased interaction with USP7.

Alternatively, one or more of the six mutated phosphorylation sites may play a role in promoting the NGN3/USP7 interaction. To investigate this possibility, we repeated the HA-NGN3 immunoprecipitation assays, including samples transfected with each of the previously described single-site HA-NGN3 mutants (S14A, S38A, S160A, S174A, S183A, S187A, S199A). USP7 successfully co-immunoprecipitated with all tested mutants (Fig. 25A). We found no significant differences between any of the mutants and wildtype HA-NGN3 in their ability to pull down USP7 (Fig. 25B). Therefore, it is unlikely that any of the individual phosphorylation sites are essential for the USP7/NGN3 interaction. To determine whether USP7 can still stabilise the different phosphorylation mutants, we overexpressed USP7 alongside each of the mutants in HEK293A cells.

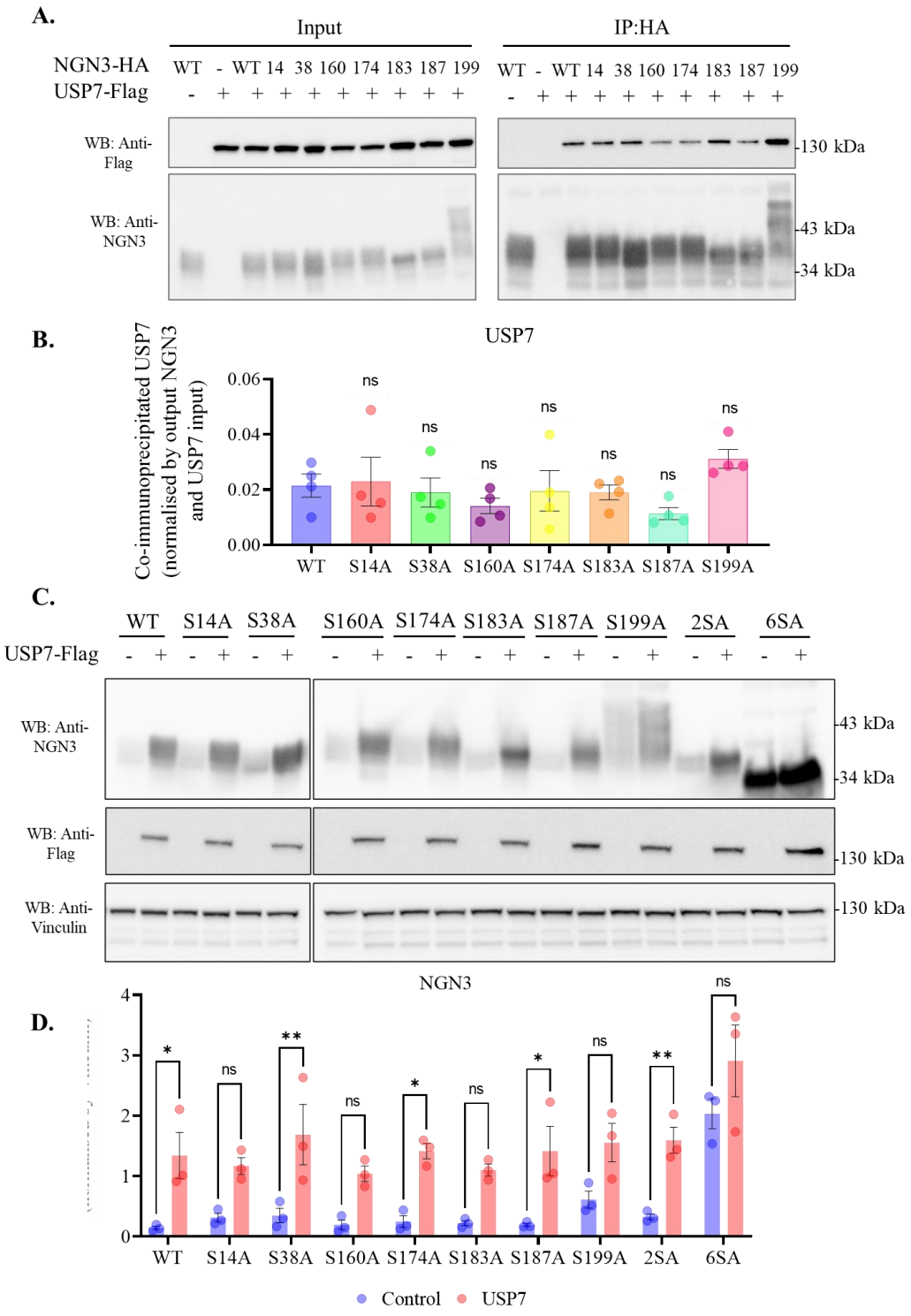

Figure 25. The NGN3/USP7 interaction is not significantly impaired by mutation at the S14, S38, S160, S174, S183, S187 or S199 predicted phosphorylation sites. A) Immunoblotting for NGN3 and Flag in an HA-NGN3 immunoprecipitation experiment. Flag-USP7 was detected in the immunoprecipitation output for WT NGN3, as well as for all single-site mutants tested. Image is representative of n=4 experiments. B) Quantification of Flag-USP7 co-immunoprecipitated with WT or mutant NGN3, normalised by NGN3 output and USP7 input from the corresponding sample, n=4. Error Bars = S.E.M, One-way ANOVA with Dunnett's multiple comparison correction. C) Immunoblotting for NGN3 in samples transfected with either Flag-USP7 or the empty pcDNA3 vector control, and NGN3 (WT or one of the tested mutants). Image is representative of n=3 experiments. D) Quantification of NGN3 (WT or mutant) protein levels from immunoblotting of samples transfected with either Flag-USP7 or pcDNA3 empty control, normalised by Vinculin, n=3. Error Bars = S.E.M, *p<0.05, **p<0.01, Two-way ANOVA with Sidak multiple comparison correction.

While all mutants seemed to be stabilised by co-transfection with USP7 (Fig. 25D), this stabilisation was only statistically significant for the wildtype HA-NGN3 (p= 0.0154), HA-NGN3-S38A (p=0.0049), HA-NGN3-S174A (p=0.0200), HA-NGN3-S187A (p=0.0128) and HA-NGN3-2SA (p=0.0091). However, as we only carried out a total of three experimental replicates, it is possible that our statistical analysis was not powerful enough to detect significant differences after correction for multiple comparisons in the case of other mutants that are visibly stabilised by USP7 overexpression (Fig. 25C). Further experimental repeats could increase the statistical power of the analysis and provide more robust evidence of the role of NGN3 phosphorylation in its interaction with USP7.

5.5 Discussion

In this chapter, we validated and characterised the interaction between NGN3 and USP7 in an overexpression HEK293A system. First, we carried out immunoprecipitation experiments for HA-NGN3 in cells transfected with both pcDNA3-HA-NGN3 and a pcDNA3.Flag-USP7 construct. Like in the case of endogenous USP7 (Fig. 13D), exogenous USP7 co-immunoprecipitates with NGN3. (Fig. 20B). Previous literature (Sancho et al. 2014), as well as our own research into HUWE1, has indicated that NGN3 phosphorylation plays an essential role in its interactions. We therefore investigated whether NGN3 phosphorylation mutants were able to interact with USP7 in the same way as the wildtype protein. While the NGN3-6SA mutant showed a significantly lower ability to pull down USP7 (Fig. 24A,B), no significant differences were observed between the single-site mutants (S14A, S38A, S160A, S174A, S183A, S187A, S199A) and wildtype. This may indicate that instead of particular NGN3 phosphorylation sites playing a role in the NGN3/USP7 interaction, a lack of overall NGN3 phosphorylation is responsible for the decrease in the NGN3-6SA/USP7 interaction. As USP7 is a deubiquitinase, and NGN3 phosphorylation at certain sites promotes NGN3 ubiquitination,

it is also possible that a lack of NGN3 ubiquitination, rather than the phosphorylation itself, prevents NGN3 from interacting with USP7, provided that NGN3 undergoes USP7-mediated deubiquitination.

Indeed, in ubiquitination assays where NGN3, USP7 and wildtype ubiquitin are overexpressed, a 1:2.5 USP7:NGN3 DNA transfection ratio is enough to significantly decrease NGN3 polyubiquitination (Fig. 21A,B). A similar decrease in NGN3 ubiquitination is not observed when Flag-USP7 is replaced with the catalytically inactive Flag-USP7^{C223A} mutant, indicating that the effect of USP7 on NGN3 ubiquitination is due to its catalytic activity as a deubiquitinase, rather than a result of other regulatory pathways, such as NGN3 transcription. By comparison, the NGN3-6SA mutant exhibits low ubiquitination levels even in the absence of USP7 overexpression (Fig. 24C,D), possibly explaining the observed decrease in the NGN3-6SA/USP7 interaction, compared to the wildtype protein.

USP7 also deubiquitinates NGN3 in experiments where wildtype ubiquitin is replaced by Ub^{K48R} and Ub^{K63R} mutants unable to form K48-linked and K63-linked polyubiquitin chains, respectively (Fig.21EF). As chains formed by the K48R mutant will be mostly K63-linked chains and vice versa, our results suggest that USP7 is able to remove both K63-linked and K48-linked polyubiquitin chains from NGN3. K48-linked ubiquitination is typically degradative, targeting its substrate to the proteasome (Swatek and Komander 2016). Therefore, by removing K48-linked chains from NGN3, USP7 could play a role in modulating NGN3 stability. As we were particularly interested in finding ways to stabilise NGN3, we decided to investigate whether USP7 overexpression could prevent its degradation. Indeed, similarly to its effect on NGN3 ubiquitination, USP7 overexpression leads to NGN3 stabilisation in a dose-dependent manner (Fig. 22A,B). Furthermore, co-transfection of NGN3 with USP7 in CHX chase experiments prevents NGN3 degradation (Fig. 22C,D), confirming that the stabilising

effect of USP7 on NGN3 stems from preventing NGN3 degradation, rather than from promoting NGN3 synthesis. These results are also mirrored in experiments where mouse HA-NGN3 is replaced with the newly generated HA-hNGN3 plasmid, inducing expression of human NGN3 (Fig. 23A-D). Despite the increased stability of hNGN3 compared to the mouse protein, USP7 overexpression still leads to significant further stabilisation. These findings are encouraging, as they indicate that targeting USP7, unlike HUWE1, could be a viable path towards NGN3 modulation during endocrine differentiation. However, additional *in vitro* and *in vivo* validation would need to be carried out, to determine whether USP7 has a similar effect on NGN3 stability within an endogenous expression system and whether the interaction has any impact on endocrine cell fate beyond the endocrine progenitor stage. As we have previously shown that Usp7 is expressed during the Ngn3 expression window in the developing human pancreas, and that the decrease in Usp7 expression precedes that of Ngn3, it is possible that USP7 is one of several interactors regulating NGN3 stability during embryonic development. While the decrease in Ngn3 transcriptional repressor HES1 early in pancreatic development provides an explanation for the initiation of the Ngn3 expression window after W8, we do not know, as of yet, what causes the sudden end of this window after W16. With HES1 expression at this timepoint still low, and expression of E3 ubiquitin ligases such as FBW7 and HUWE1 decreasing after W14, it is not excluded that another mechanism may be responsible for the decrease of NGN3 expression. Further investigation into the role of USP7 in endocrine development may therefore uncover new mechanisms that govern NGN3 expression and endocrine specification in the developing pancreas.

Chapter 6: USP7 impairment leads to reduced pancreatic endocrine differentiation

6.1 Introduction

NGN3 expression in the embryonic pancreas is transient and tightly controlled (Salisbury et al. 2014; Roark, Itzhaki, and Philpott 2012). NGN3 is not generally detected in the pancreas past W31 of human foetal development (Jennings et al. 2013; Salisbury et al. 2014) and, in the absence of NGN3+ endocrine progenitors, β cell neogenesis is not believed to occur in the adult human pancreas except as a result of stressors such as pregnancy or type 2 diabetes (Butler et al. 2010; Yoneda et al. 2013).

The pathways regulating NGN3 expression are complex. At the transcriptional level, HES1, a component of the Notch pathway, acts as a transcriptional repressor of NGN3, while SOX9 can induce Ngn3 transcription but is then downregulated by NGN3 itself, to allow for further endocrine differentiation (Shih et al. 2012). Additionally, NGN3 can act as an activator of its own transcription (Shih et al. 2012; Ejarque et al. 2013), suggesting that a layer of post-translational regulation involving enzymes such as FBW7 are required to ensure NGN3 is degraded and unable to maintain the positive auto-feedback loop, so that endocrine progenitors can progress towards a mature, functional fate. Therefore, while the results presented in the previous chapter are promising, our HEK293A system relying on NGN3 overexpression may not recapitulate normal NGN3 regulation to the extent needed for validation of the USP7/NGN3 interaction.

To address this, we collaborated with Dr Jessica Nelson from the Behrens lab on an *in vivo* mouse study, investigating the consequences of USP7 loss on the developing murine pancreas.

In particular, we assessed the effect of a Usp7 conditional knockout on the endocrine progenitor pool in mouse embryos, as well as on the size and functionality of the endocrine compartment in adult mice.

Lastly, despite the many similarities between the human and murine pancreas, some differences, particularly in NGN3 expression patterns during development, do exist. For instance, while there is biphasic NGN3 expression during mouse pancreatic development (Villasenor, Chong, and Cleaver 2008), only one expression wave has been detected in the development of the human pancreas (Jennings et al. 2013). Moreover, while NGN3 loss leads to a complete lack of endocrine cells in the murine pancreas (Gradwohl et al. 2000), low levels of c-peptide can be detected in the blood of human patients with null NGN3 mutations (Pinney et al. 2011; Rubio-Cabezas et al. 2011), indicating that a small number of β cells may still develop in the absence of NGN3. Therefore, a thorough investigation of the role of USP7 in NGN3 regulation and endocrine specification would require further validation in a system that can more closely mimic human pancreatic development, featuring endogenous NGN3 expression. To achieve this, we used a human iPSC-to-β-cell differentiation model to assess the effect of USP7 chemical inhibition on NGN3 stability and endocrine cell generation.

6.2 USP7 knockout leads to impaired endocrine differentiation in mice

In the previous chapter, we showed that USP7 can deubiquitinate NGN3 in an overexpression HEK293A system, leading to its stabilisation in the cell. To validate our findings in an *in vivo*, endogenous expression model, we collaborated with Dr Jessica Nelson (Behrens Lab, Institute for Cancer Research) to generate Pdx1-Cre $Usp7^{-/-}$ mice (Fig. 26A) and investigated the effect of Usp7 knockout on the development of the endocrine pancreas. As the knockout is conditioned by expression of Pdx1, its effects would be limited to tissues such as the pancreas

and duodenum, avoiding the previously described embryonic lethality (N. Kon et al. 2010) as a consequence of the indiscriminate knockout of Usp7. This allowed us to assess the USP7$^{-/-}$ phenotype in both embryonic and adult mice.

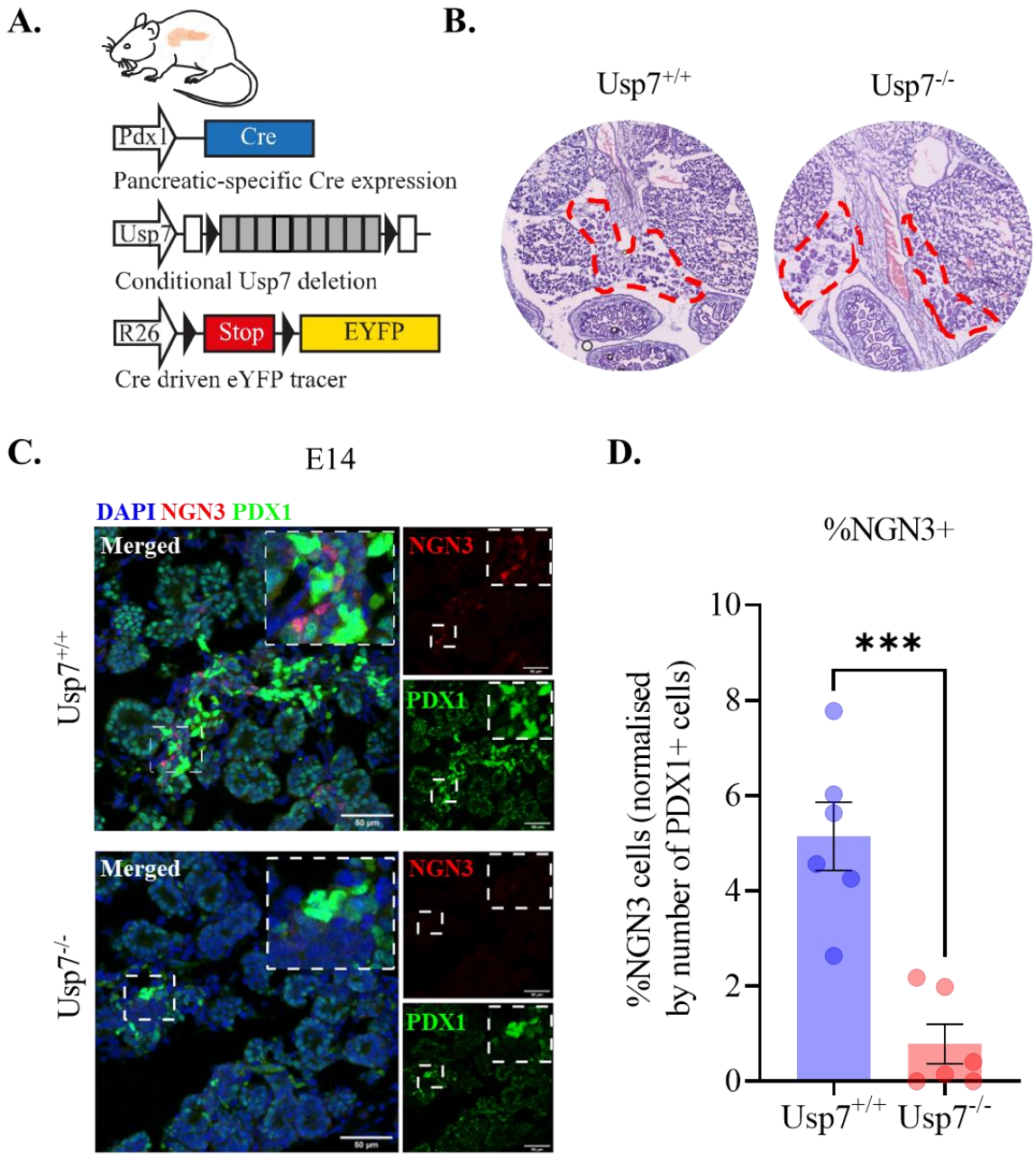

Figure 26. Conditional Usp7 knockout in the pancreas of mouse embryos depletes NGN3+ endocrine progenitors at E14. A) Schematic of pancreatic-specific Usp7 knock-out mouse. B) H&E staining of Usp7$^{+/+}$ and Usp7$^{-/-}$ mouse embryo sections. The pancreas is marked by the red dotted line. C) Immunofluorescent staining for NGN3 (red) and PDX1 (green) in the pancreas of E14 Usp7$^{+/+}$ and Usp7$^{-/-}$ mouse embryos. Scale bar = 50 µM, 40x Magnification. D) Quantification of NGN3 immunofluorescent staining in Usp7$^{+/+}$ and Usp7$^{-/-}$ mouse embryos, normalised by the number of PDX1+ cells, n=6 (6 embryos per genotype with 5 frames quantified for each embryo). Error bars = S.E.M, ***p<0.001, Unpaired Two-tailed Student t-test.

Firstly, we collected $Usp7^{+/+}$ and $Usp7^{-/-}$ mouse embryos at E14, when NGN3 should be highly expressed at protein level (Villasenor, Chong, and Cleaver 2008). H&E staining of sections generated from these embryos reveals the presence of a similarly developed pancreas in both wildtype and $Usp7^{-/-}$ embryos (Fig. 26B), indicating that at least until this developmental stage, Usp7 knockout did not produce noticeable changes in pancreas architecture. However, immunofluorescent staining for NGN3 revealed significantly fewer NGN3+ endocrine progenitors in $Usp7^{-/-}$ embryos compared to wildtype (0.79 ± 1.01% vs 5.15 ± 1.75%, p=0.0004, Unpaired Two-Tailed Student t-test) (Fig. 26C,D), indicating that USP7 plays an essential role in NGN3 stabilisation during pancreatic development.

As NGN3 expression is essential for the specification of endocrine cells in the pancreas, we next investigated how the USP7 knockout had affected the development and function of the pancreas in adult mice (5-7 weeks). Immunohistochemical staining experiments revealed visibly smaller islets in Usp7 knockout mice compared to wildtype (Fig. 27A), as emphasised by significantly decreased insulin staining ($p<0.0001$, Unpaired Two-tailed Student t-test) (Fig. 27B). Additionally, immunofluorescent staining for GCG and SST, alongside c-Peptide, shows significant decreases in the proportion of α cells and δ cells, as well as β cells in the pancreas of $Usp7^{-/-}$ mice (Fig. 27F-I). As all major endocrine cell types were affected by the knockout, this finding provides further proof of the essential role played by USP7 in endocrine cell specification through its regulation of NGN3. While knockout mice exhibit a 2x lower pancreas weight compared to control (Fig. 27D), this can be mostly explained by the lower body weight of these mice (Fig. 27C). As islets make up less than 5% of the pancreas volume (Paredes et al. 2014; Eriksson et al. 2013; Ionescu-Tirgoviste et al. 2015), it is improbable that the decrease in islet size would lead to a roughly 50% decrease in pancreas weight. In addition to lower pancreas and body weight, Usp7 knockout mice also exhibit elevated blood glucose levels (Fig. 27E) suggesting a diabetic phenotype, a likely consequence of reduced β-cell numbers.

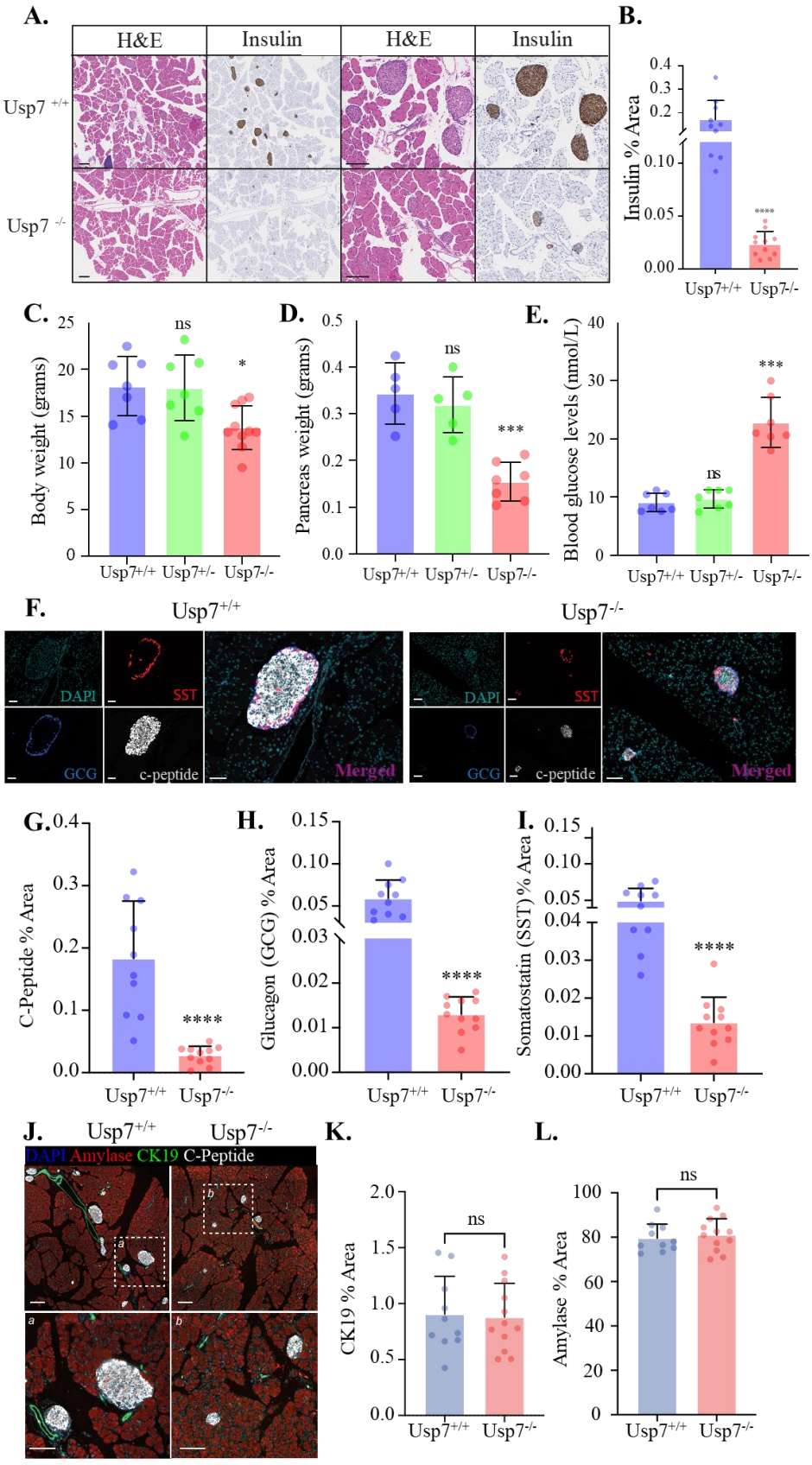

Figure 27. Conditional Usp7-/- in the pancreas during mouse embryonic development leads to decreased α, β and δ cell numbers and a diabetic phenotype. A) Histological and immunohistochemical analysis of Insulin expression in Usp7$^{+/+}$ and Usp7$^{-/-}$ pancreatic tissues from 5-7 weeks old mice. Scale bar on left is 200μm and scale bar on right is 100μm. B) Quantification of Insulin positive staining area (n=10-11). C) Whole body weight (in

grams) in indicated mice, measured in 5-7 weeks old mice. D) Weight (in grams) of pancreas in indicated mice, in 5-7 weeks old mice. E) Circulating blood glucose concentrations measured in indicate mice, in 5-7 weeks old mice. F) Representative images of immunofluorescent staining for C-peptide (white), Somatostatin (SST; red), Glucagon (GCG; blue) and DAPI (teal) in $Usp7^{+/+}$ and $Usp7^{-/-}$ pancreatic tissues from 5-7 weeks old mice. Scale bar is 50µm. G) Quantification of C-peptide positive staining area (n=10-11 mice per group). H) Quantification of Somatostatin (SST) positive staining area (n=10-11 mice per group). I) Quantification of Glucagon (GCG) positive staining area (n=10-11 mice per group). J) Representative images of immunofluorescent staining for Amylase (red), CK19 (green), C-peptide (white) and DAPI (blue) in $Usp7^{+/+}$ and $Usp7^{-/-}$ pancreatic tissues from 5-7 weeks old mice. Scale bar on top is 200µm, and scale bar on bottom is 100µm. K) Quantification of Amylase positive staining area (n=11-12 mice per group). L) Quantification of Amylase positive staining area (n=11-12 mice per group). Error bars = S.E.M, *p<0.05, **p<0.01, ***p<0.001, ****p<0.0001. All data included in this figure was collected and analysed by Dr Jessica Nelson (Behrens Lab).

Despite the dramatic effect triggered by Usp7 knockout in the endocrine compartment of the murine pancreas, no significant differences were detected in the expression of ductal marker CK19 or acinar marker Amylase (Fig. 27J-L) between knockout and wildtype mice, suggesting that the exocrine compartment was not affected by loss of USP7. Considering the decreased body and pancreas weight of knockout mice, it is not excluded that the Usp7 knockout could have additional, detrimental effects on pancreatic development. However, our findings show that endocrine cell generation in particular was disproportionately affected by USP7 loss. This is consistent with decreases in NGN3 stability and endocrine progenitor numbers during embryonic development.

6.3 USP7 inhibition during iPSC-to-β-cell differentiation *in vitro* impairs generation of β-like cells due to reduction in NGN3 stability

We previously showed that exogenous NGN3 and USP7 can interact in HEK293A cells, with USP7 deubiquitinating and stabilising NGN3. Furthermore, USP7 loss in the mouse pancreas during embryonic development leads to destabilisation of NGN3, a reduction in the endocrine progenitor pool, decreased islet size, and elevated blood glucose levels. While these findings strongly indicate a key role for USP7 in endocrine specification in the pancreas, it is still not clear whether they can be recapitulated in an endogenous NGN3 expression model of human pancreatic development. Therefore, we employed an iPSC-derived pancreatic progenitor

differentiation model to investigate the effect of USP7 inhibition on NGN3 expression and endocrine cell generation. We adapted the Hogrebe protocol (Hogrebe et al. 2020), switching from 2D to a 3D differentiation within Matrigel domes in suspension (Fig. 28A) and treated the cells with GNE6440 (Kategaya et al. 2017), a chemical inhibitor specific to USP7, for the duration of the endocrine progenitor stage (D5-12). At D12, immunofluorescent staining for NGN3 reveals a significant decrease in the percentage of NGN3+ cells after GNE6640 treatment compared to the control (5.09% ± 2.97 vs 14.88% ± 4.71, p=0.0043, Unpaired Two-tailed Student t-test), supporting our *in vivo* findings (Fig. 28B).

Immunofluorescent staining for INS, GCG and SST at D20 (end of differentiation) showed successful differentiation to β-, α- and δ-like cells in the control samples (Fig. 28D), while the percentage of INS+ β-like cells in the GNE6640-treated samples was significantly decreased (4.54% ± 3.71 vs 11.32 ± 4.96, p= 0.0403, Unpaired Two-tailed Student t-test) (Fig. 28E). However, decreases were not significant in the case of GCG (1.91% ± 0.86 vs 3.57% ± 1.57, p=0.0711, Unpaired Two-tailed Student t-test) or SST (11.01% ± 3.87 vs 15.01% ± 5.51, p=0.2214, Unpaired Two-tailed Student t-test).

Despite a lower percentage of NGN3+ cells in GNE6640-treated samples at D12, Ngn3 gene expression was not significantly decreased (Fig. 28F). This indicates that NGN3 protein stabilisation, rather than upregulated Ngn3 transcription, is responsible for the increase in NGN3+ progenitor numbers. In contrast, we found significantly decreased gene expression of Ins (0.36 ± 0.14 vs 1.09 ± 0.55 p=0.0004, Two-way ANOVA with Sidak correction) and Gcg (0.62 ± 0.35 vs 3.65 ± 3.91, p=0.0361, Two-way ANOVA with Sidak correction) in GNE6640-treated samples at D20. No change was observed in Sst gene expression in GNE6640-treated samples at D20 (6.06 ± 2.45 vs 33.43 ± 44.18, p=0.0995, Two-way ANOVA with Sidak correction).

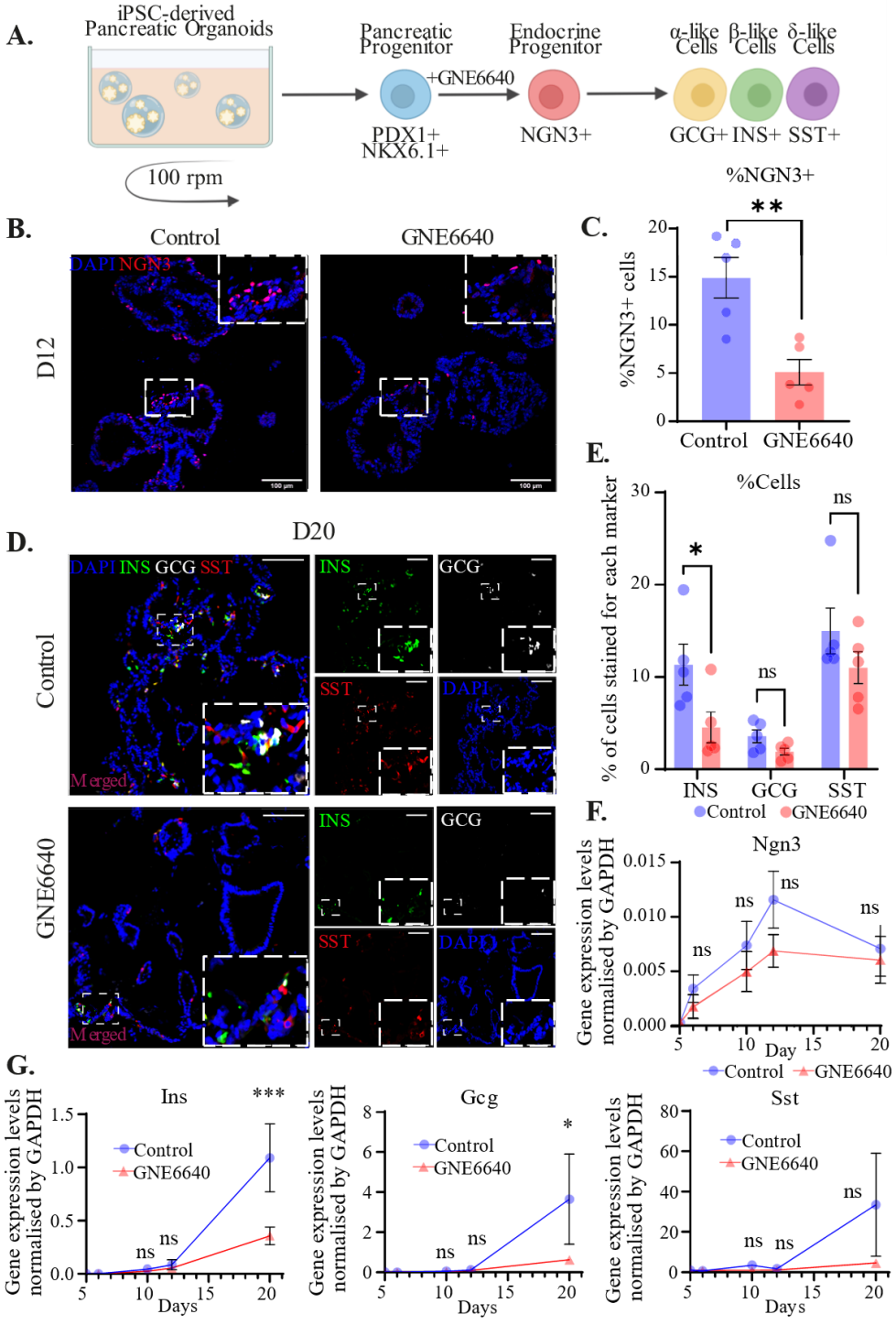

Figure 28. USP7 inhibition during iPSC-to-β-cell differentiation destabilises NGN3 and impairs endocrine specification. A) Diagram of the adapted Hogrebe protocol. B) NGN3 immunofluorescent staining in control and GNE6640-treated samples at D12. C) Quantification of NGN3 immunofluorescent staining in D12 control and GNE6640-treated samples. Datapoints represent separate differentiation experiments. Error bars = S.E.M, n=5, Student t-test. D) Immunofluorescent staining for INS, GCG and SST in D20 control and GNE6640-treated samples. Scale bar = 100 µM E) Quantification of INS, GCG and SST immunostaining in control and GNE6640-treated samples. Datapoints represent separate differentiation experiments. Error bars = S.E.M, n=5, Unpaired two-tailed Student t-test. F) Ngn3 gene expression normalised by Gapdh in GNE6640-treated and control samples. Error bars = S.E.M, n=4, Two-way ANOVA with Sidak multiple comparison correction; Comparison against Control sample from the same timepoint. G) Ins, Gcg and Sst gene expression normalised by Gapdh in GNE6640-treated and control samples. Error bars = S.E.M, n=3, *p<0.05, ***p<0.001, Two-way ANOVA with Sidak multiple comparison correction; Comparison against Control sample from the same timepoint.

6.4 Discussion

In this chapter, we investigated the role of USP7 in the regulation of NGN3 and endocrine specification in two systems featuring endogenous expression of NGN3. Firstly, we addressed how USP7 loss affected the development of the endocrine compartment of the pancreas in mice, by assessing the size of the endocrine progenitor pool in mouse embryos with a conditional Usp7 knockout genotype. We found that USP7 loss led to a considerable reduction in NGN3+ endocrine progenitor numbers at E14 (Fig. 26C,D), which translated to greatly reduced islet size in the adult mouse (Fig. 27A). While the proportion of the pancreas occupied by α, β, and δ cells was significantly decreased as a result of the Usp7 knockout (Fig. 27F-I), the proportion occupied by exocrine cells, such as ductal or acinar cells, was not significantly affected (Fig. 27J-L), indicating that the knockout specifically affected the endocrine pancreas. This would be consistent with USP7 playing an important role in NGN3 stabilisation, as NGN3 expression pushes cells towards an endocrine fate during pancreatic development (Sheets et al. 2018; Pinney et al. 2011).

Despite USP7 loss not affecting the proportion of ductal and acinar cells within the pancreas, knockout mice did exhibit decreased pancreas weight, alongside decreased body weight and increased blood glucose levels (Fig. 27C-E). While the increase in blood glucose levels can be easily explained by the reduction in islet size and β-cell numbers, the decrease in pancreas and body weight may be similarly caused by insulin deficiency, as this was shown to affect foetal growth (Fowden 1992). As islets represent only a small percentage of pancreatic weight, the reduction in islet size alone cannot account for the notable reduction in pancreas size, suggesting that while the proportion of acinar and ductal cells making up the pancreas remains unchanged, there is likely a reduction in the absolute numbers of these cell types after Usp7 knockout.

Previous studies have shown that USP7 inhibition can affect cell proliferation, due to the role of USP7 in stabilising substrates such as PLK1 (Y. Peng et al. 2019; Galarreta et al. 2021). While the decrease in the pancreas size of adult knockout mice could be due to the insulin deficiency caused by reduced β-cell numbers, as the Usp7 knockout is induced by Pdx1 expression, we cannot exclude the possibility that one side-effect of the knockout is a decrease in the proliferation of PDX1+ pancreatic progenitors. This would lead to a reduction in pancreas size even before the appearance of NGN3+ endocrine progenitors, and, in turn, to a smaller NGN3+ progenitor pool, independent of the effect of Usp7 knockout on NGN3 stability. However, in the quantification of NGN3+ endocrine progenitors in E14 embryos, Usp7 knockout embryos showed a reduction in NGN3+ cell numbers even after normalisation by the number of PDX1+ pancreatic cells, indicating that even after controlling for a potential effect of Usp7 knockout on proliferation, USP7 loss still disproportionately impacts endocrine cell populations through its effect on NGN3 stability.

We next validated our findings in and *in vitro* iPSC-to-β-cell differentiation model, starting with pancreatic progenitors derived from healthy human donor iPSC line Kute-4. We chemically inhibited USP7 for the entire duration of the endocrine differentiation stage (D5-12 of our differentiation protocol) and analysed the effect of this inhibition on NGN3 stability and endocrine cell generation (Fig. 28B-G). USP7 inhibition led to a 3x decrease in NGN3+ endocrine progenitors at the end of the endocrine differentiation stage, which translated to a decrease in INS+ β-like cells by D20 (end of differentiation). We found no significant differences in Ngn3 gene expression between treated and untreated samples throughout the differentiation, suggesting that the effect of USP7 inhibition on NGN3+ cell numbers is likely due to decreased NGN3 stability, rather than due to a decrease in its transcription. On the other hand, USP7 inhibition resulted in lower Ins and Gcg gene expression at D20, which also translated to a decrease at protein level, in the case of INS. This is consistent with the

hypothesis that USP7 inhibition during the endocrine differentiation stage affects NGN3 protein stability, which in turn has a knock-on effect on endocrine differentiation, leading to decreased Ins gene expression and finally, to lower numbers of INS+ cells. While we also see a decrease in Gcg gene expression, this does not result in a significant decrease in GCG+ cells.

These results mostly reflect our previous findings in Usp7 knockout mice. As in our *in vitro* assays USP7 is only inhibited during the NGN3 expression window (D5-12), we are able to exclude possible side-effects of USP7 inhibition during other differentiation stages, in contrast to our previous *in vivo* experiments. This could explain why GCG+ and SST+ cell populations do not seem to be impacted by USP7 inhibition in the same way they were in Usp7 knockout mice. It has been previously suggested that endocrine progenitors generated at different developmental timepoints during mouse pancreatic development may be biased towards specific endocrine cell fates (Scavuzzo et al. 2018). It is not clear whether this is recapitulated by *in vitro* differentiation assays. However, if this was the case, it could explain why USP7 inhibition for a limited timeframe during the differentiation had a disproportionate effect on the generation of certain types of endocrine cells and not others. Alternatively, as we have shown that $Usp7^{+/-}$ mice do not exhibit a visible phenotype, and as previous literature has not described a pancreatic phenotype in patients with Usp7 heterozygous loss-of-function mutations (Fountain et al. 2019), it is likely that even a considerable reduction in USP7 activity, like in the case of our USP7 chemical inhibition assays, will not have as great an impact on endocrine specification as a complete Usp7 knockout.

Our findings in both mouse and human iPSC models confirm the essential role played by USP7 in NGN3 regulation and endocrine pancreas development, indicating that USP7 modulation could be a valid strategy for NGN3 stabilisation. In turn, this stabilisation may be able to boost exocrine-to-endocrine plasticity as well as iPSC-to-β-cell differentiation *in vitro*. While several

USP7 small molecule inhibitors exist, to our knowledge, no small molecule activators of USP7 have been described. Therefore, future research could investigate different approaches to boost USP7 activity, and their effect on pancreatic plasticity and β cell generation.

Chapter 7: Discussion

7.1 Introduction

This thesis aimed to validate new regulators of NGN3 stability and investigate their role in pancreatic endocrine specification. We carried out an IP-MS experiment to identify NGN3 interactors that may play a role in NGN3 post-translational regulation and further investigated these interactions and their mechanisms in HEK293A cells, iPSC-derived pancreatic progenitors, and, in the case of USP7, in a Usp7 knockout mouse model.

As phosphorylation has been shown to play a role in NGN3 stability, in chapter 3, we generated and characterised several phosphorylation mutants of murine and human NGN3 for use in future experiments. We then identified USP7 and HUWE1 as potential NGN3 interactors and confirmed the ability of these endogenous proteins to co-immunoprecipitate with exogenous NGN3 in HEK293A cells. Furthermore, the analysis of an scRNAseq public dataset containing human foetal pancreas samples at different timepoints throughout development revealed that both Huwe1 and Usp7 are expressed during the Ngn3 expression window, suggesting a possible role of these factors in NGN3 regulation and pancreatic development.

In chapter 4, we focused on the interaction between NGN3 and HUWE1, investigating the role of NGN3 phosphorylation in the interaction and the effect of HUWE1 inhibition on NGN3 ubiquitination and stability. We found that exogenous NGN3 interacts with endogenous HUWE1 in HEK293A cells, and that a lack of phosphorylation close to the C-terminus of NGN3 impairs the interaction. While treatment with an inhibitor of HECT E3 ubiquitin ligases (Heclin) reduced NGN3 ubiquitination, treatment with the specific HUWE1 inhibitor BI8622 did not have a significant impact on NGN3 ubiquitination, and neither treatment led to NGN3 stabilisation in our HEK293A cell system. Furthermore, Heclin treatment did not stabilise

NGN3 or boost β-like cell differentiation in an iPSC-derived pancreatic progenitor system, suggesting that HUWE1 may not be a regulator of NGN3 stability under the tested experimental condition.

Finally, in chapters 5 and 6, we validated the interaction of NGN3 with USP7 and described the essential role that USP7 plays in NGN3 post-translational regulation and endocrine specification during pancreatic development. We showed that USP7 overexpression leads to a decrease in NGN3 ubiquitination, including K48-linked polyubiquitin chains, which are mainly responsible for targeting their substrate to the proteasome for degradation. As a result, co-transfection of NGN3 with USP7 leads to NGN3 stabilisation in HEK293A cells, while USP7 inhibition during iPSC-to-β-cell differentiation leads to a decrease in NGN3+ endocrine progenitor numbers and in the generation of β-like cells. USP7 loss in the mouse embryonic pancreas leads to a similar decrease in NGN3+ progenitors at E14, with smaller islets and a diabetic phenotype observed in the adult mice.

This study proposes a novel mechanism for NGN3 post-translational regulation during pancreatic development, dependent on USP7-mediated deubiquitination (Fig. 29). This mechanism is key for NGN3 stabilisation, facilitating endocrine specification in pancreatic progenitors and ensuring the normal development of pancreatic islets.

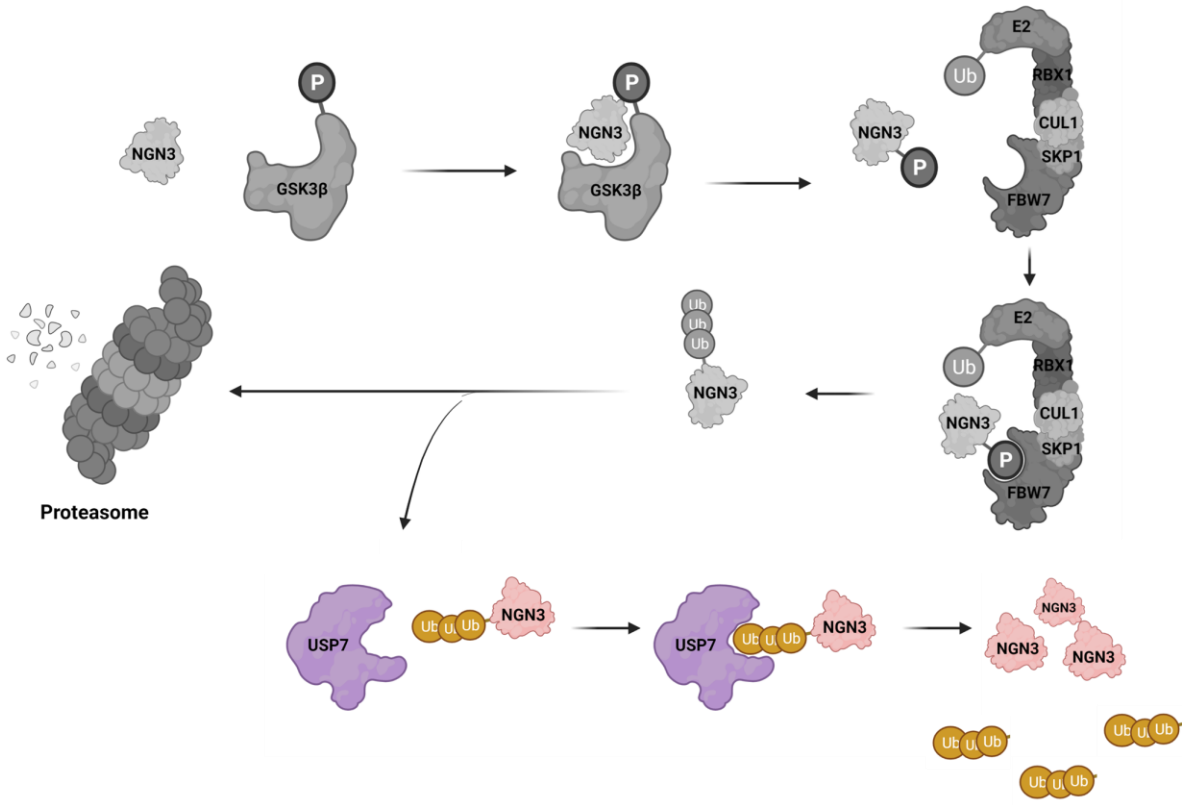

Figure 29. Updated diagram of NGN3 proteasomal degradation pathway. Greyscale: previously known interactions. Colour: Mechanism described in this study. USP7 interacts with ubiquitinated NGN3 and cleaves off ubiquitin chains, preventing NGN3 degradation.

7.2 Phosphorylation plays an integral part in NGN3 post-translational regulation

Phosphorylation can modulate NGN3 stability, with NGN3-6SA, a form of NGN3 with mutations at six different predicted phosphorylation sites, being significantly more stable than the wildtype protein (Azzarelli et al. 2017). While the importance of NGN3 phosphorylation at residues S183 and S187 in the context of its interaction with FBW7 has been previously described (Sancho et al. 2014), little was known about the role other phosphorylation sites mutated in the NGN3-6SA mutant played in NGN3 regulation and function. In this study we show that phosphorylation sites closer to the C-terminus of NGN3, such as S174, S183, S187 and possibly also S199 promote the interaction of exogenous NGN3 with endogenous HUWE1

in a HEK293A *in vitro* system. Mutating these sites impairs the NGN3/HUWE1 interaction, indicating that a similar mechanism could be at play for the recognition of NGN3 by HUWE1 as for its recognition by FBW7.

To our knowledge, only the S183 and S187 sites have been studied in connection with the NGN3/FBW7 interaction so far, as they can be phosphorylated by GSK3β (Sancho et al. 2014). GSK3β phosphorylates other substrates such as NOTCH1 and c-MYC (G. Wu et al. 2001; Welcker et al. 2004) and targets them to FBW7 for ubiquitination, suggesting that GSK3β-meditated phosphorylation may play a similar role in the case of NGN3. For this reason, S183 and S187, predicted GSK3β phosphorylation sites, initially provided the most promising targets for investigations into the NGN3/FBW7 interaction mechanism. However, we have now shown that the NGN3-2SA mutant protein, in which both S183 and S187 are mutated, can still be stabilised by treatment with the GSK3β inhibitor CHIR99021, while the 6SA mutant shows no stabilisation. These results indicate that aside from S183, one or more of the five other sites mutated in the NGN3-6SA mutant may undergo GSK3β-meditated phosphorylation under normal circumstances, contributing to NGN3 degradation. They may therefore be involved in the interaction of NGN3 with FBW7, requiring further investigation.

The NGN3-6SA mutant showed a decreased ability to interact with USP7 when compared to NGN3 WT. However, as USP7 is a deubiquitinase, we wondered whether the impairment of the interaction was a direct consequence of the lower NGN3 phosphorylation levels, or a secondary effect of a decrease in NGN3 ubiquitination as a result of lower phosphorylation. We showed that the NGN3-6SA mutant exhibits low ubiquitination at baseline levels, with no significant reduction after USP7 overexpression. Furthermore, when analysing the effect of each of the six phosphorylation sites separately, none of the single-site mutants showed significant decreases in their ability to pull down USP7, suggesting that the NGN3/USP7

interaction is not dependent on a single phosphorylation site. It is therefore likely that a lack of ubiquitination in the NGN3-6SA mutant, rather than a lack of phosphorylation, leads to a reduction in the protein's interaction with USP7.

Besides contributing to the interactions between NGN3 and enzymes such as FBW7 or HUWE1, phosphorylation may also affect NGN3 function. In our experiments, some NGN3 phosphorylation mutants, such as S160, 2SA and 6SA showed a significantly decreased ability to induce expression of Nkx2.2, a target of NGN3-mediated transcriptional activation. However, further experiments using the human NGN3 protein and the corresponding phosphorylation mutants would be necessary to validate these findings, as it is possible that, although limited, the differences between the structures of mouse and human NGN3 affect the function of certain NGN3 mutants in the human HEK293A system, while this may not be the case for similar mutants of human NGN3. Indeed, mutating the same residue in mouse and human NGN3 can have radically different consequences on NGN3 post-translational regulation, as illustrated by the mutation of the S199 site in either the mouse or human protein. Despite the serine being mutated to an alanine residue in the mouse protein, and to a phenylalanine residue in the human one, to reflect the S199F SNP previously identified in the human population, the differences between the two amino acids may not be sufficient to explain the dramatic differences in NGN3 post-translational modification, as they are both hydrophobic, non-polar residues. The more likely explanation is that the serine residue at position 199 is subjected to different post-translational modification events in mice and humans, and thus its mutation leads to different outcomes for NGN3.

Lastly, while here we focused on seven predicted phosphorylation sites that were previously studied in connection with the degradation pathway of mouse NGN3 (S14, S38, S160, S174, S183, S187, S199) (Azzarelli et al. 2017; Sancho et al. 2014), other serine, threonine and

tyrosine residues on NGN3 could be sites for phosphorylation. Therefore, a lot is still unknown about how specific phosphorylation events affect the stability and function of NGN3, and which kinases, other than GSK3β, play a role in NGN3 post-translational regulation. Answering these questions could provide new targets for NGN3 modulation and could allow for optimisation of differentiation protocols aiming to generate specific pancreatic cell types.

7.3 HUWE1 inhibition does not significantly stabilise NGN3

One of the NGN3 interactors we identified in our IP-MS experiment was E3 ubiquitin ligase HUWE1. While research into HUWE1 function within the pancreas has been limited, one study has investigated the effect of a pancreas specific Huwe1 knockout in mice, showing a detrimental effect on β cell mass (L. Wang et al. 2014). However, the reduction was attributed to p53-mediated β cell apoptosis and the aging process aggravated this phenotype. Therefore, it is unlikely that this decrease in β cell mass is due to an effect of HUWE1 on NGN3 regulation, as any such effect would precede the existence of mature β cells in the pancreas. As NGN3 is not generally expressed in the mouse pancreas after E18.5 (Villasenor, Chong, and Cleaver 2008; Mellitzer et al. 2004), the severity of the phenotype would most likely become apparent soon after birth, rather than being exacerbated by age. Instead, with p53 being a known substrate of HUWE1 (D. Yang et al. 2018), HUWE1 loss leads to a decrease in p53 ubiquitination and an increase in its stability, which, in turn, results in apoptosis. While this does not exclude an additional effect of HUWE1 loss on NGN3 stability during pancreatic development, the study did not investigate the effect of HUWE1 loss during pancreas embryonic development, or mice younger than 1 month.

We found that endogenous HUWE1 co-immunoprecipitates with exogenous NGN3 in HEK293A cells, and that this interaction is promoted by phosphorylation at the C-terminus of NGN3. However, while we observed a reduction in NGN3 ubiquitination upon treatment with

a broad HECT E3 ubiquitin ligase inhibitor (Heclin), this was not recapitulated in experiments where BI8622, a specific HUWE1 inhibitor, was used. Furthermore, no NGN3 stabilisation was observed in HEK293A cells after either of the two treatments, or in iPSC-derived endocrine progenitors after Heclin treatment, indicating that HUWE1 may not significantly contribute to NGN3 ubiquitination and proteasomal degradation under our experimental conditions. It is also possible that our 24 h Heclin treatment window, especially during the iPSC-to-β-cell differentiation experiments, was too short to induce a detectable change in NGN3 levels. A similar experiment aiming to inhibit USP7 activity yielded a considerable change in NGN3+ cell numbers after maintaining treatment for the chemical inhibition of USP7 for the entire duration of the NGN3 protein expression window. Additional experiments with an extended window of Heclin or BI8622 treatment may result in a more noticeable stabilisation of NGN3.

Another way to investigate the NGN3/HUWE1 interaction would be to analyse how NGN3 ubiquitination and stability are affected by HUWE1 overexpression, as opposed to its chemical inhibition, in similar experiments as have been carried out for USP7. However, due to the large size of the HUWE1 sequence, we have encountered obstacles in generating, expanding and transducing a plasmid vector that would induce full length HUWE1 overexpression. Future experiments could explore ways to optimise this process, for instance using adenoviral transduction systems.

7.4 USP7 deubiquitinates and stabilises pro-endocrine transcription factor NGN3

In addition to HUWE1, we identified USP7 as another interactor of NGN3 in our IP-MS experiment. This was of particular interest as it was the first known interaction between NGN3 and a deubiquitinase, providing further insight into the post-translational regulation of NGN3

through the ubiquitin-proteasome system. Our experiments showed that exogenous NGN3 can interact with both endogenous and exogenous USP7 in HEK293A cells, with USP7 overexpression resulting in reduced NGN3 ubiquitination and increase stability. These findings were further recapitulated in an iPSC-to-β-cell differentiation model, where USP7 inhibition during the endocrine differentiation stage led to a significant decrease in the proportion of NGN3+ cells and to a reduction in Ins and Gcg gene expression and in INS+ β-like cell numbers by the end of the differentiation. Conditional Usp7 knockout in the mouse embryonic pancreas leads to a similar reduction in NGN3+ endocrine progenitors at E14, while adult mice exhibit a decreased proportion of endocrine cells in the pancreas, decreased body and pancreas mass and increased blood glucose levels, reminiscent of a diabetic phenotype. We therefore demonstrated that USP7 plays an essential role in endocrine specification in the pancreas, through its ability to deubiquitinate and stabilise NGN3. However, no impact of Usp7 heterozygous loss-of-function mutations on the pancreas has been described so far in human patients, despite an otherwise strong phenotype, with symptoms such as intellectual disability, seizures, hypotonia and autism spectrum disorders (Fountain et al. 2019). This is consistent with the lack of phenotype we observed in our $Usp7^{+/-}$ mice (Fig. 27C-E), indicating that only a complete ablation of USP7 will result in a noticeably impacted pancreatic endocrine compartment. No patients with homozygous loss-of-function mutations in Usp7 have been identified. As complete Usp7 knockout in mice leads to early embryonic lethality (N. Kon et al. 2010), this is likely also the case for human embryos, explaining the lack of $Usp7^{-/-}$ patients.

We showed that NGN3 is a substrate for USP7, and that NGN3 ubiquitination, rather than phosphorylation, promotes this interaction. However, we have not yet investigated whether post-translational modifications on USP7 could affect substrate recognition. It has been previously revealed that CK2-mediated phosphorylation of USP7 at residue S18 modulates its affinity for certain substrates. For instance, the phosphorylated form of USP7 is more likely to

bind MDM2, while the dephosphorylated form favours p53 binding (Khoronenkova et al. 2012). Therefore, to investigate which form of USP7 has a higher affinity for NGN3 binding, NGN3/USP7 immunoprecipitation assays could be repeated using a $USP7^{S18A}$ mutant plasmid. As phosphatase PPM1G can dephosphorylate USP7 at S18 (Khoronenkova et al. 2012), future experiments could modulate either CK2 or PPM1G activity to promote the post-translational modification that boosts the USP7/NGN3 interaction. One option for CK2 inhibition is ATP-competitive inhibitor CX-4945 (Chon et al. 2015), while cadmium has been found to inhibit PPM1G (C. Pan et al. 2013). While we have previously shown that endogenous NGN3 can be destabilised by USP7 inhibition during pancreatic endocrine differentiation, these experiments would help establish whether it is possible to stabilise it instead, by boosting USP7 activity. Additionally, previous studies have achieved exocrine-to-endocrine cell transdifferentiation by using an adenoviral construct to induce NGN3 overexpression in ductal or acinar cells (Weida Li et al. 2014; Zhou et al. 2008; Demcollari, Cujba, and Sancho 2017), or knocking out FBW7, an E3 ubiquitin ligase responsible for NGN3 ubiquitination and degradation (Sancho et al. 2014). Therefore, future assays could assess whether inducing USP7 overexpression in ductal or acinar cells using an adenoviral construct could result in similar exocrine-to-endocrine plasticity.

Lastly, while transient NGN3 expression is necessary for the endocrine specification of pancreatic progenitors, loss of NGN3 expression is also required for successful maturation of endocrine cells. During our iPSC-to-β-cell differentiation experiments, we found that although Ngn3 gene expression declined after D12, it was still relatively high by D20 (end of differentiation) compared to expression at D5, before the start of the endocrine differentiation stage (Fig. 28F). If this phenomenon were to be recapitulated at protein level, the maintained NGN3 expression could slow down β-cell maturation. As improving the maturation of β-cells generated *in vitro* has long been an aim in the field of diabetes and stem cell research

(Hohmeier, An, and Newgard 2019), it would be interesting to investigate whether USP7 chemical inhibition after D12 could accelerate the endocrine cell maturation process by destabilising NGN3 once endocrine specification has been achieved.

7.5 Research limitations

While in this project we identify USP7 as a potential regulator of NGN3 stability and endocrine specification in the pancreas, our research, in its current state, does pose certain limitations. Firstly, an NGN3 overexpression system in HEK293A cells was used to identify possible NGN3 interactors and to investigate the NGN3/USP7 interaction *in vitro*, as generating sufficient numbers of NGN3+ iPSC-derived endocrine progenitor cells for experiments such as immunoprecipitation assays was not feasible using currently available differentiation protocols. To our knowledge, no immortalised pancreatic cell lines with endogenous NGN3 expression exist, at present. However, a possible improved model to study NGN3 interactors could be the pancreatic adenocarcinoma cell line PANC-1. While lower transfection efficiency in this cell line compared to HEK293A cells prevented us from using it widely for our experiments, the generation of a stable line of PANC-1 cells with doxycycline-inducible expression of NGN3 could help provide a more biologically relevant alternative for the study of NGN3 interactions.

Secondly, while our preliminary IP-MS experiment did uncover USP7 as a possible interactor of NGN3, due to the reduced number of sample replicates (two NGN3-HA samples and one pcDNA3.HA control) and the lack of additional controls (e.g. other HA-tagged proteins) it is likely that many of the hits identified in the experiment could be false positives that would require extensive additional validation. Repeating this assay with additional replicates and controls, in a more biologically relevant system (e.g. PANC-1 cells), could validate our existing findings, or identify new interactors of NGN3.

Finally, while USP7 overexpression seems to stabilise ectopic NGN3 in our *in vitro* HEK293A system, we cannot exclude the possibility that the phenotype observed in mice and iPSC-derived pancreatic progenitors after USP7 inhibition or loss could be independent of NGN3-destabilisation. USP7 is known to interact with substrates involved in cell proliferation and apoptosis, such as p53. While we attempted to control for this effect in our experiments by normalisation to either the number of PDX1+ pancreatic cells in mice, or to total number of cells in our *in vitro* iPSC differentiation assays, this would not account for an additional effect USP7 loss could have on the survival of NGN3+ endocrine progenitors in particular. Immunofluorescent staining for apoptosis markers such as Caspase-3 in both the wildtype and $Usp7^{-/-}$ E14 mouse embryo sections and the iPSC-to-β-cell differentiation dome sections could determine whether USP7 loss disproportionally triggered apoptosis in NGN3+ endocrine progenitors. Similarly, while in our *in vitro* differentiation experiments USP7 inhibition was limited to the endocrine progenitor stage, in our Pdx1;Cre $Usp7^{-/-}$ mouse model USP7 loss was maintained during endocrine cell maturation, meaning that additional effects of USP7 loss on endocrine cell maturation and function could contribute to the observed phenotype in adult mice. To further investigate this, mouse models for Usp7 knockout at different pancreatic developmental stages and in different cell types could be generated, such as a MafA;Cre $Usp7^{-/-}$ model to investigate the effect of USP7 on β-cell maturation. Additionally, to further validate whether the effect of USP7 loss on the endocrine compartment in the murine pancreas is due to NGN3 destabilisation, wildtype and $Usp7^{-/-}$ embryos from earlier developmental timepoints post-knockout but before the emergence of NGN3 expression (e.g. E10) could be harvested. A comparison of the size and morphology of the wildtype and $Usp7^{-/-}$ pancreas in these embryos would elucidate whether USP7 loss affects pancreatic development previously to the NGN3 expression window.

7.6 Concluding remarks

In the present study, we identify two potential interactors of proendocrine transcription factor NGN3 and explore the mechanisms and consequences of these interactions. While both Usp7 and Huwe1 are expressed in the human foetal pancreas, of the two, USP7 shows great promise as a possible target for the modulation of NGN3 stability. Experiments in HEK293A cells reveal that USP7 overexpression leads to exogenous NGN3 deubiquitination and stabilisation, while USP7 inhibition in iPSC-derived pancreatic endocrine progenitors destabilises NGN3 and impairs β-like cell differentiation. Furthermore, a conditional Usp7 knockout in the pancreas of mouse embryos leads to a reduction in the NGN3+ endocrine progenitor pool and impairs endocrine specification, resulting in a diabetic phenotype. These findings are consistent with USP7 playing an essential role in endocrine specification in the developing pancreas through its ability to stabilise NGN3.

USP7 has been intensely researched as a target for cancer therapies, due to its regulation of substrates such as p53 and its role in cell proliferation (H. Chen et al. 2020; W. Zhang et al. 2020). However, to our knowledge, this is the first study that links USP7 to the pancreas in the context of healthy pancreatic development. As NGN3 stabilisation in ductal cells has been shown to promote exocrine-to-endocrine transdifferentiation (Sancho et al. 2014), it is possible that chemically boosting the deubiquitinating activity of USP7 could help achieve similar effect without the need for NGN3 overexpression through viral vectors. Additional research would be needed to assess the effect of increased USP7 activation on endocrine differentiation *in vitro* and *in vivo*, as well as on processes such as cell proliferation and tumorigenesis in the pancreas, in order to further determine the suitability of USP7 as a target for *in situ* NGN3 modulation. Nevertheless, the current study identifies USP7 as a key facilitator of endocrine specification

during pancreatic development, providing valuable insight into the complex post-translational regulation network of NGN3.

References

Adda, G., L. Hannoun, and J. Loygue. 1984. “Development of the Human Pancreas: Variations and Pathology. A Tentative Classification.” *Anatomia Clinica* 5 (4): 275–83. https://doi.org/10.1007/BF01798752.

Adhikary, Sovana, Federica Marinoni, Andreas Hock, Esther Hulleman, Nikita Popov, Rudi Beier, Sandra Bernard, et al. 2005. “The Ubiquitin Ligase HectH9 Regulates Transcriptional Activation by Myc and Is Essential for Tumor Cell Proliferation.” *Cell* 123 (3): 409–21. https://doi.org/10.1016/J.CELL.2005.08.016/ATTACHMENT/3675A098-E912-4B74-8A5F-28815ACFC9EE/MMC1.PDF.

Ali, Amjad, Rameez Raja, Sabihur Rahman Farooqui, Shaista Ahmad, and Akhil C. Banerjea. 2017. “USP7 Deubiquitinase Controls HIV-1 Production by Stabilizing Tat Protein.” *The Biochemical Journal* 474 (10): 1653–68. https://doi.org/10.1042/BCJ20160304.

Ali, Fahad R, Kevin Cheng, Peter Kirwan, Su Metcalfe, Frederick J Livesey, Roger A Barker, and Anna Philpott. 2014. “The Phosphorylation Status of Ascl1 Is a Key Determinant of Neuronal Differentiation and Maturation in Vivo and in Vitro.” https://doi.org/10.1242/dev.106377.

Alonso-De Vega, Ignacio, Yusé Martín, Veronique Aj Smits, and Yus E Martín. 2015. “Cell Cycle USP7 Controls Chk1 Protein Stability by Direct Deubiquitination USP7 Controls Chk1 Protein Stability by Direct Deubiquitination.” https://doi.org/10.4161/15384101.2014.973324.

Andey, Terrick, Michael M. Attah, Nana Adwoa Akwaaba-Reynolds, Sana Cheema, Sara Parvin-Nejad, and George K. Acquaah-Mensah. 2020. “Enhanced Immortalization, HUWE1 Mutations and Other Biological Drivers of Breast Invasive Carcinoma in Black/African American Patients.” *Gene* 763 (December): 100030. https://doi.org/10.1016/J.GENE.2020.100030.

Andralojc, K. M., A. Mercalli, K. W. Nowak, L. Albarello, R. Calcagno, L. Luzi, E. Bonifacio, C. Doglioni, and L. Piemonti. 2009. “Ghrelin-Producing Epsilon Cells in the Developing and Adult Human Pancreas.” *Diabetologia* 52 (3): 486–93. https://doi.org/10.1007/S00125-008-1238-Y/FIGURES/5.

Apelqvist, Åsa, Hao Li, Lukas Sommer, Paul Beatus, David J. Anderson, Tasuku Honjo, Martin Hrabě De Angelis, Urban Lendahl, and Helena Edlund. 1999. “Notch Signalling Controls Pancreatic Cell Differentiation.” *Nature 1999 400:6747* 400 (6747): 877–81. https://doi.org/10.1038/23716.

Aprigliano, Rossana, Merdane Ezgi Aksu, Stefano Bradamante, Boris Mihaljevic, Wei Wang, Kristin Rian, Nicola P. Montaldo, et al. 2021. “Increased P53 Signaling Impairs Neural Differentiation in HUWE1-Promoted Intellectual Disabilities.” *Cell Reports Medicine* 2 (4). https://doi.org/10.1016/J.XCRM.2021.100240.

Aramata, Shinsaku, Song Iee Han, Kunio Yasuda, and Kohsuke Kataoka. 2005. “Synergistic Activation of the Insulin Gene Promoter by the Beta-Cell Enriched Transcription Factors MafA, Beta2, and Pdx1.” *Biochimica et Biophysica Acta* 1730 (1): 41–46. https://doi.org/10.1016/J.BBAEXP.2005.05.009.

Aravind, L. 2001. “The WWE Domain: A Common Interaction Module in Protein Ubiquitination and ADP Ribosylation.” *Trends in Biochemical Sciences* 26 (5): 273–75. https://doi.org/10.1016/s0968-0004(01)01787-x.

Ariyachet, Chaiyaboot, Alessio Tovaglieri, Guanjue Xiang, Jiaqi Lu, Manasvi S. Shah, Camilla A. Richmond, Catia Verbeke, et al. 2016. “Reprogrammed Stomach Tissue as a Renewable Source of Functional β Cells for Blood Glucose Regulation.” *Cell Stem Cell* 18 (3): 410–21. https://doi.org/10.1016/j.stem.2016.01.003.

Arosio, Maura, Cristina L. Ronchi, Carlotta Gebbia, Vincenzo Cappiello, Paolo Beck-Peccoz, and Maddalena Peracchi. 2003. “Stimulatory Effects of Ghrelin on Circulating Somatostatin and Pancreatic Polypeptide Levels.” *The Journal of Clinical Endocrinology and Metabolism* 88 (2): 701–4. https://doi.org/10.1210/JC.2002-021161.

Artner, Isabella, Yan Hang, Magdalena Mazur, Tsunehiko Yamamoto, Min Guo, Jill Lindner, Mark A. Magnuson, and Roland Stein. 2010. “MafA and MafB Regulate Genes Critical to Beta-Cells in a Unique Temporal Manner.” *Diabetes* 59 (10): 2530–39. https://doi.org/10.2337/DB10-0190.

Ashton, Nicholas W., Gabrielle J. Valles, Nancy Jaiswal, Irina Bezsonova, and Roger Woodgate. 2021. “DNA Polymerase ι Interacts with Both the TRAF-like and UBL1-2 Domains of USP7.” *Journal of Molecular Biology* 433 (2): 166733. https://doi.org/10.1016/J.JMB.2020.166733.

Atkinson, Mark A, George S Eisenbarth, and Aaron W Michels. 2014. “Type 1 Diabetes.” *The Lancet* 383 (9911): 69–82. https://doi.org/10.1016/S0140-6736(13)60591-7.

Auton, Adam, Gonçalo R. Abecasis, David M. Altshuler, Richard M. Durbin, David R. Bentley, Aravinda Chakravarti, Andrew G. Clark, et al. 2015. “A Global Reference for Human Genetic Variation.” *Nature* 526 (7571): 68. https://doi.org/10.1038/NATURE15393.

Azizoglu, D. Berfin, and Ondine Cleaver. 2016. “Blood Vessel Crosstalk during Organogenesis—Focus on Pancreas and Endothelial Cells.” *Wiley Interdisciplinary Reviews: Developmental Biology* 5 (5): 598–617. https://doi.org/10.1002/WDEV.240.

Azzarelli, Roberta, Christopher Hurley, Magdalena K. Sznurkowska, Steffen Rulands, Laura Hardwick, Ivonne Gamper, Fahad Ali, et al. 2017a. “Multi-Site Neurogenin3 Phosphorylation Controls Pancreatic Endocrine Differentiation.” *Developmental Cell* 41 (3): 274. https://doi.org/10.1016/J.DEVCEL.2017.04.004.

Banga, A., E. Akinci, L. V. Greder, J. R. Dutton, and J. M. W. Slack. 2012. “In Vivo Reprogramming of Sox9+ Cells in the Liver to Insulin-Secreting Ducts.” *Proceedings of the National Academy of Sciences* 109 (38): 15336–41. https://doi.org/10.1073/pnas.1201701109.

Bocian-Sobkowska, Joanna, Maciej Zabel, Witold Wozniak, and Joanna Surdyk-Zasada. 1999. “Polyhormonal Aspect of the Endocrine Cells of the Human Fetal Pancreas.” *Histochemistry and Cell Biology* 112 (2): 147–53. https://doi.org/10.1007/S004180050401.

Boj, Sylvia F., Chang Il Hwang, Lindsey A. Baker, Iok In Christine Chio, Dannielle D. Engle, Vincenzo Corbo, Myrthe Jager, et al. 2015. “Organoid Models of Human and Mouse Ductal Pancreatic Cancer.” *Cell* 160 (0): 324. https://doi.org/10.1016/J.CELL.2014.12.021.

Bonazzoli, Elena, Stefania Bellone, Luca Zammataro, Barbara Gnutti, Adele Guglielmi, Silvia Pelligra, Nupur Nagarkatti, et al. 2020. “Derangements in HUWE1/c-MYC Pathway Confer Sensitivity to the BET Bromodomain Inhibitor GS-626510 in Uterine Cervical Carcinoma.” *Gynecologic Oncology* 158 (3): 769–75. https://doi.org/10.1016/J.YGYNO.2020.06.484.

Bonner-Weir, Susan, Brooke A. Sullivan, and Gordon C. Weir. 2015. “Human Islet Morphology Revisited: Human and Rodent Islets Are Not So Different After All.” *Journal of Histochemistry and Cytochemistry* 63 (8): 604. https://doi.org/10.1369/0022155415570969.

Bosshard, Matthias, Rossana Aprigliano, Cristina Gattiker, Vuk Palibrk, Enni Markkanen, Paul Hoff Backe, Stefania Pellegrino, et al. 2017. “Impaired Oxidative Stress Response Characterizes HUWE1-Promoted X-Linked Intellectual Disability.” *Scientific Reports* 7 (1). https://doi.org/10.1038/S41598-017-15380-Y.

Breslin, Mary B., Hong Wei Wang, Amy Pierce, Rebecca Aucoin, and Michael S. Lan. 2007. “Neurogenin 3 Recruits CBP Co-Activator to Facilitate Histone H3/H4 Acetylation in the Target Gene INSM1.” *FEBS Letters* 581 (5): 949. https://doi.org/10.1016/J.FEBSLET.2007.01.087.

Butler, A. E., L. Cao-Minh, R. Galasso, R. A. Rizza, A. Corradin, C. Cobelli, and P. C. Butler. 2010. “Adaptive Changes in Pancreatic Beta Cell Fractional Area and Beta Cell Turnover in Human Pregnancy.” *Diabetologia* 53 (10): 2167. https://doi.org/10.1007/S00125-010-1809-6.

Cabrera, Over, Dora M. Berman, Norma S. Kenyon, Camillo Ricordi, Per Olof Berggren, and Aiejandro Caicedo. 2006. “The Unique Cytoarchitecture of Human Pancreatic Islets Has Implications for Islet Cell Function.” *Proceedings of the National Academy of Sciences of the United States of America* 103 (7): 2334–39. https://doi.org/10.1073/PNAS.0510790103.

Cadwell, Ken, and Laurent Coscoy. 2005. “Ubiquitination on Nonlysine Residues by a Viral E3 Ubiquitin Ligase.” *Science (New York, N.Y.)* 309 (5731): 127–30. https://doi.org/10.1126/science.1110340.

Carrà, Giovanna, Cristina Panuzzo, Davide Torti, Guido Parvis, Sabrina Crivellaro, Ubaldo Familiari, Marco Volante, et al. 2017. “Therapeutic Inhibition of USP7-PTEN Network in Chronic Lymphocytic Leukemia: A Strategy to Overcome TP53 Mutated/Deleted Clones.” *Oncotarget* 8 (22): 35508–22. https://doi.org/10.18632/ONCOTARGET.16348.

Chavoshi, Sara, Olga Egorova, Ira Kay Lacdao, Sahar Farhadi, Yi Sheng, and Vivian Saridakis. 2016. “Identification of Kaposi Sarcoma Herpesvirus (KSHV) VIRF1 Protein as a Novel Interaction Partner of Human Deubiquitinase USP7.” *The Journal of Biological Chemistry* 291 (12): 6281. https://doi.org/10.1074/JBC.M115.710632.

Chen, Hao, Xiaoling Zhu, Rong Sun, Panpan Ma, Erhao Zhang, Zhou Wang, Yihui Fan, Guoxiong Zhou, and Renfang Mao. 2020. “Ubiquitin-Specific Protease 7 Is a Druggable Target That Is Essential for Pancreatic Cancer Growth and Chemoresistance.” *Investigational New Drugs* 38 (6): 1707–16. https://doi.org/10.1007/S10637-020-00951-0/FIGURES/4.

Chen, Yi Ju, Stacy R. Finkbeiner, Daniel Weinblatt, Matthew J. Emmett, Feven Tameire, Maryam Yousefi, Chenghua Yang, et al. 2014. “De Novo Formation of Insulin-Producing ‘Neo-β Cell Islets’ from Intestinal Crypts.” *Cell Reports* 6 (6): 1046. https://doi.org/10.1016/J.CELREP.2014.02.013.

Cheng, Yen Fu, Mingjie Tong, and Albert S.B. Edge. 2016. “Destabilization of Atoh1 by E3 Ubiquitin Ligase Huwe1 and Casein Kinase 1 Is Essential for Normal Sensory Hair Cell Development.” *The Journal of Biological Chemistry* 291 (40): 21096–109. https://doi.org/10.1074/JBC.M116.722124.

Chera, Simona, Delphine Baronnier, Luiza Ghila, Valentina Cigliola, Jan N. Jensen, Guoqiang Gu, Kenichiro Furuyama, et al. 2014. “Diabetes Recovery by Age-Dependent Conversion of

Pancreatic δ-Cells into Insulin Producers." *Nature* 514 (7523): 503–7. https://doi.org/10.1038/NATURE13633.

Choe, Katherine N, Claudia M Nicolae, Daniel Constantin, Yuka Imamura Kawasawa, Maria Rocio Delgado-Diaz, Subhajyoti De, Raimundo Freire, Veronique AJ Smits, and George-Lucian Moldovan. 2016. "HUWE1 Interacts with PCNA to Alleviate Replication Stress." *EMBO Reports* 17 (6): 874. https://doi.org/10.15252/EMBR.201541685.

Chon, Hae J., Kyoung J. Bae, Yura Lee, and Jiyeon Kim. 2015. "The Casein Kinase 2 Inhibitor, CX-4945, as an Anti-Cancer Drug in Treatment of Human Hematological Malignancies." *Frontiers in Pharmacology* 6 (MAR): 70. https://doi.org/10.3389/FPHAR.2015.00070/BIBTEX.

Collombat, Patrick, Jacob Hecksher-Sørensen, Vania Broccoli, Jens Krull, Ilaria Ponte, Tabea Mundiger, Julian Smith, Peter Gruss, Palle Serup, and Ahmed Mansouri. 2005. "The Simultaneous Loss of Arx and Pax4 Genes Promotes a Somatostatin-Producing Cell Fate Specification at the Expense of the Alpha- and Beta-Cell Lineages in the Mouse Endocrine Pancreas." *Development (Cambridge, England)* 132 (13): 2969–80. https://doi.org/10.1242/DEV.01870.

Collombat, Patrick, Jacob Hecksher-Sørensen, Jens Krull, Joachim Berger, Dietmar Riedel, Pedro L. Herrera, Palle Serup, and Ahmed Mansouri. 2007. "Embryonic Endocrine Pancreas and Mature Beta Cells Acquire Alpha and PP Cell Phenotypes upon Arx Misexpression." *The Journal of Clinical Investigation* 117 (4): 961–70. https://doi.org/10.1172/JCI29115.

Collombat, Patrick, Xiaobo Xu, Philippe Ravassard, Beatriz Sosa-Pineda, Sébastien Dussaud, Nils Billestrup, Ole D. Madsen, Palle Serup, Harry Heimberg, and Ahmed Mansouri. 2009. "The Ectopic Expression of Pax4 in the Mouse Pancreas Converts Progenitor Cells into Alpha and Subsequently Beta Cells." *Cell* 138 (3): 449–62. https://doi.org/10.1016/J.CELL.2009.05.035.

Crawford, Lisa J., David C. Campbell, Jonathan J. Morgan, Michelle A. Lawson, Jennifer M. Down, Dharminder Chauhan, Roisin M. McAvera, et al. 2020. "The E3 Ligase HUWE1 Inhibition as a Therapeutic Strategy to Target MYC in Multiple Myeloma." *Oncogene* 39 (27): 5001. https://doi.org/10.1038/S41388-020-1345-X.

Dadson, Keith, Ludger Hauck, Zhenyue Hao, Daniela Grothe, Vivek Rao, Tak W. Mak, and Filio Billia. 2017. "The E3 Ligase Mule Protects the Heart against Oxidative Stress and Mitochondrial Dysfunction through Myc-Dependent Inactivation of Pgc-1α and Pink1." *Scientific Reports 2017 7:1* 7 (1): 1–14. https://doi.org/10.1038/srep41490.

Dai, C., M. Brissova, Y. Hang, C. Thompson, G. Poffenberger, A. Shostak, Z. Chen, R. Stein, and A. C. Powers. 2012. "Islet-Enriched Gene Expression and Glucose-Induced Insulin Secretion in Human and Mouse Islets." *Diabetologia* 55 (3): 707–18. https://doi.org/10.1007/S00125-011-2369-0.

Dassaye, Reshmi, Strini Naidoo, and Marlon E. Cerf. 2016. "Transcription Factor Regulation of Pancreatic Organogenesis, Differentiation and Maturation." *Islets* 8 (1): 13. https://doi.org/10.1080/19382014.2015.1075687.

Demcollari, Theoni Ingrid, Ana-Maria Cujba, and Rocio Sancho. 2017a. "Phenotypic Plasticity in the Pancreas: New Triggers, New Players." *Current Opinion in Cell Biology* 49 (December): 38–46. https://doi.org/10.1016/J.CEB.2017.11.014.

Desai, Biva M., Jennifer Oliver-Krasinski, Diva D. de Leon, Cyrus Farzad, Nankang Hong, Steven D. Leach, and Doris A. Stoffers. 2007. “Preexisting Pancreatic Acinar Cells Contribute to Acinar Cell, but Not Islet Beta Cell, Regeneration.” *The Journal of Clinical Investigation* 117 (4): 971–77. https://doi.org/10.1172/JCI29988.

Deutsch, G., J. Jung, M. Zheng, J. Lóra, and K. S. Zaret. 2001. “A Bipotential Precursor Population for Pancreas and Liver within the Embryonic Endoderm.” *Development* 128 (6): 871–81. https://doi.org/10.1242/DEV.128.6.871.

Dolenšek, Jurij, Marjan Slak Rupnik, and Andraž Stožer. 2015. “Structural Similarities and Differences between the Human and the Mouse Pancreas.” *Islets* 7 (1). https://doi.org/10.1080/19382014.2015.1024405.

Dominguez-Brauer, Carmen, Zhenyue Hao, Andrew J. Elia, Jérôme M. Fortin, Robert Nechanitzky, Patrick M. Brauer, Yi Sheng, et al. 2016. “Mule Regulates the Intestinal Stem Cell Niche via the Wnt Pathway and Targets EphB3 for Proteasomal and Lysosomal Degradation.” *Cell Stem Cell* 19 (2): 205. https://doi.org/10.1016/J.STEM.2016.04.002.

Ejarque, Miriam, Sara Cervantes, Gemma Pujadas, Anna Tutusaus, Lidia Sanchez, and Rosa Gasa. 2013. “Neurogenin3 Cooperates with Foxa2 to Autoactivate Its Own Expression.” *The Journal of Biological Chemistry* 288 (17): 11705. https://doi.org/10.1074/JBC.M112.388173.

Elia, Andrew E.H., Alexander P. Boardman, David C. Wang, Edward L. Huttlin, Robert A. Everley, Noah Dephoure, Chunshui Zhou, Itay Koren, Steven P. Gygi, and Stephen J. Elledge. 2015. “Quantitative Proteomic Atlas of Ubiquitination and Acetylation in the DNA Damage Response.” *Molecular Cell* 59 (5): 867. https://doi.org/10.1016/J.MOLCEL.2015.05.006.

Eriksson, Anna U., Christoffer Svensson, Andreas Hörnblad, Abbas Cheddad, Elena Kostromina, Maria Eriksson, Nils Norlin, et al. 2013. “Near Infrared Optical Projection Tomography for Assessments of β-Cell Mass Distribution in Diabetes Research.” *Journal of Visualized Experiments : JoVE*, no. 71: 50238. https://doi.org/10.3791/50238.

Faesen, Alex C., Annette M.G. Dirac, Anitha Shanmugham, Huib Ovaa, Anastassis Perrakis, and Titia K. Sixma. 2011. “Mechanism of USP7/HAUSP Activation by Its C-Terminal Ubiquitin-like Domain and Allosteric Regulation by GMP-Synthetase.” *Molecular Cell* 44 (1): 147–59. https://doi.org/10.1016/J.MOLCEL.2011.06.034/ATTACHMENT/B928868D-831B-421C-ACC5-429D3E99FB9A/MMC1.PDF.

Faesen, Alex C., Mark P.A. Luna-Vargas, Paul P. Geurink, Marcello Clerici, Remco Merkx, Willem J. Van Dijk, Dharjath S. Hameed, Farid El Oualid, Huib Ovaa, and Titia K. Sixma. 2011. “The Differential Modulation of USP Activity by Internal Regulatory Domains, Interactors and Eight Ubiquitin Chain Types.” *Chemistry & Biology* 18 (12): 1550–61. https://doi.org/10.1016/J.CHEMBIOL.2011.10.017.

Fernández-Montalván, Amaury, Tewis Bouwmeester, Gerard Joberty, Robert Mader, Marion Mahnke, Benoit Pierrat, Jean Marc Schlaeppi, Susanne Worpenberg, and Bernd Gerhartz. 2007. “Biochemical Characterization of USP7 Reveals Post-Translational Modification Sites and Structural Requirements for Substrate Processing and Subcellular Localization.” *The FEBS Journal* 274 (16): 4256–70. https://doi.org/10.1111/J.1742-4658.2007.05952.X.

Ferré-D'Amaré, Adrian R., George C. Prendergast, Edward B. Ziff, and Stephen K. Burley. 1993. "Recognition by Max of Its Cognate DNA through a Dimeric b/HLH/Z Domain." *Nature* 363 (6424): 38–45. https://doi.org/10.1038/363038A0.

Forget, Antoine, Laure Bihannic, Sara Maria Cigna, Coralie Lefevre, Marc Remke, Monia Barnat, Sophie Dodier, et al. 2014. "Shh Signaling Protects Atoh1 from Degradation Mediated by the E3Ubiquitin Ligase Huwe1 in Neural Precursors." *Developmental Cell* 29 (6): 649–61. https://doi.org/10.1016/J.DEVCEL.2014.05.014/ATTACHMENT/282E7386-D904-44CC-871E-E06288EB4D92/MMC1.PDF.

Fountain, Michael D., David S. Oleson, Megan E. Rech, Lara Segebrecht, Jill V. Hunter, John M. McCarthy, Philip J. Lupo, et al. 2019. "Pathogenic Variants in USP7 Cause a Neurodevelopmental Disorder with Speech Delays, Altered Behavior, and Neurologic Anomalies." *Genetics in Medicine* 21 (8): 1797. https://doi.org/10.1038/S41436-019-0433-1.

Fowden, A L. 1992. "The Role of Insulin in Fetal Growth." *Early Human Development* 29 (1–3): 177–81. https://doi.org/10.1016/0378-3782(92)90135-4.

Franklin, Isobel, Jesper Gromada, Asllan Gjinovci, Sten Theander, and Claes B. Wollheim. 2005. "β-Cell Secretory Products Activate α-Cell ATP-Dependent Potassium Channels to Inhibit Glucagon Release." *Diabetes* 54 (6): 1808–15. https://doi.org/10.2337/DIABETES.54.6.1808.

Friez, Michael J., Susan Sklower Brooks, Roger E. Stevenson, Michael Field, Monica J. Basehore, Lesley C. Adès, Courtney Sebold, et al. 2016. "HUWE1 Mutations in Juberg-Marsidi and Brooks Syndromes: The Results of an X-Chromosome Exome Sequencing Study." *BMJ Open* 6 (4). https://doi.org/10.1136/BMJOPEN-2015-009537.

Froyen, Guy, Mark Corbett, Joke Vandewalle, Irma Jarvela, Owen Lawrence, Cliff Meldrum, Marijke Bauters, et al. 2008. "Submicroscopic Duplications of the Hydroxysteroid Dehydrogenase HSD17B10 and the E3 Ubiquitin Ligase HUWE1 Are Associated with Mental Retardation." *American Journal of Human Genetics* 82 (2): 432. https://doi.org/10.1016/J.AJHG.2007.11.002.

Galarreta, Antonio, Pablo Valledor, Patricia Ubieto-Capella, Vanesa Lafarga, Eduardo Zarzuela, Javier Mu˜ Noz, Marcos Malumbres, Emilio Lecona, and Oscar Fernandez-Capetillo. 2021. "USP7 Limits CDK1 Activity throughout the Cell Cycle." *The EMBO Journal* 40 (11): e99692. https://doi.org/10.15252/EMBJ.201899692.

Gasa, Rosa, Caroline Mrejen, Francis C. Lynn, Peter Skewes-Cox, Lidia Sanchez, Katherine Y. Yang, Chin Hsing Lin, Ramon Gomis, and Michael S. German. 2008. "Induction of Pancreatic Islet Cell Differentiation by the Neurogenin-NeuroD Cascade." *Differentiation* 76 (4): 381–91. https://doi.org/10.1111/J.1432-0436.2007.00228.X.

Gillotin, Sébastien, John D. Davies, and Anna Philpott. 2018. "Subcellular Localisation Modulates Ubiquitylation and Degradation of Ascl1." *Scientific Reports 2018 8:1* 8 (1): 1–13. https://doi.org/10.1038/s41598-018-23056-4.

Giovinazzi, S., V. M. Morozov, M. K. Summers, W. C. Reinhold, and A. M. Ishov. 2013. "USP7 and Daxx Regulate Mitosis Progression and Taxane Sensitivity by Affecting Stability of Aurora-A Kinase." *Cell Death and Differentiation* 20 (5): 721–31. https://doi.org/10.1038/CDD.2012.169.

Gradwohl, Gérard, Andrée Dierich, Marianne LeMeur, and François Guillemot. 2000. "Neurogenin3 Is Required for the Development of the Four Endocrine Cell Lineages of the Pancreas."

Proceedings of the National Academy of Sciences of the United States of America 97 (4): 1607. https://doi.org/10.1073/PNAS.97.4.1607.

Greenberg, G. R., T. E. Adrian, J. H. Baron, R. F. Mccloy, V. S. Chadwick, and S. R. Bloom. 1978. "INHIBITION OF PANCREAS AND GALLBLADDER BY PANCREATIC POLYPEPTIDE." *The Lancet* 312 (8103): 1280–82. https://doi.org/10.1016/S0140-6736(78)92042-1.

Hao, Yi Heng, Michael D. Fountain, Klementina Fon Tacer, Fan Xia, Weimin Bi, Sung Hae L. Kang, Ankita Patel, et al. 2015. "USP7 Acts as a Molecular Rheostat to Promote WASH-Dependent Endosomal Protein Recycling and Is Mutated in a Human Neurodevelopmental Disorder." *Molecular Cell* 59 (6): 956. https://doi.org/10.1016/J.MOLCEL.2015.07.033.

Hebrok, M., S. K. Kim, B. St-Jacques, A. P. McMahon, and D. A. Melton. 2000. "Regulation of Pancreas Development by Hedgehog Signaling." *Development* 127 (22): 4905–13. https://doi.org/10.1242/DEV.127.22.4905.

Hebrok, Matthias. 2012. "Generating β Cells from Stem Cells—The Story So Far." *Cold Spring Harbor Perspectives in Medicine* 2 (6). https://doi.org/10.1101/CSHPERSPECT.A007674.

Hebrok, Matthias, Seung K. Kim, and Douglas A. Melton. 1998. "Notochord Repression of Endodermal Sonic Hedgehog Permits Pancreas Development." *Genes & Development* 12 (11): 1705. https://doi.org/10.1101/GAD.12.11.1705.

Henry, Brandon Michael, Bendik Skinningsrud, Karolina Saganiak, Przemysław A. Pękala, Jerzy A. Walocha, and Krzysztof A. Tomaszewski. 2019. "Development of the Human Pancreas and Its Vasculature — An Integrated Review Covering Anatomical, Embryological, Histological, and Molecular Aspects." *Annals of Anatomy - Anatomischer Anzeiger* 221 (January): 115–24. https://doi.org/10.1016/J.AANAT.2018.09.008.

Hicke, Linda, and Rebecca Dunn. 2003. "Regulation of Membrane Protein Transport by Ubiquitin and Ubiquitin-Binding Proteins." *Http://Dx.Doi.Org/10.1146/Annurev.Cellbio.19.110701.154617* 19 (November): 141–72. https://doi.org/10.1146/ANNUREV.CELLBIO.19.110701.154617.

Hingorani, Sunil R., Emanuel F. Petricoin, Anirban Maitra, Vinodh Rajapakse, Catrina King, Michael A. Jacobetz, Sally Ross, et al. 2003. "Preinvasive and Invasive Ductal Pancreatic Cancer and Its Early Detection in the Mouse." *Cancer Cell* 4 (6): 437–50. https://doi.org/10.1016/S1535-6108(03)00309-X.

Hofmann, K, and P Bucher. 1996. "The UBA Domain: A Sequence Motif Present in Multiple Enzyme Classes of the Ubiquitination Pathway." *Trends in Biochemical Sciences* 21 (5): 172–73.

Hogrebe, Nathaniel J., Punn Augsornworawat, Kristina G. Maxwell, Leonardo Velazco-Cruz, and Jeffrey R. Millman. 2020. "Targeting the Cytoskeleton to Direct Pancreatic Differentiation of Human Pluripotent Stem Cells." *Nature Biotechnology* 38 (4): 460. https://doi.org/10.1038/S41587-020-0430-6.

Hohmeier, Hans E, Jie An, and Christopher B Newgard. 2019. "Improving Human β-Cell Maturation in Vitro." *Nature Cell Biology* 21 (2): 119–21. https://doi.org/10.1038/s41556-019-0277-6.

Holowaty, Melissa N., Yi Sheng, Tin Nguyen, Cheryl Arrowsmith, and Lori Frappier. 2003. "Protein Interaction Domains of the Ubiquitin-Specific Protease, USP7/HAUSP." *The Journal of Biological Chemistry* 278 (48): 47753–61. https://doi.org/10.1074/JBC.M307200200.

Hu, Min, Lichuan Gu, Muyang Li, Philip D. Jeffrey, Wei Gu, and Yigong Shi. 2006. “Structural Basis of Competitive Recognition of P53 and MDM2 by HAUSP/USP7: Implications for the Regulation of the P53–MDM2 Pathway.” *PLoS Biology* 4 (2): 228–39. https://doi.org/10.1371/JOURNAL.PBIO.0040027.

Hu, Min, Pingwei Li, Muyang Li, Wenyu Li, Tingting Yao, Jia Wei Wu, Wei Gu, Robert E. Cohen, and Yigong Shi. 2002. “Crystal Structure of a UBP-Family Deubiquitinating Enzyme in Isolation and in Complex with Ubiquitin Aldehyde.” *Cell* 111 (7): 1041–54. https://doi.org/10.1016/S0092-8674(02)01199-6.

Huang, Hsiang-Po, Min Liu, Heithem M. El-Hodiri, Khoi Chu, Milan Jamrich, and Ming-Jer Tsai. 2000. “Regulation of the Pancreatic Islet-Specific Gene BETA2 (NeuroD) by Neurogenin 3.” *Molecular and Cellular Biology* 20 (9): 3292. https://doi.org/10.1128/MCB.20.9.3292-3307.2000.

Huising, Mark O., Talitha van der Meulen, Jessica L. Huang, Mohammad S. Pourhosseinzadeh, and Glyn M. Noguchi. 2018. “The Difference δ-Cells Make in Glucose Control.” *Physiology* 33 (6): 403. https://doi.org/10.1152/PHYSIOL.00029.2018.

Hussain, Sajjad, Ying Zhang, and Paul J. Galardy. 2009. “DUBs and Cancer: The Role of Deubiquitinating Enzymes as Oncogenes, Non-Oncogenes and Tumor Suppressors.” *Https://Doi.Org/10.4161/Cc.8.11.8739* 8 (11): 1688–97. https://doi.org/10.4161/CC.8.11.8739.

Inoue, Satoshi, Zhenyue Hao, Andrew J. Elia, David Cescon, Lily Zhou, Jennifer Silvester, Bryan Snow, et al. 2013. “Mule/Huwe1/Arf-BP1 Suppresses Ras-Driven Tumorigenesis by Preventing c-Myc/Miz1-Mediated down-Regulation of P21 and P15.” *Genes & Development* 27 (10): 1101. https://doi.org/10.1101/GAD.214577.113.

Ionescu-Tirgoviste, Constantin, Paul A. Gagniuc, Elvira Gubceac, Liliana Mardare, Irinel Popescu, Simona Dima, and Manuella Militaru. 2015. “A 3D Map of the Islet Routes throughout the Healthy Human Pancreas.” *Scientific Reports 2015 5:1* 5 (1): 1–14. https://doi.org/10.1038/srep14634.

Jackson, Alan E., Paul G. Casell, Bernard V. North, Shanti Vijayaraghavan, Susan V. Gelding, Ambady Ramachandran, Chamukuttan Snehalatha, and Graham A. Hitman. 2004. “Polymorphic Variations in the Neurogenic Differentiation-1, Neurogenin-3, and Hepatocyte Nuclear Factor-1alpha Genes Contribute to Glucose Intolerance in a South Indian Population.” *Diabetes* 53 (8): 2122–25. https://doi.org/10.2337/DIABETES.53.8.2122.

Jacquemin, Patrick, Serge M. Durviaux, Jan Jensen, Catherine Godfraind, Gerard Gradwohl, François Guillemot, Ole D. Madsen, et al. 2000. “Transcription Factor Hepatocyte Nuclear Factor 6 Regulates Pancreatic Endocrine Cell Differentiation and Controls Expression of the Proendocrine Gene Ngn3.” *Molecular and Cellular Biology* 20 (12): 4445. https://doi.org/10.1128/MCB.20.12.4445-4454.2000.

Jacquemin, Patrick, Hideyuki Yoshitomi, Yasushige Kashima, Guy G. Rousseau, Frederic P. Lemaigre, and Kenneth S. Zaret. 2006. “An Endothelial-Mesenchymal Relay Pathway Regulates Early Phases of Pancreas Development.” *Developmental Biology* 290 (1): 189–99. https://doi.org/10.1016/J.YDBIO.2005.11.023.

Jennings, Rachel E., Andrew A. Berry, Rebecca Kirkwood-Wilson, Neil A. Roberts, Thomas Hearn, Rachel J. Salisbury, Jennifer Blaylock, Karen Piper Hanley, and Neil A. Hanley. 2013.

"Development of the Human Pancreas from Foregut to Endocrine Commitment." *Diabetes* 62 (10): 3514–22. https://doi.org/10.2337/DB12-1479/-/DC1.

Jensen, J N, L Hansen, C T Ekstrùm, F Pociot, J Nerup, T Hansen, and O Pedersen. 2001. "Polymorphisms in the Neurogenin 3 Gene (NEUROG) and Their Relation to Altered Insulin Secretion and Diabetes in the Danish Caucasian Population." *Diabetologia* 44: 123–26.

Jensen, Jan N, Louise C Rosenberg, Jacob Hecksher-Sørensen, and Palle Serup. 2007. "Mutant Neurogenin-3 in Congenital Malabsorptive Diarrhea." *The New England Journal of Medicine*. United States. https://doi.org/10.1056/NEJMc063247.

Ji, Lei, Bo Lu, Raffaella Zamponi, Olga Charlat, Robert Aversa, Zinger Yang, Frederic Sigoillot, et al. 2019. "USP7 Inhibits Wnt/β-Catenin Signaling through Promoting Stabilization of Axin." *Nature Communications 2019 10:1* 10 (1): 1–14. https://doi.org/10.1038/s41467-019-12143-3.

Jonsson, Jörgen, Lena Carlsson, Thomas Edlund, and Helena Edlund. 1994. "Insulin-Promoter-Factor 1 Is Required for Pancreas Development in Mice." *Nature* 371 (6498): 606–9. https://doi.org/10.1038/371606A0.

Jørgensen, Mette Christine, Jonas Ahnfelt-Rønne, Jacob Hald, Ole D. Madsen, Palle Serup, and Jacob Hecksher-Sørensen. 2007. "An Illustrated Review of Early Pancreas Development in the Mouse." *Endocrine Reviews* 28 (6): 685–705. https://doi.org/10.1210/ER.2007-0016.

Kategaya, Lorna, Paola Di Lello, Lionel Rougé, Richard Pastor, Kevin R. Clark, Jason Drummond, Tracy Kleinheinz, et al. 2017. "USP7 Small-Molecule Inhibitors Interfere with Ubiquitin Binding." *Nature* 550 (7677): 534–38. https://doi.org/10.1038/NATURE24006.

Katsarou, Anastasia, Soffia Gudbjörnsdottir, Araz Rawshani, Dana Dabelea, Ezio Bonifacio, Barbara J. Anderson, Laura M. Jacobsen, Desmond A. Schatz, and Ake Lernmark. 2017. "Type 1 Diabetes Mellitus." *Nature Reviews Disease Primers 2017 3:1* 3 (1): 1–17. https://doi.org/10.1038/nrdp.2017.16.

Kawahira, Hiroshi, Nancy H. Ma, Emmanouhl S. Tzanakakis, Andrew P. McMahon, Pao Tien Chuang, and Matthias Hebrok. 2003. "Combined Activities of Hedgehog Signaling Inhibitors Regulate Pancreas Development." *Development (Cambridge, England)* 130 (20): 4871–79. https://doi.org/10.1242/DEV.00653.

Khoronenkova, Svetlana V., and Grigory L. Dianov. 2013. "USP7S-Dependent Inactivation of Mule Regulates DNA Damage Signalling and Repair." *Nucleic Acids Research* 41 (3): 1750. https://doi.org/10.1093/NAR/GKS1359.

Khoronenkova, Svetlana V., Irina I. Dianova, Nicola Ternette, Benedikt M. Kessler, Jason L. Parsons, and Grigory L.D. Dianov. 2012. "ATM-Dependent Downregulation of USP7/HAUSP by PPM1G Activates P53 Response to DNA Damage." *Molecular Cell* 45 (6): 801–13. https://doi.org/10.1016/J.MOLCEL.2012.01.021.

Kim, Abraham, Kevin Miller, Junghyo Jo, German Kilimnik, Pawel Wojcik, and Manami Hara. 2009. "Islet Architecture: A Comparative Study." *Islets* 1 (2): 129–36. https://doi.org/10.4161/ISL.1.2.9480.

Kim, Robbert Q., and Titia K. Sixma. 2017. "Regulation of USP7: A High Incidence of E3 Complexes." *Journal of Molecular Biology* 429 (22): 3395–3408. https://doi.org/10.1016/J.JMB.2017.05.028.

Kim, Seung K., Matthias Hebrok, En Li, S. Paul Oh, Heinrich Schrewe, Erin B. Harmon, Joon S. Lee, and Douglas A. Melton. 2000. “Activin Receptor Patterning of Foregut Organogenesis.” *Genes & Development* 14 (15): 1866. https://doi.org/10.1101/gad.14.15.1866.

Kim, Seung K., Matthias Hebrok, and Douglas A. Melton. 1997. “Notochord to Endoderm Signaling Is Required for Pancreas Development.” *Development* 124 (21): 4243–52. https://doi.org/10.1242/DEV.124.21.4243.

Kitabchi, Abbas E., Guillermo E. Umpierrez, John M. Miles, and Joseph N. Fisher. 2009. “Hyperglycemic Crises in Adult Patients With Diabetes.” *Diabetes Care* 32 (7): 1335. https://doi.org/10.2337/DC09-9032.

Kon, N., Y. Kobayashi, M. Li, C. L. Brooks, T. Ludwig, and W. Gu. 2010. “Inactivation of HAUSP in Vivo Modulates P53 Function.” *Oncogene* 29 (9): 1270. https://doi.org/10.1038/ONC.2009.427.

Kon, N., J. Zhong, Y. Kobayashi, M. Li, M. Szabolcs, T. Ludwig, P. D. Canoll, and W. Gu. 2011. “Roles of HAUSP-Mediated P53 Regulation in Central Nervous System Development.” *Cell Death and Differentiation* 18 (8): 1366–75. https://doi.org/10.1038/CDD.2011.12.

Kon, Ning, Jiayun Zhong, Li Qiang, Domenico Accili, and Wei Gu. 2012. “Inactivation of Arf-Bp1 Induces P53 Activation and Diabetic Phenotypes in Mice.” *The Journal of Biological Chemistry* 287 (7): 5102. https://doi.org/10.1074/JBC.M111.322867.

Krentz, Nicole A.J., Dennis van Hoof, Zhongmei Li, Akie Watanabe, Mei Tang, Cuilan Nian, Michael S. German, and Francis C. Lynn. 2017. “Phosphorylation of NEUROG3 Links Endocrine Differentiation to the Cell Cycle in Pancreatic Progenitors.” *Developmental Cell* 41 (2): 129. https://doi.org/10.1016/J.DEVCEL.2017.02.006.

Lammert, E., O. Cleaver, and D. Melton. 2001. “Induction of Pancreatic Differentiation by Signals from Blood Vessels.” *Science (New York, N.Y.)* 294 (5542): 564–67. https://doi.org/10.1126/SCIENCE.1064344.

Lee, Catherine S., Nathalie Perreault, John E. Brestelli, and Klaus H. Kaestner. 2002. “Neurogenin 3 Is Essential for the Proper Specification of Gastric Enteroendocrine Cells and the Maintenance of Gastric Epithelial Cell Identity.” *Genes & Development* 16 (12): 1488–97. https://doi.org/10.1101/GAD.985002.

Lee, Jane C., Stewart B. Smith, Hirotaka Watada, Joseph Lin, David Scheel, Juehu Wang, Raghavendra G. Mirmira, and Michael S. German. 2001. “Regulation of the Pancreatic Pro-Endocrine Gene Neurogenin3.” *Diabetes* 50 (5): 928–36. https://doi.org/10.2337/DIABETES.50.5.928.

Li, J., A. Bergmann, M. Reimann, J. Schulze, S. R. Bornstein, and P. E.H. Schwarz. 2008. “Genetic Variation of Neurogenin 3 Is Slightly Associated with Hyperproinsulinaemia and Progression toward Type 2 Diabetes.” *Experimental and Clinical Endocrinology & Diabetes : Official Journal, German Society of Endocrinology [and] German Diabetes Association* 116 (3): 178–83. https://doi.org/10.1055/S-2007-992156.

Li, Wei, Mario H Bengtson, Axel Ulbrich, Akio Matsuda, Venkateshwar A Reddy, Anthony Orth, Sumit K Chanda, Serge Batalov, and Claudio A P Joazeiro. 2008. “Genome-Wide and Functional Annotation of Human E3 Ubiquitin Ligases Identifies MULAN, a Mitochondrial E3 That Regulates the Organelle’s Dynamics and Signaling.” *PloS One* 3 (1): e1487. https://doi.org/10.1371/journal.pone.0001487.

Li, Weida, Mio Nakanishi, Adrian Zumsteg, Matthew Shear, Christopher Wright, Douglas A. Melton, and Qiao Zhou. 2014. “In Vivo Reprogramming of Pancreatic Acinar Cells to Three Islet Endocrine Subtypes.” *ELife* 3 (3): 1846. https://doi.org/10.7554/ELIFE.01846.

Liu, Zhiqian, Dengsheng Miao, Qingwen Xia, Louis Hermo, and Simon S Wing. 2007. “Regulated Expression of the Ubiquitin Protein Ligase, E3(Histone)/LASU1/Mule/ARF-BP1/HUWE1, during Spermatogenesis.” *Developmental Dynamics : An Official Publication of the American Association of Anatomists* 236 (10): 2889–98. https://doi.org/10.1002/dvdy.21302.

Longo, Patti A., Jennifer M. Kavran, Min Sung Kim, and Daniel J. Leahy. 2013. “Transient Mammalian Cell Transfection with Polyethylenimine (PEI).” *Methods in Enzymology* 529 (January): 227–40. https://doi.org/10.1016/B978-0-12-418687-3.00018-5.

Louet, J. F., S. B. Smith, J. F. Gautier, M. Molokhia, M. L. Virally, J. P. Kevorkian, P. J. Guillausseau, et al. 2008. “Gender and Neurogenin3 Influence the Pathogenesis of Ketosis-Prone Diabetes.” *Diabetes, Obesity and Metabolism* 10 (10): 912–20. https://doi.org/10.1111/J.1463-1326.2007.00830.X.

Lyttle, B. M., J. Li, M. Krishnamurthy, F. Fellows, M. B. Wheeler, C. G. Goodyer, and R. Wang. 2008. “Transcription Factor Expression in the Developing Human Fetal Endocrine Pancreas.” *Diabetologia* 51 (7): 1169–80. https://doi.org/10.1007/S00125-008-1006-Z/FIGURES/7.

Ma, Jianhong, John D. Martin, Yu Xue, Leng A. Lor, Karen M. Kennedy-Wilson, Robert H. Sinnamon, Thau F. Ho, et al. 2010. “C-Terminal Region of USP7/HAUSP Is Critical for Deubiquitination Activity and Contains a Second Mdm2/P53 Binding Site.” *Archives of Biochemistry and Biophysics* 503 (2): 207–12. https://doi.org/10.1016/J.ABB.2010.08.020.

Masuya, D., C. Huang, D. Liu, T. Nakashima, H. Yokomise, M. Ueno, N. Nakashima, and S. Sumitomo. 2006. “The HAUSP Gene Plays an Important Role in Non-Small Cell Lung Carcinogenesis through P53-Dependent Pathways.” *The Journal of Pathology* 208 (5): 724–32. https://doi.org/10.1002/PATH.1931.

McGrath, Patrick S., Carey L. Watson, Cameron Ingram, Michael A. Helmrath, and James M. Wells. 2015. “The Basic Helix-Loop-Helix Transcription Factor Neurog3 Is Required for Development of the Human Endocrine Pancreas.” *Diabetes* 64 (7): 2497–2505. https://doi.org/10.2337/DB14-1412/-/DC1.

Mei, Yide, Allison Alcivar Hahn, Shimin Hu, and Xiaolu Yang. 2011. “The USP19 Deubiquitinase Regulates the Stability of C-IAP1 and c-IAP2.” *The Journal of Biological Chemistry* 286 (41): 35380. https://doi.org/10.1074/JBC.M111.282020.

Mellitzer, Georg, Stefan Bonné, Reini F. Luco, Mark Van De Casteele, Nathalie Lenne-Samuel, Patrick Collombat, Ahmed Mansouri, et al. 2006. “IA1 Is NGN3-Dependent and Essential for Differentiation of the Endocrine Pancreas.” *The EMBO Journal* 25 (6): 1344. https://doi.org/10.1038/SJ.EMBOJ.7601011.

Mellitzer, Georg, Marjorie Sidhoum-Jenny, Christophe Orvain, Jochen Barths, Philip A Seymour, Maike Sander, and Rard Gradwohl. 2004. “Pancreatic Islet Progenitor Cells in Neurogenin 3-Yellow Fluorescent Protein Knock-Add-On Mice.” *Molecular Endocrinology* 18: 2765–76. https://doi.org/10.1210/me.2004-0243.

Metzger, Meredith B., Jonathan N. Pruneda, Rachel E. Klevit, and Allan M. Weissman. 2014. “RING-Type E3 Ligases: Master Manipulators of E2 Ubiquitin-Conjugating enzymes and

Ubiquitination." *Biochimica et Biophysica Acta* 1843 (1): 47. https://doi.org/10.1016/J.BBAMCR.2013.05.026.

Meulen, Talitha Van Der, Cynthia J. Donaldson, Elena Cáceres, Anna E. Hunter, Christopher Cowing-Zitron, Lynley D. Pound, Michael W. Adams, Andreas Zembrzycki, Kevin L. Grove, and Mark O. Huising. 2015. "Urocortin3 Mediates Somatostatin-Dependent Negative Feedback Control of Insulin Secretion." *Nature Medicine* 21 (7): 769. https://doi.org/10.1038/NM.3872.

Michel, Martin A., Kirby N. Swatek, Manuela K. Hospenthal, and David Komander. 2017. "Ubiquitin Linkage-Specific Affimers Reveal Insights into K6-Linked Ubiquitin Signaling." *Molecular Cell* 68 (1): 233. https://doi.org/10.1016/J.MOLCEL.2017.08.020.

Molland, Katrina, Qing Zhou, and Andrew D. Mesecar. 2014. "A 2.2 Å Resolution Structure of the USP7 Catalytic Domain in a New Space Group Elaborates upon Structural Rearrangements Resulting from Ubiquitin Binding." *Acta Crystallographica Section F:Structural Biology Communications* 70 (3): 283–87. https://doi.org/10.1107/S2053230X14002519/TT5045SUP2.TIF.

Morotti, A., C. Panuzzo, S. Crivellaro, B. Pergolizzi, U. Familiari, A. H. Berger, G. Saglio, and P. P. Pandolfi. 2014. "BCR-ABL Disrupts PTEN Nuclear-Cytoplasmic Shuttling through Phosphorylation-Dependent Activation of HAUSP." *Leukemia* 28 (6): 1326–33. https://doi.org/10.1038/LEU.2013.370.

Murre, Cornelis, Patrick Schonleber McCaw, H. Vaessin, M. Caudy, L. Y. Jan, Y. N. Jan, Carlos v. Cabrera, et al. 1989. "Interactions between Heterologous Helix-Loop-Helix Proteins Generate Complexes That Bind Specifically to a Common DNA Sequence." *Cell* 58 (3): 537–44. https://doi.org/10.1016/0092-8674(89)90434-0.

Muthusamy, Babylakshmi, Thong T. Nguyen, Aravind K. Bandari, Salah Basheer, Lakshmi Dhevi N. Selvan, Deepshikha Chandel, Jesna Manoj, et al. 2019. "Exome Sequencing Reveals a Novel Splice Site Variant in HUWE1 Gene in Patients with Suspected Say-Meyer Syndrome." *European Journal of Medical Genetics* 63 (1): 103635. https://doi.org/10.1016/J.EJMG.2019.02.007.

Nalepa, Grzegorz, Mark Rolfe, and J Wade Harper. 2006. "Drug Discovery in the Ubiquitin–Proteasome System." *Nature Reviews Drug Discovery* 5 (7): 596–613. https://doi.org/10.1038/nrd2056.

Nava, C., F. Lamari, D. Héron, C. Mignot, A. Rastetter, B. Keren, D. Cohen, et al. 2012. "Analysis of the Chromosome X Exome in Patients with Autism Spectrum Disorders Novel Candidate Genes, Including TMLHE." *Translational Psychiatry* 2 (10): e179. https://doi.org/10.1038/TP.2012.102.

Nishimura, Wataru, Satoru Takahashi, and Kazuki Yasuda. 2015. "MafA Is Critical for Maintenance of the Mature Beta Cell Phenotype in Mice." *Diabetologia* 58 (3): 566–74. https://doi.org/10.1007/S00125-014-3464-9.

Offield, Martin F., Tom L. Jetton, Patricia A. Labosky, Michael Ray, Roland W. Stein, Mark A. Magnuson, Brigid L.M. Hogan, and Christopher V.E. Wright. 1996. "PDX-1 Is Required for Pancreatic Outgrowth and Differentiation of the Rostral Duodenum." *Development* 122 (3): 983–95. https://doi.org/10.1242/DEV.122.3.983.

Ohsako, Shunji, Jeanette Hyer, Grace Panganiban, Ian Oliver, and Michael Caudy. 1994. "Hairy Function as a DNA-Binding Helix-Loop-Helix Repressor of Drosophila Sensory Organ Formation." *Genes & Development* 8 (22): 2743–55. https://doi.org/10.1101/GAD.8.22.2743.

Okada, T., K. Tobe, K. Hara, K. Yasuda, Y. Kawaguchi, H. Ikegami, C. Ito, and T. Kadowaki. 2001. "Variants of Neurogenin 3 Gene Are Not Associated with Type II Diabetes in Japanese Subjects." *Diabetologia* 44 (2): 241–44. https://doi.org/10.1007/S001250051606.

Oliver-Krasinski, Jennifer M., Margaret T. Kasner, Juxiang Yang, Michael F. Crutchlow, Anil K. Rustgi, Klaus H. Kaestner, and Doris A. Stoffers. 2009. "The Diabetes Gene Pdx1 Regulates the Transcriptional Network of Pancreatic Endocrine Progenitor Cells in Mice." *The Journal of Clinical Investigation* 119 (7): 1888–98. https://doi.org/10.1172/JCI37028.

Pagliuca, Felicia W., and Douglas A. Melton. 2013. "How to Make a Functional β-Cell." *Development (Cambridge, England)* 140 (12): 2472. https://doi.org/10.1242/DEV.093187.

Pagliuca, Felicia W., Jeffrey R. Millman, Mads Gürtler, Michael Segel, Alana Van Dervort, Jennifer Hyoje Ryu, Quinn P. Peterson, Dale Greiner, and Douglas A. Melton. 2014. "Generation of Functional Human Pancreatic β Cells in Vitro." *Cell* 159 (2): 428–39. https://doi.org/10.1016/J.CELL.2014.09.040/ATTACHMENT/3FCB8D19-8B7A-42F9-A32B-2F981B085625/MMC3.XLS.

Pan, Chang, Hong Da Liu, Zheng Gong, Xiao Yu, Xu Ben Hou, Di Dong Xie, Xi Bin Zhu, et al. 2013. "Cadmium Is a Potent Inhibitor of PPM Phosphatases and Targets the M1 Binding Site." *Scientific Reports 2013 3:1* 3 (1): 1–11. https://doi.org/10.1038/srep02333.

Pan, Fong Cheng, and Marcela Brissova. 2014. "Pancreas Development in Humans." *Current Opinion in Endocrinology, Diabetes, and Obesity* 21 (2): 77. https://doi.org/10.1097/MED.0000000000000047.

Pan, Fong Cheng, and Chris Wright. 2011. "Pancreas Organogenesis: From Bud to Plexus to Gland." *Developmental Dynamics* 240 (3): 530–65. https://doi.org/10.1002/DVDY.22584.

Pandya, Renuka K., James R. Partridge, Kerry Routenberg Love, Thomas U. Schwartz, and Hidde L. Ploegh. 2010. "A Structural Element within the HUWE1 HECT Domain Modulates Self-Ubiquitination and Substrate Ubiquitination Activities." *The Journal of Biological Chemistry* 285 (8): 5664. https://doi.org/10.1074/JBC.M109.051805.

Paredes, Jose L., Abrahim I. Orabi, Taimur Ahmad, Iman Benbourenane, Kimimasa Tobita, Sameh Tadros, Kyongtae T. Bae, and Sohail Z. Husain. 2014. "A Non-Invasive Method of Quantifying Pancreatic Volume in Mice Using Micro-MRI." *PLoS ONE* 9 (3): 92263. https://doi.org/10.1371/JOURNAL.PONE.0092263.

Parsons, Jason L., Phillip S. Tait, David Finch, Irina I. Dianova, Mariola J. Edelmann, Svetlana V. Khoronenkova, Benedikt M. Kessler, Ricky A. Sharma, W. Gillies McKenna, and Grigory L. Dianov. 2009. "Ubiquitin Ligase ARF-BP1/Mule Modulates Base Excision Repair." *The EMBO Journal* 28 (20): 3207. https://doi.org/10.1038/EMBOJ.2009.243.

Peng, Jing, Ying Wang, Fang He, Chen Chen, Li Wen Wu, Li Fen Yang, Yu Ping Ma, et al. 2018. "Novel West Syndrome Candidate Genes in a Chinese Cohort." *CNS Neuroscience & Therapeutics* 24 (12): 1196. https://doi.org/10.1111/CNS.12860.

Peng, Yuchong, Youhong Liu, Yingxue Gao, Bowen Yuan, Xuli Qi, Yuxin Fu, Qianling Zhu, et al. 2019. "USP7 Is a Novel Deubiquitinase Sustaining PLK1 Protein Stability and Regulating Chromosome Alignment in Mitosis." *Journal of Experimental & Clinical Cancer Research : CR* 38 (1). https://doi.org/10.1186/S13046-019-1457-8.

Petroski, Matthew D, and Raymond J Deshaies. 2003. “Context of Multiubiquitin Chain Attachment Influences the Rate of Sic1 Degradation.” *Molecular Cell* 11 (6): 1435–44. https://doi.org/10.1016/s1097-2765(03)00221-1.

Pictet, Raymond L., William R. Clark, Robert H. Williams, and William J. Rutter. 1972. “An Ultrastructural Analysis of the Developing Embryonic Pancreas.” *Developmental Biology* 29 (4): 436–67. https://doi.org/10.1016/0012-1606(72)90083-8.

Pinney, Sara E., Jennifer Oliver-Krasinski, Linda Ernst, Nkecha Hughes, Puja Patel, Doris A. Stoffers, Pierre Russo, and Diva D. De León. 2011. “Clinical Case Seminar: Neonatal Diabetes and Congenital Malabsorptive Diarrhea Attributable to a Novel Mutation in the Human Neurogenin-3 Gene Coding Sequence.” *The Journal of Clinical Endocrinology and Metabolism* 96 (7): 1960. https://doi.org/10.1210/JC.2011-0029.

Pozhidaeva, Alexandra, and Irina Bezsonova. 2019. “USP7: Structure, Substrate Specificity, and Inhibition.” *DNA Repair* 76 (April): 30. https://doi.org/10.1016/J.DNAREP.2019.02.005.

Rall, L. B., R. L. Pictet, R. H. Williams, and W. J. Rutter. 1973. “Early Differentiation of Glucagon-Producing Cells in Embryonic Pancreas: A Possible Developmental Role for Glucagon.” *Proceedings of the National Academy of Sciences of the United States of America* 70 (12 Pt 1-2): 3478. https://doi.org/10.1073/PNAS.70.12.3478.

Rankin, Matthew M., and Jake A. Kushner. 2009. “Adaptive Beta-Cell Proliferation Is Severely Restricted with Advanced Age.” *Diabetes* 58 (6): 1365–72. https://doi.org/10.2337/DB08-1198.

Reverdy, Céline, Susan Conrath, Roman Lopez, Cécile Planquette, Cédric Atmanene, Vincent Collura, Jane Harpon, et al. 2012. “Discovery of Specific Inhibitors of Human USP7/HAUSP Deubiquitinating Enzyme.” *Chemistry & Biology* 19 (4): 467–77. https://doi.org/10.1016/J.CHEMBIOL.2012.02.007.

Rickels, Michael R., and R. Paul Robertson. 2019. “Pancreatic Islet Transplantation in Humans: Recent Progress and Future Directions.” *Endocrine Reviews* 40 (2): 631. https://doi.org/10.1210/ER.2018-00154.

Roark, Ryan, Laura Itzhaki, and Anna Philpott. 2012. “Complex Regulation Controls Neurogenin3 Proteolysis.” *Biology Open* 1 (12): 1264. https://doi.org/10.1242/BIO.20121750.

Rose, Scott D., Galvin H. Swift, Michael J. Peyton, Robert E. Hammer, and Raymond J. MacDonald. 2001. “The Role of PTF1-P48 in Pancreatic Acinar Gene Expression.” *The Journal of Biological Chemistry* 276 (47): 44018–26. https://doi.org/10.1074/JBC.M106264200.

Roze, S., J. Smith-Palmer, W. Valentine, S. de Portu, K. Nørgaard, and J. C. Pickup. 2015. “Cost-Effectiveness of Continuous Subcutaneous Insulin Infusion versus Multiple Daily Injections of Insulin in Type 1 Diabetes: A Systematic Review.” *Diabetic Medicine* 32 (11): 1415–24. https://doi.org/10.1111/dme.12792.

Rubio-Cabezas, Oscar, Jan N. Jensen, Maria I. Hodgson, Ethel Codner, Sian Ellard, Palle Serup, and Andrew T. Hattersley. 2011. “Permanent Neonatal Diabetes and Enteric Anendocrinosis Associated with Biallelic Mutations in NEUROG3.” *Diabetes* 60 (4): 1349–53. https://doi.org/10.2337/DB10-1008/-/DC1.

Ruckert, Mariana Tannús, Annet Z Brouwers-Vos, Luis Fernando P Nagano, Jan Jacob Schuringa, and Vanessa Silva Silveira. 2020. “HUWE1 Cooperates with RAS Activation to Control Leukemia Cell

Proliferation and Human Hematopoietic Stem Cells Differentiation Fate." *Cancer Gene Therapy* 27 (10–11): 830–33. https://doi.org/10.1038/s41417-020-0198-3.

Russ, Holger A, Audrey V Parent, Jennifer J Ringler, Thomas G Hennings, Gopika G Nair, Mayya Shveygert, Tingxia Guo, et al. 2015. "Controlled Induction of Human Pancreatic Progenitors Produces Functional Beta-like Cells in Vitro." *The EMBO Journal* 34 (13): 1759. https://doi.org/10.15252/EMBJ.201591058.

Saedi, Elham, Mohammad Reza Gheini, Firoozeh Faiz, and Mohammad Ali Arami. 2016. "Diabetes Mellitus and Cognitive Impairments." *World Journal of Diabetes* 7 (17): 412. https://doi.org/10.4239/WJD.V7.I17.412.

Saisho, Yoshifumi. 2015. "β-Cell Dysfunction: Its Critical Role in Prevention and Management of Type 2 Diabetes." *World Journal of Diabetes* 6 (1): 109. https://doi.org/10.4239/WJD.V6.I1.109.

Salisbury, Rachel J., Jennifer Blaylock, Andrew A. Berry, Rachel E. Jennings, Ronald De Krijger, Karen Piper Hanley, and Neil A. Hanley. 2014. "The Window Period of NEUROGENIN3 during Human Gestation." *Islets* 6 (3). https://doi.org/10.4161/19382014.2014.954436.

Samols, E., G. Marri, and V. Marks. 1966. "Interrelationship of Glucagon, Insulin and Glucose: The Insulinogenic Effect of Glucagon." *Diabetes* 15 (12): 855–66. https://doi.org/10.2337/DIAB.15.12.855.

Sancho, Rocio, Ralph Gruber, Guoqiang Gu, and Axel Behrens. 2014. "Loss of Fbw7 Reprograms Adult Pancreatic Ductal Cells into α, δ, and β Cells." *Cell Stem Cell* 15 (2): 139–53. https://doi.org/10.1016/J.STEM.2014.06.019.

Sander, Bodo, Wenshan Xu, Martin Eilers, Nikita Popov, and Sonja Lorenz. 2017. "A Conformational Switch Regulates the Ubiquitin Ligase HUWE1." *ELife* 6 (February). https://doi.org/10.7554/ELIFE.21036.

Saridakis, Vivian, Yi Sheng, Feroz Sarkari, Melissa N. Holowaty, Kathy Shire, Tin Nguyen, Rongguang G. Zhang, et al. 2005. "Structure of the P53 Binding Domain of HAUSP/USP7 Bound to Epstein-Barr Nuclear Antigen 1 Implications for EBV-Mediated Immortalization." *Molecular Cell* 18 (1): 25–36. https://doi.org/10.1016/J.MOLCEL.2005.02.029.

Sato, Mai, Ruth Rodriguez-Barrueco, Jiyang Yu, Catherine Do, Jose M. Silva, and Jean Gautier. 2015. "MYC Is a Critical Target of FBXW7." *Oncotarget* 6 (5): 3292. https://doi.org/10.18632/ONCOTARGET.3203.

Sayar, Ersin, Ali Islek, Aygen Yilmaz, Mustafa Akcam, Sarah E. Flanagan, and Reha Artan. 2013. "Extremely Rare Cause of Congenital Diarrhea: Enteric Anendocrinosis." *Pediatrics International* 55 (5): 661–63. https://doi.org/10.1111/PED.12169.

Scavuzzo, Marissa A., Matthew C. Hill, Jolanta Chmielowiec, Diane Yang, Jessica Teaw, Kuanwei Sheng, Yuelin Kong, et al. 2018. "Endocrine Lineage Biases Arise in Temporally Distinct Endocrine Progenitors during Pancreatic Morphogenesis." *Nature Communications* 9 (1). https://doi.org/10.1038/S41467-018-05740-1.

Schaffer, Ashleigh E., Kristine K. Freude, Shelley B. Nelson, and Maike Sander. 2010. "Ptf1a and Nkx6 Transcription Factors Function as Antagonistic Lineage Determinants in Multipotent Pancreatic Progenitors." *Developmental Cell* 18 (6): 1022. https://doi.org/10.1016/J.DEVCEL.2010.05.015.

Shahjalal, Hussain Md, Ahmed Abdal Dayem, Kyung Min Lim, Tak Il Jeon, and Ssang Goo Cho. 2018. "Generation of Pancreatic β Cells for Treatment of Diabetes: Advances and Challenges." *Stem Cell Research & Therapy* 9 (1). https://doi.org/10.1186/S13287-018-1099-3.

Sheets, Timothy P., Ki Eun Park, Chi Hun Park, Steven M. Swift, Anne Powell, David M. Donovan, and Bhanu P. Telugu. 2018. "Targeted Mutation of NGN3 Gene Disrupts Pancreatic Endocrine Cell Development in Pigs." *Scientific Reports* 8 (1). https://doi.org/10.1038/S41598-018-22050-0.

Sheng, Yi, Vivian Saridakis, Feroz Sarkari, Shili Duan, Tianne Wu, Cheryl H. Arrowsmith, and Lori Frappier. 2006. "Molecular Recognition of P53 and MDM2 by USP7/HAUSP." *Nature Structural & Molecular Biology* 13 (3): 285–91. https://doi.org/10.1038/NSMB1067.

Shih, Hung Ping, Janel L. Kopp, Manbir Sandhu, Claire L. Dubois, Philip A. Seymour, Anne Grapin-Botton, and Maike Sander. 2012. "A Notch-Dependent Molecular Circuitry Initiates Pancreatic Endocrine and Ductal Cell Differentiation." *Development (Cambridge, England)* 139 (14): 2488–99. https://doi.org/10.1242/DEV.078634.

Smith, Stuart B., Rosa Gasa, Hirotaka Watada, Juehu Wang, Steven C. Griffen, and Michael S. German. 2003. "Neurogenin3 and Hepatic Nuclear Factor 1 Cooperate in Activating Pancreatic Expression of Pax4." *Journal of Biological Chemistry* 278 (40): 38254–59. https://doi.org/10.1074/JBC.M302229200.

Sommer, L, Q Ma, and D J Anderson. 1996. "Neurogenins, a Novel Family of Atonal-Related BHLH Transcription Factors, Are Putative Mammalian Neuronal Determination Genes That Reveal Progenitor Cell Heterogeneity in the Developing CNS and PNS." *Molecular and Cellular Neurosciences* 8 (4): 221–41. https://doi.org/10.1006/mcne.1996.0060.

Soyer, Josselin, Lydie Flasse, Wolfgang Raffelsberger, Anthony Beucher, Christophe Orvain, Bernard Peers, Philippe Ravassard, et al. 2010. "Rfx6 Is an Ngn3-Dependent Winged Helix Transcription Factor Required for Pancreatic Islet Cell Development." *Development* 137 (2): 203–12. https://doi.org/10.1242/DEV.041673/-/DC1.

Srinivas, Shankar, Tomoko Watanabe, Chyuan-Sheng Lin, Chris M William, Yasuto Tanabe, Thomas M Jessell, and Frank Costantini. 2001. "Cre Reporter Strains Produced by Targeted Insertion of EYFP and ECFP into the ROSA26 Locus." *BMC Developmental Biology*. Vol. 1.

Stoffers, Doris A., Noah T. Zinkin, Violeta Stanojevic, William L. Clarke, and Joel F. Habener. 1997. "Pancreatic Agenesis Attributable to a Single Nucleotide Deletion in the Human IPF1 Gene Coding Sequence." *Nature Genetics* 15 (1): 106–10. https://doi.org/10.1038/NG0197-106.

Su, Chen, Tao Wang, Jiabao Zhao, Jia Cheng, and Jingjing Hou. 2019. "Meta-Analysis of Gene Expression Alterations and Clinical Significance of the HECT Domain-Containing Ubiquitin Ligase HUWE1 in Cancer." *Oncology Letters* 18 (3): 2292. https://doi.org/10.3892/OL.2019.10579.

Swatek, Kirby N., and David Komander. 2016. "Ubiquitin Modifications." *Cell Research* 26 (4): 399. https://doi.org/10.1038/CR.2016.39.

Tavana, Omid, Dawei Li, Chao Dai, Gonzalo Lopez, Debarshi Banerjee, Ning Kon, Chao Chen, et al. 2016. "HAUSP Deubiquitinates and Stabilizes N-Myc in Neuroblastoma." *Nature Medicine* 22 (10): 1180–86. https://doi.org/10.1038/NM.4180.

Teta, Monica, Matthew M. Rankin, Simon Y. Long, Geneva M. Stein, and Jake A. Kushner. 2007. "Growth and Regeneration of Adult Beta Cells Does Not Involve Specialized Progenitors." *Developmental Cell* 12 (5): 817–26. https://doi.org/10.1016/J.DEVCEL.2007.04.011.

Tripathi, Vivek, Ekjot Kaur, Suhas Sampat Kharat, Mansoor Hussain, Arun Prasath Damodaran, Swati Kulshrestha, and Sagar Sengupta. 2019. "Abrogation of FBW7α-Dependent P53 Degradation Enhances P53's Function as a Tumor Suppressor." *The Journal of Biological Chemistry* 294 (36): 13224–32. https://doi.org/10.1074/JBC.AC119.008483.

Trotman, Lloyd C., Xinjiang Wang, Andrea Alimonti, Zhenbang Chen, Julie Teruya-Feldstein, Haijuan Yang, Nikola P. Pavletich, et al. 2007. "Ubiquitination Regulates PTEN Nuclear Import and Tumor Suppression." *Cell* 128 (1): 141. https://doi.org/10.1016/J.CELL.2006.11.040.

Trott, Jamie, Ee Kim Tan, Sheena Ong, Drew M. Titmarsh, Simon L.I.J. Denil, Maybelline Giam, Cheng Kit Wong, et al. 2017. "Long-Term Culture of Self-Renewing Pancreatic Progenitors Derived from Human Pluripotent Stem Cells." *Stem Cell Reports* 8 (6): 1675. https://doi.org/10.1016/J.STEMCR.2017.05.019.

Turner, Robert. 1998. "Effect of Intensive Blood-Glucose Control with Metformin on Complications in Overweight Patients with Type 2 Diabetes (UKPDS 34)." *The Lancet* 352 (9131): 854–65. https://doi.org/10.1016/S0140-6736(98)07037-8.

Uhlén, Mathias, Linn Fagerberg, Bjö M. Hallström, Cecilia Lindskog, Per Oksvold, Adil Mardinoglu, Åsa Sivertsson, et al. 2015. "Tissue-Based Map of the Human Proteome." *Science* 347 (6220). https://doi.org/10.1126/SCIENCE.1260419/SUPPL_FILE/1260419_UHLEN.SM.PDF.

Ünlüsoy Aksu, Aysel, Ödül Eğritaş Gürkan, Sinan Sarı, Zeliha Demirtaş, Canan Türkyılmaz, Aylar Poyraz, and Buket Dalgıç. 2016. "Mutant Neurogenin-3 in a Turkish Boy with Congenital Malabsorptive Diarrhea." *Pediatrics International* 58 (5): 379–82. https://doi.org/10.1111/PED.12783.

Urbán, Noelia, Debbie L.C. Van Den Berg, Antoine Forget, Jimena Andersen, Jeroen A.A. Demmers, Charles Hunt, Olivier Ayrault, and François Guillemot. 2016. "Return to Quiescence of Murine Neural Stem Cells by Degradation of a Pro-Activation Protein." *Science (New York, N.Y.)* 353 (6296): 292. https://doi.org/10.1126/SCIENCE.AAF4802.

Valles, Gabrielle J., Irina Bezsonova, Roger Woodgate, and Nicholas W. Ashton. 2020. "USP7 Is a Master Regulator of Genome Stability." *Frontiers in Cell and Developmental Biology* 8 (August). https://doi.org/10.3389/FCELL.2020.00717.

VanDussen, Kelli L., Alexis J. Carulli, Theresa M. Keeley, Sanjeevkumar R. Patel, Brent J. Puthoff, Scott T. Magness, Ivy T. Tran, et al. 2012. "Notch Signaling Modulates Proliferation and Differentiation of Intestinal Crypt Base Columnar Stem Cells." *Development (Cambridge, England)* 139 (3): 488–97. https://doi.org/10.1242/DEV.070763.

Varshavsky, Alexander. 2017. "The Ubiquitin System, Autophagy, and Regulated Protein Degradation." *Https://Doi.Org/10.1146/Annurev-Biochem-061516-044859* 86 (June): 123–28. https://doi.org/10.1146/ANNUREV-BIOCHEM-061516-044859.

Villasenor, Alethia, Diana C. Chong, and Ondine Cleaver. 2008. "Biphasic Ngn3 Expression in the Developing Pancreas." *Developmental Dynamics : An Official Publication of the American Association of Anatomists* 237 (11): 3270. https://doi.org/10.1002/DVDY.21740.

Viner, Russell, Billy White, and Deborah Christie. 2017. “Type 2 Diabetes in Adolescents: A Severe Phenotype Posing Major Clinical Challenges and Public Health Burden.” *The Lancet* 389 (10085): 2252–60. https://doi.org/10.1016/S0140-6736(17)31371-5.

Vojtek, Anne B., Jennifer Taylor, Stacy L. DeRuiter, Jenn-Yah Yu, Claudia Figueroa, Roland P. S. Kwok, and David L. Turner. 2003. “Akt Regulates Basic Helix-Loop-Helix Transcription Factor-Coactivator Complex Formation and Activity during Neuronal Differentiation.” *Molecular and Cellular Biology* 23 (13): 4417. https://doi.org/10.1128/MCB.23.13.4417-4427.2003.

Wang, Linyuan, Cynthia T. Luk, Stephanie A. Schroer, Alannah M. Smith, Xie Li, Erica P. Cai, Herbert Gaisano, et al. 2014. “Dichotomous Role of Pancreatic HUWE1/MULE/ARF-BP1 in Modulating Beta Cell Apoptosis in Mice under Physiological and Genotoxic Conditions.” *Diabetologia* 57 (9): 1889–98. https://doi.org/10.1007/S00125-014-3295-8/FIGURES/6.

Wang, Qian, Shuai Ma, Nan Song, Xin Li, Ling Liu, Shangda Yang, Xiang Ding, et al. 2016. “Stabilization of Histone Demethylase PHF8 by USP7 Promotes Breast Carcinogenesis.” *The Journal of Clinical Investigation* 126 (6): 2205. https://doi.org/10.1172/JCI85747.

Wang, Xiaoli, Roger A. Herr, Wei Jen Chua, Lonnie Lybarger, Emmanuel J.H.J. Wiertz, and Ted H. Hansen. 2007. “Ubiquitination of Serine, Threonine, or Lysine Residues on the Cytoplasmic Tail Can Induce ERAD of MHC-I by Viral E3 Ligase MK3.” *The Journal of Cell Biology* 177 (4): 613. https://doi.org/10.1083/JCB.200611063.

Wang, Zhiru, Wenting Kang, Yinghua You, Jingru Pang, Hongmei Ren, Zhenhe Suo, Hongmin Liu, and Yichao Zheng. 2019. “USP7: Novel Drug Target in Cancer Therapy.” *Frontiers in Pharmacology* 10 (APR): 427. https://doi.org/10.3389/FPHAR.2019.00427/BIBTEX.

Welcker, Markus, Amir Orian, Jianping Jin, Jonathan A. Grim, J. Wade Harper, Robert N. Eisenman, and Bruce E. Clurman. 2004. “The Fbw7 Tumor Suppressor Regulates Glycogen Synthase Kinase 3 Phosphorylation-Dependent c-Myc Protein Degradation.” *Proceedings of the National Academy of Sciences of the United States of America* 101 (24): 9085–90. https://doi.org/10.1073/PNAS.0402770101/SUPPL_FILE/02770FIG8.PDF.

Wenzel, Dawn M., Alexei Lissounov, Peter S. Brzovic, and Rachel E. Klevit. 2011. “UbcH7 Reactivity Profile Reveals Parkin and HHARI to Be RING/HECT Hybrids.” *Nature* 474 (7349): 105. https://doi.org/10.1038/NATURE09966.

Wickliffe, Katherine E., Adam Williamson, Hermann Josef Meyer, Aileen Kelly, and Michael Rape. 2011. “K11-Linked Ubiquitin Chains as Novel Regulators of Cell Division.” *Trends in Cell Biology* 21 (11): 656. https://doi.org/10.1016/J.TCB.2011.08.008.

Wilkinson, C R, M Seeger, R Hartmann-Petersen, M Stone, M Wallace, C Semple, and C Gordon. 2001. “Proteins Containing the UBA Domain Are Able to Bind to Multi-Ubiquitin Chains.” *Nature Cell Biology* 3 (10): 939–43. https://doi.org/10.1038/ncb1001-939.

Wu, Guangyu, Svetlana Lyapina, Indranil Das, Jinhe Li, Mark Gurney, Adele Pauley, Inca Chui, Raymond J. Deshaies, and Jan Kitajewski. 2001. “SEL-10 Is an Inhibitor of Notch Signaling That Targets Notch for Ubiquitin-Mediated Protein Degradation.” *Molecular and Cellular Biology* 21 (21): 7403–15. https://doi.org/10.1128/MCB.21.21.7403-7415.2001/ASSET/D92D330A-BBA2-49C1-B768-48E05BF7537B/ASSETS/GRAPHIC/MB2110099007.JPEG.

Wu, Yanling, Yanping Ding, Yoshimasa Tanaka, and Wen Zhang. 2014. “Risk Factors Contributing to Type 2 Diabetes and Recent Advances in the Treatment and Prevention.” *International Journal of Medical Sciences* 11 (11): 1185. https://doi.org/10.7150/IJMS.10001.

Xu, Ping, Duc M Duong, Nicholas T Seyfried, Dongmei Cheng, Yang Xie, Jessica Robert, John Rush, Mark Hochstrasser, Daniel Finley, and Junmin Peng. 2009. “Quantitative Proteomics Reveals the Function of Unconventional Ubiquitin Chains in Proteasomal Degradation.” *Cell* 137 (1): 133–45. https://doi.org/10.1016/j.cell.2009.01.041.

Xu, Yi ming, Qiang Gao, Jin zhao Zhang, Yun tao Lu, Dong ming Xing, Yan qing Qin, and Jing Fang. 2020. “Prolyl Hydroxylase 3 Controls the Intestine Goblet Cell Generation through Stabilizing ATOH1.” *Cell Death and Differentiation* 27 (7): 2131. https://doi.org/10.1038/S41418-020-0490-7.

Xu, Yue, D. Eric Anderson, and Yihong Ye. 2016. “The HECT Domain Ubiquitin Ligase HUWE1 Targets Unassembled Soluble Proteins For.” *Cell Discovery* 2 (November): 16040. https://doi.org/10.1038/CELLDISC.2016.40.

Yang, Dong, Daomei Cheng, Qiu Tu, Huihui Yang, Bin Sun, Lanzhen Yan, Hongjuan Dai, et al. 2018. “HUWE1 Controls the Development of Non-Small Cell Lung Cancer through down-Regulation of P53.” *Theranostics* 8 (13): 3517–29. https://doi.org/10.7150/THNO.24401.

Yang, Y., B. H.J. Chang, V. Yechoor, W. Chen, L. Li, M. J. Tsai, and L. Chan. 2011. “The Krüppel-like Zinc Finger Protein GLIS3 Transactivates Neurogenin 3 for Proper Fetal Pancreatic Islet Differentiation in Mice.” *Diabetologia* 54 (10): 2595–2605. https://doi.org/10.1007/S00125-011-2255-9.

Yi, Juan, Guang Lu, Li Li, Xiaozhen Wang, Li Cao, Ming Lin, Sha Zhang, and Genze Shao. 2015. “DNA Damage-Induced Activation of CUL4B Targets HUWE1 for Proteasomal Degradation.” *Nucleic Acids Research* 43 (9): 4579. https://doi.org/10.1093/NAR/GKV325.

Yoneda, S, S Uno, H Iwahashi, Y Fujita, A Yoshikawa, J Kozawa, K Okita, et al. 2013. “Predominance of β-Cell Neogenesis Rather Than Replication in Humans With an Impaired Glucose Tolerance and Newly Diagnosed Diabetes.” *The Journal of Clinical Endocrinology & Metabolism* 98 (5): 2053–61. https://doi.org/10.1210/jc.2012-3832.

Yoon, Ji-Won, and Hee-Sook Jun. 2005. “Autoimmune Destruction of Pancreatic Beta Cells.” *American Journal of Therapeutics* 12 (6): 580–91.

Yu, Xin Xin, Wei Lin Qiu, Liu Yang, Yan Chun Wang, Mao Yang He, Dan Wang, Yu Zhang, et al. 2021. “Sequential Progenitor States Mark the Generation of Pancreatic Endocrine Lineages in Mice and Humans.” *Cell Research* 31 (8): 886–903. https://doi.org/10.1038/S41422-021-00486-W.

Zapata, Juan M., Krzysztof Pawlowski, Elvira Haas, Carl F. Ware, Adam Godzik, and John C. Reed. 2001. “A Diverse Family of Proteins Containing Tumor Necrosis Factor Receptor-Associated Factor Domains *.” *Journal of Biological Chemistry* 276 (26): 24242–52. https://doi.org/10.1074/JBC.M100354200.

Zhang, Wei, Jingxin Zhang, Chenzhou Xu, Shiqing Zhang, Saiyan Bian, Feng Jiang, Wenkai Ni, et al. 2020. “Ubiquitin-Specific Protease 7 Is a Drug-Able Target That Promotes Hepatocellular Carcinoma and Chemoresistance.” *Cancer Cell International* 20 (1): 1–12. https://doi.org/10.1186/S12935-020-1109-2/FIGURES/6.

Zhang, Xinghao, Patrick S Mcgrath, Joseph Salomone, Rhett Kovall, Brian Gebelein, and James M Wells Correspondence. 2019. “A Comprehensive Structure-Function Study of Neurogenin3 Disease-Causing Alleles during Human Pancreas and Intestinal Organoid Development.” *Developmental Cell* 50: 367–80. https://doi.org/10.1016/j.devcel.2019.05.017.

Zhong, Qing, Wenhua Gao, Fenghe Du, and Xiaodong Wang. 2005. “Mule/ARF-BP1, a BH3-Only E3 Ubiquitin Ligase, Catalyzes the Polyubiquitination of Mcl-1 and Regulates Apoptosis.” *Cell* 121 (7): 1085–95. https://doi.org/10.1016/j.cell.2005.06.009.

Zhou, Qiao, Juliana Brown, Andrew Kanarek, Jayaraj Rajagopal, and Douglas A. Melton. 2008. “In Vivo Reprogramming of Adult Pancreatic Exocrine Cells to β-Cells.” *Nature 2008 455:7213* 455 (7213): 627–32. https://doi.org/10.1038/nature07314.

Zhu, Yaxi, Qian Liu, Zhiguang Zhou, and Yasuhiro Ikeda. 2017. “PDX1, Neurogenin-3, and MAFA: Critical Transcription Regulators for Beta Cell Development and Regeneration.” *Stem Cell Research and Therapy* 8 (1): 1–7. https://doi.org/10.1186/S13287-017-0694-Z/FIGURES/1.

Zinger, Adar, and Gil Leibowitz. 2014. “Islet Transplantation in Type 1 Diabetes: Hype, Hope and Reality - a Clinician’s Perspective.” *Diabetes/Metabolism Research and Reviews* 30 (2): 83–87. https://doi.org/10.1002/dmrr.2484.